# Palos Verdes Shelf Oceanographic Study: Data Report for Observations December 2007–April 2008

By Kurt Rosenberger, Marlene A. Noble, Christopher R. Sherwood, Marinna M. Martini, Joanne T. Ferreira, and Ellyn Montgomery

Open-File Report 2010–1240

**U.S. Department of the Interior**
**U. S. Geological Survey**

**U.S. Department of the Interior**
KEN SALAZAR, Secretary

**U.S. Geological Survey**
Marcia K. McNutt, Director

U.S. Geological Survey, Reston, Virginia: 2011

For more information on the USGS—the Federal source for science about the Earth, its natural and living resources, natural hazards, and the environment—visit *http://www.usgs.gov* or call 1–888–ASK–USGS

For an overview of USGS information products, including maps, imagery, and publications, visit *http://www.usgs.gov/pubprod*

Suggested citation:
Rosenberger, Kurt, Noble, M.A., Sherwood, C.R., Martini, M.M., Ferreira, J.T., and Montgomery, Ellyn, 2011, Palos Verdes Shelf oceanographic study; data report for observations December 2007–April 2008: U.S. Geological Survey Open-File Report 2010–1240, 118 p., available at *http://pubs.usgs.gov/of/2010/1240/*.

# Contents

## Appendixes



## Figures

## Tables

# Palos Verdes Shelf Oceanographic Study: Data Report for Observations December 2007–April 2008

By Kurt Rosenberger[1], Marlene A. Noble[2], Christopher R. Sherwood[3], Marinna M. Martini[3], Joanne T. Ferreira[2], and Ellyn Montgomery[3]

## Abstract

Beginning in 1997, the Environmental Protection Agency (EPA) defined a contaminated section of the Palos Verdes Shelf region in southern California as a Superfund Site, initiating a continuing investigation of this area. The investigation involved the EPA, the U.S. Geological Survey (USGS), Science Applications International Corporation (SAIC), Los Angeles County Sanitation Districts (LACSD) data, and other allied agencies.

In mid-2007, the Palos Verdes Shelf project team identified the need for additional data on the sediment properties and oceanographic conditions at the Palos Verdes Superfund Site and deployed seven bottom platforms, three subsurface moorings, and three surface moorings on the shelf. This additional data was needed to support ongoing modeling and feasibility studies and to improve our ability to model the fate of the effluent-affected deposit over time. It provided more detail on the spatial variability and magnitude of resuspension of the deposit during multiple storms that are expected to transit the region during a winter season.

The operation began in early December 2007 and ended in early April 2008. The goal was to measure the sediment response (threshold of resuspension, suspended-sediment concentrations, and suspended-sediment transport rates) to bed stresses associated with waves and currents. Other objectives included determining the structure of the bottom boundary layer (BBL) relating nearbed currents with those measured at 10 m above bottom (mab) and comparing those with the long-term data from the LACSD Acoustic Doppler Current Profiler (ADCP) deployments for nearbed current speed and direction. Low-profile tripods with high-frequency ADCPs co-located with two of the large tripods were selected for this goal.

This report describes the data obtained during the field program, the instruments and data-processing procedures used, and the archive that contains the data sets that have passed our quality-assurance procedures.

## Introduction

The Palos Verdes Shelf is a narrow section of continental shelf just west of Los Angeles, Calif., that lies between Santa Monica and San Pedro Bays (fig. 1). Beginning in 1937 and peaking around 1971, the pesticide dichlorodiphenyltricloroethane (DDT), combined with polychlorinated biphenyls (PCBs), metals, and other contaminants, were discharged onto the shelf through the Whites Point treated wastewater outfall operated by the Los Angeles County

[1] U.S. Geological Survey, Santa Cruz, Calif.
[2] U.S. Geological Survey, Menlo Park, Calif.
[3] U.S. Geological Survey, Woods Hole, Mass.

Sanitation Districts (LACSD). Since then, continuous improvements in treatment have reduced the load of suspended solids and contaminants, culminating in November 2002 when all discharge began to receive secondary treatment. Sediment from the outfalls has combined with material from other sources (most notably, erosion at the toe of the Portuguese Bend landslide off Palos Verdes) to form an effluent-affected deposit on the Palos Verdes Shelf upcoast of the outfall.

In 1992, the USGS Coastal and Marine Geology Team, in collaboration with other agencies, conducted an extensive survey of the deposit and the sediment and pollutant transport processes in the region (Lee and Wiberg, 2002). They found that the effluent-affected deposit ranged in thickness from 5 to 60 cm, had a volume of more than 9 M $m^3$, and covered 40 $km^2$ on the shelf and adjacent continental slope (Lee and Wiberg, 2002). The Palos Verdes Shelf became an Environmental Protection Agency (EPA) Superfund Site in 1997, which initiated an investigation of the region. The EPA has defined the Palos Verdes Shelf region of interest to include the area from Point Fermin in the southeast to the southern edge of Redondo Canyon, which lies northwest of the Palos Verdes peninsula. Brown lines show LACSD municipal sewer outfall pipes.

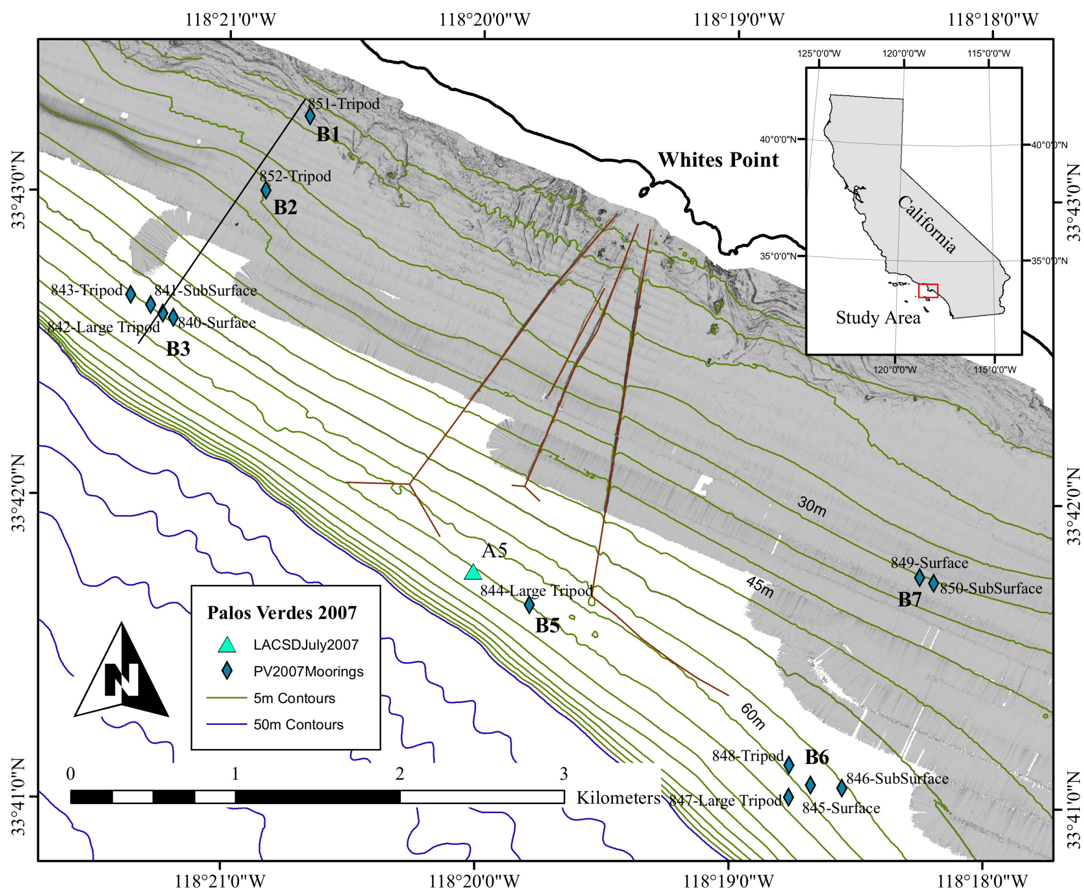


**Figure 1.** Map of Palos Verdes Shelf, along the California coast, showing deployment locations.

Subsequently, the USGS and other agencies such as LACSD, EPA, the U.S. Army Corps of Engineers (ACOE), and SAIC collected or supported the collection of many more data sets (Stull and others, 1996). Some of the goals of these projects were to (1) monitor sediment and contaminant resuspension and transport processes and (2) use the analysis products from these multiple data sets to improve numerical models that predict the eventual fate of the sediments and contaminants. As part of this program, the USGS and SAIC, supported partly by the EPA, conducted an oceanographic measurement program in the region from early March 2004 to early July 2004 (SAIC, 2004, 2005, 2009; Sherwood and others, unpub. data, 2010) to improve our understanding of the natural processes that resuspend and transport sediment, especially in the region southeast of the outfall where earlier measurements were thought to be deficient. Figure 1 shows the locations of the moorings deployed in the 2007 program, as well as the location of the 2007 LACSD mooring in the region. Unfortunately, too few major storms that enhance resuspension and transport processes occurred during our winter field program (December 2007–April 2008) to obtain adequate data. Another measurement and analysis program was instituted to further refine our understanding of transport processes of polluted sediment over the Palos Verdes Shelf.

## Background and Objectives

In mid-2007 the Palos Verdes Shelf project team identified the need for additional data on the sediment properties and oceanographic conditions at the Palos Verdes Superfund Site. This additional data was needed to support ongoing modeling and feasibility studies and improve our ability to model the fate of the effluent-affected deposit over time. It could provide more detailed data on the spatial variability and magnitude of resuspension of the contaminated, effluent-affected deposit during multiple storms expected to transit the region during a winter season. Multiple objectives were identified for the 2007–2008 field program:

- Measure sediment transport events at several locations on the effluent-affected deposit. Specifically, measure the sediment response (threshold of resuspension, suspended-sediment concentrations, and suspended-sediment transport rates) to bed stresses associated with waves and currents. Pursue the hypothesis that net erosion or deposition of the deposit is related to alongshore gradients in sediment transport caused primarily by gradients in sediment erodibility, but also examine alongshelf gradients in forcing, particularly that of internal tides. Multiple heavily instrumented tripods were necessary to accomplish this goal.
- Determine the structure of the BBL and relate near-bed currents with those measured at 10 mab. Relate the valuable long-term data from the LACSD ADCP deployments to near-bed current speed and direction. Low-profile tripods with high-frequency ADCPs co-located with two of the large tripods were selected for this goal.
- Measure nearshore circulation and sediment fluxes on the inner and middle shelf near the Portuguese Bend landslide in an attempt to understand the dispersal and pathways of landslide material over the effluent-affected deposit. Two tripods with ADCPs and near-bottom current and suspended-sediment sensors in a cross-shore array were deployed to fulfill this need. In addition, one tripod was equipped with a sediment trap to sample for later analysis of size and mineralogy of suspended sediment.

- Evaluate the cross-shelf evolution of internal motions. Thermistor strings at 60-m and 30-m sites were deployed to observe changes in internal wave character as they propagate onshore. The thermistor strings deployed by the USGS and thermistor arrays deployed by LACSD provided additional data on the alongshelf variability of internal motions.
- Obtain field measurements to assess the temporal and spatial variation in the potential erodability of Palos Verdes Shelf sediment (co-located with current meter measurements) via sediment coring and on-board erodibility measurements on cores obtained.
- Support deployment of EPA/URI polyethylene sheets as passive DDT samplers (for absorbing DDT from the water column).

The USGS conducted an oceanographic measurement program on the Palos Verdes Shelf beginning in early December 2007 and ending in early April 2008 to meet these project needs. This report describes the data obtained during the field program, the instruments and data-processing procedures used, and the archive that contains the data sets that have passed our quality-assurance procedures.

Related field activity identification numbers and their metadata follow:

S-4-07-SC *http://walrus.wr.usgs.gov/infobank/s/s407sc/html/s-4-07-sc.meta.html*
S-R3-08-SC *http://walrus.wr.usgs.gov/infobank/s/sr308sc/html/s-r3-08-sc.meta.html*

# Field Program

## Tripods and Moorings

To meet the measurement objectives listed above, the USGS deployed seven bottom platforms, three subsurface moorings, and three surface moorings on the Palos Verdes Shelf. Locations of instrument packages deployed are shown in figure 1, along with the concurrent LACSD deployment locations. Two sites previously occupied by USGS in 2004 (Sites B3 and B6) were re-occupied with heavily instrumented BBL tripods to meet the first objective. Site B3 had to be moved into slightly shallower water to 55-m water depth due to depth constraints of the instruments on the large tripod. A similar BBL tripod was deployed near LACSD at Site A5 (near the end of the outfall pipe, occupied by LACSD from 2000 through the measurement program) to fulfill both the first and the second objectives (USGS Site B5). Two low-profile tripods with upward-facing ADCPs were also deployed at Sites B3 and B6 to measure the structure of the BBL currents in the lower 10 m, covering the gap between the ADCP and near-bottom current meters on the large tripods. A small tripod with an ADCP and a near-bottom current meter was deployed in the nearshore region near Portuguese Bend at Site B1. This tripod and another tripod placed halfway between Sites B3 and B1 (Site B2) met the third objective. Thermistor strings at Sites B6 and B7 (formerly occupied by SAIC in 2004) were deployed to meet the fourth measurement objective. Table 1 lists the mooring locations, measurement goals, and deployment dates. Figure 2 shows a diagram of the Geoprobe tripod used and a diagram of the locations of instruments used.

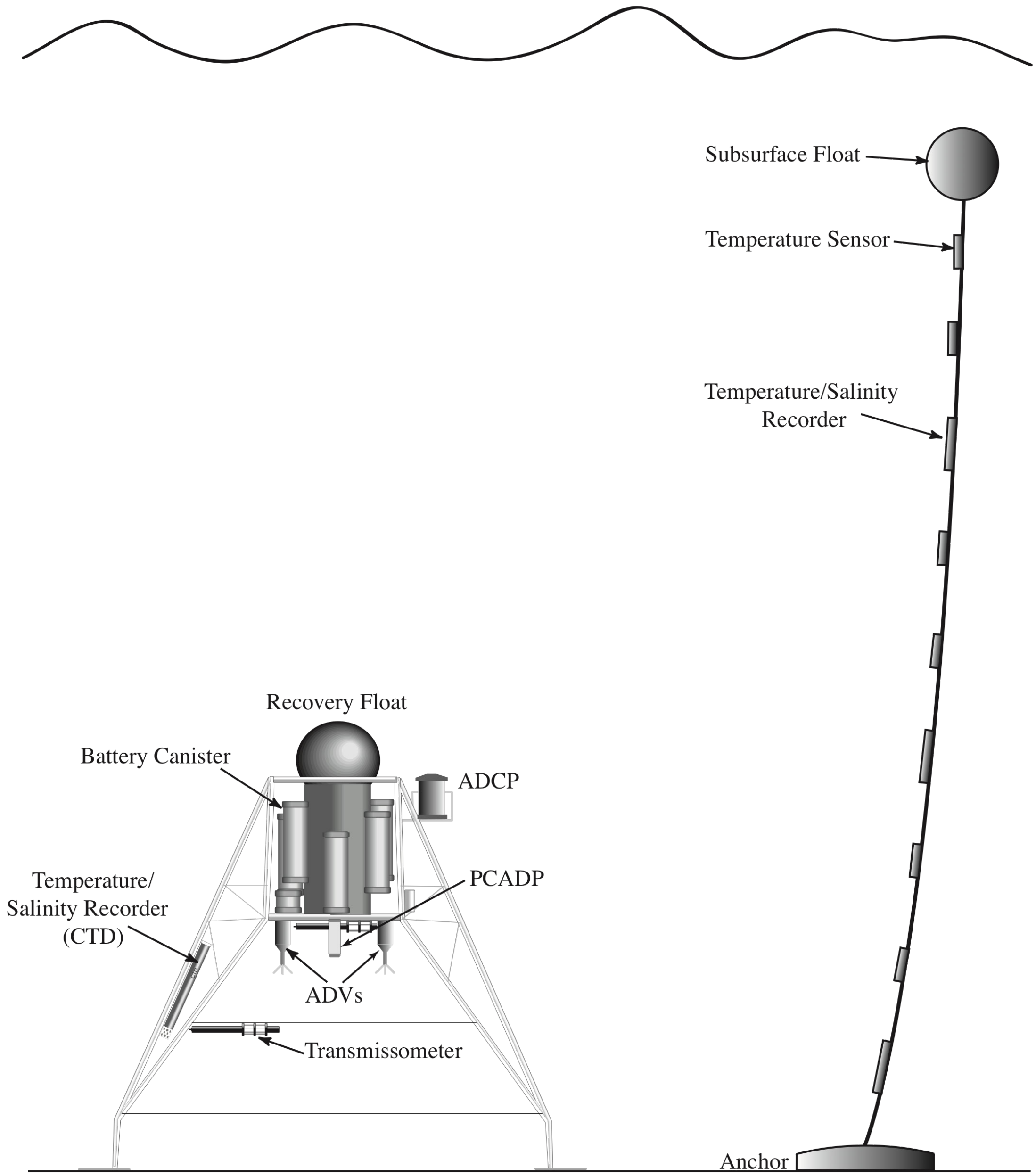


**Figure 2.** Representative diagram of a large tripod and a subsurface mooring used in the Palos Verdes Shelf 2007-2008 measurement program.

Each large BBL tripod housed two near-bottom single-point current meters capable of directional wave measurements, one temperature and salinity (T/S) sensor, two temperature (T) sensors at different depths, three turbidity measurement instruments (either optical backscatter or transmissometer or both; see descriptions below) at different depths to estimate suspended-sediment load, a downward-facing acoustic backscatter profiler (for profiles of turbidity), a downward-facing pulse-coherent current profiler to obtain detailed profiles of currents down to the seabed, and an upward-facing ADCP to obtain profiles of currents from the transducer to the sea surface. The tripods at Sites B3 and B6 had additional optical sensors to measure turbidity. Detailed descriptions of the individual instruments and the sampling schemes utilized are presented in the next section. Table 2 lists the instruments, parameters measured, and measurement depths of each moored platform.

**Table 1.** List of mooring locations, measurement goals, and deployment dates

| Site | Platform | Measurement goal | Latitude (north) | Longitude (west) | Depth (m) | Deployment date and time (PST) |
|---|---|---|---|---|---|---|
| B1 | Small tripod | Near-shore currents, waves and suspended sediment | 33° 43.254′ | 118° 20.681′ | 18.7 | Dec. 5, 2007, 13:10 |
| B2 | Medium tripod | Water column current profile, near-bottom currents and waves | 33° 43.007' | -118° 20.851' | 28.7 | Dec. 4, 2007, 10:21 |
| B3 | Surface buoy | Thermistor string (upper water column) | 33° 42.585′ | 118° 21.208′ | 52 | Dec. 5, 2007, 14:38 |
| B3 | Subsurface mooring | Thermistor string (lower water column) Mid-column suspended sediment | 33° 42.626″ | 118° 21.299″ | 54 | Dec. 5, 2007, 17:28 |
| B3 | Large tripod | Water column current profile, intensive BBL currents, waves and suspended sediment | 33° 42.598″ | 118° 21.250″ | 54 | Dec. 4, 2007, 15:54 |
| B3 | Small tripod | Near-bottom current profile | 33° 42.658″ | 118° 21.378″ | 55.1 | Dec. 5, 2007, 9:54 |
| B5 | Large tripod | Water column current profile, intensive BBL currents, waves and suspended sediment | 33° 41.652″ | 118° 19.793″ | 65 | Dec. 4, 2007, 8:20 |
| B6 | Surface buoy | Meteorological station, thermistor string (upper water column) | 33° 41.070″ | 118° 18.677″ | 57 | Dec. 4, 2007, 12:34 |

**Table 1, cont.**

| | | | | | | |
|---|---|---|---|---|---|---|
| B6 | Subsurface mooring | Thermistor string, (lower water column) Mid-column suspended sediment | 33° 41.062″ | 118° 18.554″ | 57 | Dec. 5, 2007, 19:17 |
| B6 | Large tripod | Water column current profile, intensive BBL currents, waves and suspended sediment | 33° 41.03″ | 118° 18.529″ | 57 | Dec. 4, 2007, 14:10 |
| B6 | Small tripod | Near-bottom current profile | 33° 41.135″ | 118° 18.763″ | 60 | Dec. 5, 2007, 11:54 |
| B7 | Surface buoy | Thermistor string (upper water column) | 33° 41.759″ | 118° 18.258″ | 32.5 | Dec. 5, 2007, 20:20 |
| B7 | Subsurface mooring | Thermistor string (lower water column) Mid-column suspended sediment, waves | 33° 41.740″ | 118° 18.203″ | 32.4 | Dec. 4, 2007, 19:01 |

Subsurface taut-wire moorings supporting vertical arrays of T/S recorders were deployed by the USGS to make time-series measurements of water-column properties at Sites B3, B6, and B7. The arrays at Sites B3 and B6 (deep sites) had T loggers every 5 m from the surface to bottom and T/S recorders approximately every 10 m, while the array at Site B7 had instruments spaced 3 m apart, alternating between T and T/S recorders. These moorings also supported turbidity and T/S sensors mounted approximately 9 mab at Sites B3 and B6 and ~5.5 mab at Site B7. Figure 2 also shows a diagram of a representative subsurface T/S array at Site B6. Because these subsurface arrays did not extend through the entire water column, separate surface buoys were also deployed with a T/S sensor at 5 m below the surface and with T at 10 m. The surface buoy at Site B6 also housed a meteorological station.

Following is a description of each instrument used in the measurement program and the sampling schemes employed to meet measurement objectives. Several of the instruments employed in this program use Doppler shifts of sound reflected from particles in the water to measure velocity. The differences between them are in the use of signal frequency or measurement frequency, and point samples or measurements profiles made at various distances from the transducer.

## Acoustic Doppler Current Profilers (ADCP)

An ADCP estimates current velocity in the water by sending an acoustic pulse into the water column and measuring the Doppler shift of the returned echo, which is reflected back by suspended particulate matter. The instrument can obtain a profile of current velocity by measuring the shift at different time lags, which correspond to different distances away from the instrument.

**Table 2.** Detailed list of instruments deployed, measurement depths, parameters measured, sampling schemes, and dates of data recovery of each moored instrument. Depth is the depth of the instrument in meters below the sea surface for the moorings; in meters above the seabed for the tripods. [CP, current profile; DW, directional wave data; NBC, near-bottom currents; NBCP, near-bottom current profile; NBSSP, near-bottom suspended sediment profile; P, water pressure ; S, salinity;
SS, suspended sediment; T, temperature; W, nondirectional wave data]

| Mooring | Instrument | Depth (meters) | Parameters Measured | Sampling Scheme | Processed File(s) | Date Ranges |
|---|---|---|---|---|---|---|
| **840 - B3 - Surface - 52m** | | | | | | |
| 8401 | MicroCat | 0.58 | T,S | 3 minute | 8401mc.nc | 12/5/07-4/2/08 |
| 8402 | Branker Temp | 5.2 | T | 3 minute | 8402bt.nc | 12/5/07-4/2/08 |
| 8403 | Branker Temp | 10 | T | 3 minute | 8403bt.nc | 12/5/07-3/31/08 |
| **841 - B3 - Subsurface - 54m** | | | | | | |
| 8411 | SeaCat | 14 | T,S | 3 minute | 8411sc.nc | 12/6/07-1/28/08 |
| 8412 | Branker Temp | 19 | T | 3 minute | 8412bt.nc | 12/6/07-4/2/08 |
| 8413 | MicroCat | 24 | T,S | 3 minute | 8413mc.nc | 12/6/07-4/2/08 |
| 8414 | Branker Temp | 29 | T | 3 minute | 8414bt.nc | 12/6/07-4/2/08 |
| 8415 | Branker Temp | 34 | T | 3 minute | 8415bt.nc | 12/6/07-4/2/08 |
| 8416 | MicroCat | 39 | T,S | 3 minute | 8416mc.nc | 12/6/07-4/2/08 |
| 8417 | SeaCat | 44.8 | T,S,SS | 3 minute | 8417sc.nc | 12/6/07-2/13/08 |
| 8418 | SeaCat | 49.7 | T,S | 3 minute | 8418sc.nc | 12/6/07-4/2/08 |
| **842 - B3 - Large Tripod - 54m** | | | | | | |
| 8421 | 300 kHz ADCP | 3.12 | CP,T | 3 minute | 8421wh.nc | 12/4/07-2/29/08 |
| 8422 | Branker Logger | 2.69 | SS | 3 minute | 8422bl-att.nc | 12/4/07-12/26/08 |
| 8423 | MicroCat | 2.63 | T,S | 3 minute | 8423mc.nc | 12/4/07-2/29/08 |
| 8424 | PCADP | 1.05 | NBCP,T,P,S,SS | 17.5min@1Hz/Hr | 8424pc* | 12/3/07-2/29/08 |
| 8425 | ADV | 0.55 | NBC,T,P,SS | 17.5min@10Hz/Hr | 8425adv* | 12/3/07-2/29/08 |
| 8426 | ADV | 0.55 | NBC,T,P,SS | 17.5min@10Hz/Hr | 8426adv* | 12/3/07-2/25/08 |
| 8427 | ABS | 0.99 | NBSSP | 14min@1Hz/Hr | 8427abs* | 12/4/07-2/29/08 |
| 8428 | Branker Temp | 0.44 | T | 3 minute | 8428bt.nc | 12/4/07-2/29/08 |
| **843 - B3 - Small Tripod - 55m** | | | | | | |
| 8431 | 1200 kHz ADCP | 0.8 | NBCP,T | 3 minute | 8431wh.nc | 12/5/07-12/27/08 |

**Table 2, cont.**

| | | | | | | |
|---|---|---|---|---|---|---|
| **844 - B5 - Large Tripod - 65m** | | | | | | |
| 8441 | 300 kHz ADCP | 3.3 | CP,T | 3 minute | 8441wh.nc | 12/4/07-4/2/08 |
| 8442 | MicroCat | 3.1 | T,S | 3 minute | 8442mc.nc | 12/4/07-4/2/08 |
| 8443 | Branker Temp | 1.2 | T | 3 minute | 8443bt.nc | 12/4/07-4/2/08 |
| 8444 | PCADP | 1.04 | NBCP,T,P,S,SS | 17.5min@1Hz/Hr | 8444pc* | 12/4/07-4/4/08 |
| 8445 | ABS | 0.99 | NBSSP | 14min@1Hz/Hr | 8445adv* | 12/4/07-4/2/08 |
| 8446 | ADV | 0.58 | NBC,T,P,SS | 17.5min@10Hz/Hr | 8446adv* | 12/4/07-4/3/08 |
| 8447 | ADV | 0.58 | NBC,T,P,SS | 17.5min@10Hz/Hr | 8447abs* | 12/4/07-4/3/08 |
| 8448 | Branker Temp | 0.4 | T | 3 minute | 8448bt.nc | 12/4/07-4/2/08 |
| **845 - B6 - Surface - 57m** | | | | | | |
| 8451 | Met Station | 3 | Meteorological Data | 5 minute | 8451met.nc | 12/4/07-4/2/08 |
| 8452 | Branker Temp | 5 | T | 3 minute | 8452mc.nc | 12/4/07-3/31/08 |
| 8453 | MicroCat | 10 | T,S | 3 minute | 8453mc.nc | 12/4/07-4/2/08 |
| **846 - B6 - Subsurface - 57m** | | | | | | |
| 8461 | MicroCat | 12 | T,S | 3 minute | 8461mc.nc | 12/6/07-4/2/08 |
| 8462 | SBE-39 | 17 | T,P | 3 minute | 8462pr.nc | 12/6/07-4/2/08 |
| 8463 | MicroCat | 22 | T,S | 3 minute | 8463mc.nc | 12/6/07-4/2/08 |
| 8464 | Branker Temp | 27 | T | 3 minute | 8464bt.nc | 12/6/07-4/2/08 |
| 8465 | Branker Temp | 32 | T | 3 minute | 8465bt.nc | 12/6/07-4/2/08 |
| 8466 | MicroCat | 37 | T,S | 3 minute | 8466mc.nc | 12/6/07-4/2/08 |
| 8467 | Branker Temp | 42 | T | 3 minute | 8467bt.nc | 12/6/07-4/2/08 |
| **847 - B6 - Geoprobe Tripod - 57m** | | | | | | |
| 8471 | 300 kHz ADCP | 3.14 | CP,T | 3 minute | 8471wh.nc | 12/4/07-4/10/08 |
| 8472 | SeaCat | 2.6 | T,S,SS | 3 minute | 8472sc.nc | 12/4/07-3/20/08 |
| 8473 | PCADP | 1.04 | NBCP,T,P,S,SS | 17.5min@1Hz/Hr | 8473pc* | 12/4/07-4/11/08 |
| 8474 | ADV | 74.5 | NBC,T,P,SS | 17.5min@10Hz/Hr | 8474adv* | 12/4/07-4/11/08 |
| 8475 | ADV | 74.5 | NBC,T,P,SS | 17.5min@10Hz/Hr | 8475adv* | 12/4/07-4/11/08 |
| 8477 | Branker Temp | 0.42 | T | 3 minute | 8477bt.nc | 12/4/07-4/10/08 |
| **848 - B6 - Tophat Tripod - 60m** | | | | | | |
| 8481 | 1200 kHz ADCP | 0.7 | NBCP,T | 3 minute | 8481wh.nc | 12/5/07-2/26/08 |
| 8482 | LISST-100 | 0.31 | SS Distribution | 6 minute | 8482lisst.nc | 12/5/07-2/26/08 |

**Table 2, cont.**

| | | | | | | |
|---|---|---|---|---|---|---|
| **849 - B7 - Surface - 32.5m** | | | | | | |
| 8491 | Branker Temp | 3 | T | 3 minute | 8491bt.nc | 12/6/07-4/3/08 |
| 8492 | Branker Temp | 6 | T | 3 minute | 8492bt.nc | 12/6/07-4/3/08 |
| 8493 | Branker Temp | 9 | T | 3 minute | 8493bt.nc | 12/6/07-4/3/08 |
| **850 - B7 - SubSurface - 32.4m** | | | | | | |
| 8501 | MicroCat | 14.4 | T,S | 3 minute | 8501mc.nc | 12/5/07-4/3/08 |
| 8502 | Branker Temp | 17.4 | T | 3 minute | 8502bt.nc | 12/5/07-4/3/08 |
| 8503 | SeaCat | 20.4 | T,S | 3 minute | 8503sc.nc | 12/5/07-4/3/08 |
| 8504 | Branker Temp | 23.4 | T | 3 minute | 8504bt.nc | 12/5/07-4/3/08 |
| 8505 | SeaCat | 27 | T,S,SS | 3 minute | 8505sc.nc | 12/5/07-3/30/08 |
| 8506 | Branker Temp | 29.9 | T | 3 minute | 8506bt.nc | 12/5/07-4/3/08 |
| 8507 | Seagauge | 31.9 | T,P,W | 3 minute | 8507sg-tid.nc | 12/5/07-4/3/08 |
| **851 - B1 - Small Tripod - 18.7m** | | | | | | |
| 8511 | 600 kHz ADCP | 0.78 | CP,T,DW | 3 minute-2hr waves | 8511wh.nc | 12/5/07-4/29/08 |
| 8512 | Aquadopp | 0.8 | NBC,T,P,SS | 3 minute | 8512aq.nc | 12/5/07-4/10/08 |
| 8513 | Branker Temp | 0.62 | T | 3 minute | 8513bt.nc | 12/5/07-3/31/08 |
| **852 - B2 - Medium Tripod - 28.7m** | | | | | | |
| 8521 | 600 kHz ADCP | *2.07* | CP,T,DW | 3 minute-2hr waves | 8521wh.nc | 12/4/07-4/2/08 |
| 8522 | SeaCat | 1.48 | T,S | 3 minute | 8522sc.nc | 12/4/07-4/2/08 |
| 8523 | ADV | 0.92 | NBC,T,P,SS | 17.5min@10Hz/Hr | 8523adv* | 12/5/07-3/30/08 |

* Multiple files per instrument

One RDI Workhorse 300-KHz ADCP was mounted on each large tripod on the outer continental shelf and oriented so that the beams were facing upward to obtain current profiles of the entire water column. The transducer head on the tripod at Site B3 was mounted 3.11 mab and was configured to obtain profiles of currents in 27 bins 2 m in length that were centered at elevations ranging from 7.29 to 59.29 mab. The transducer head on the tripod at Site B5 was mounted 3.3 mab and was configured to measure velocities in 30 2-m bins at elevations ranging from 7.47 to 65.47 mab. The transducer head on the tripod at Site B6 was mounted 3.14 mab and was configured to measure velocities in 29 bins 2 m in length at elevations ranging from 4.17 to 60.17 mab. Each instrument used 60 pings per ensemble to calculate an average velocity measurement every 3 mi.

The small tripods at Sites B3 and B6 housed 1,200-kHz ADCPs set to record current profiles of the BBL in 0.25-m vertical bins, from 1.36 to 14.1 mab. The tripod at Site B2 housed a 600-kHz ADCP, mounted 2.07 mab, which measured current profiles at 3-min intervals in 1-m vertical bins from 4.17 to 29.17 mab. The small tripod at Site B1 housed a 600-kHz ADCP, mounted 0.78 mab, which measured current profiles at 3-min intervals, in 1-m vertical bins from 2.88 to 18.88 mab. The latter two instruments also measured directional wave parameters at the site at 2-hr intervals.

### Acoustic Doppler Velocimeters (ADV)

An ADV measures current speed and direction at a single point in a small sampling volume using the Doppler principle to calculate velocity along three axes.

Two models manufactured by Sontek/YSI, Inc., were used in this experiment: the field version (ADVF) and the ocean version (ADVO). The ADVF operates with a sound frequency of 10 MHz and measures velocities in a sample volume of about 0.3 $cm^3$ located ~5 cm from the acoustic transmitter. The ADVF transducers are smaller and separated from the signal conditioning electronics module by a 30-cm-long rod. ADVFs can sample at rates up to 40 Hz. The ADVO is a more rugged instrument with larger transducers mounted closer to the signal conditioning model. ADVOs operate at lower sound frequencies (5 mHz) and measure velocities in a larger sample volume (2 $cm^3$) located ~18 cm from the acoustic transmitter. The data from either model is logged using the Sontek Hydra data logger. The Hydra can also log data from Seabird MicroCAT conductivity and temperature (CT) sensors, pressure measurements from external pressure sensors like the Paroscientific Digiquartz sensor, and analog data from a wide range of sensors that produce 0–5 V or 0–10 V output. Each instrument recorded data from two external optical channels, a transmissometer, and an optical backscatter sensor (OBS) (with the exception of one ADV at Site B5 that only recorded one OBS). The Hydra can also be cabled with another Hydra or other instrument and either provide or receive an electronic signal to initiate synchronous measurements.

The purpose of having paired ADV current meters on each tripod is to be able to extract information about the turbulence in the BBL that is not associated with surface gravity wave-driven flow. Hence, the paired ADV sensors on each tripod were set to sample at the same height. The sampling height for a given tripod was determined by the horizontal separation between sensors, with the height itself a function of how the tripod is constructed. The ADVs were set to sample at 0.45 mab at Site B3, 0.4 mab at Site B5, and 0.57 mab at Site B6. All were set to measure high-frequency current and pressure information at 10 Hz for a 17.5-min period, once every hour, resulting in 10,500 samples per hour.

### Pulse-Coherent Acoustic Doppler Profilers (PCADP)

The Sontek PCADP makes higher frequency measurements than the ACDP and has the capability to make higher resolution measurements (in smaller bins) along the profile, but it is limited by a shorter overall range.

Each PCADP was set to record data at 1 Hz for a 17.5-min period, once every hour, with 6 vertical bins 0.125 cm in length, including a blanking distance of 0.3 m.

### Single-Point Acoustic Doppler Current Meter (AQD)

A Nortek Aquadopp single-point acoustic Doppler current meter was deployed on the small tripod at Site B1 and averaged current measurements over a 1.5-min period every 3 min at a single-point 0.8 mab. In addition, the instrument logged optical backscatter data from a Campbell Scientific OBS3 sensor on the same time interval as the current data. The instrument successfully recorded current data for 128 days.

### Optical Backscatter Sensors (OBS)

An OBS measures turbidity by sending a beam of infrared light into the water and then measuring the quantity of light that is reflected back to its sensor from suspended particles. Suspended-sediment concentration can then be determined by calibrating the sensors with in situ sediment in the laboratory.

Each large tripod had OBS sensors at approximately 0.4 mab, 0.6 mab, and 1 mab. The medium tripod at Site B2 had an OBS sensor at 0.42 mab, and the small tripod inshore at B1 had an OBS sensor at 0.6 mab.

### Transmissometers

A transmissometer measures the transmission of red collimated light (650 nm wavelength) from an LED along a fixed path through the water. Transmissometer data can either be represented as a percent light transmission (from 0 to 100, where 0 is completely occluded), or as 1/m (utilizing another linear conversion). The advantage of presenting the data as 1/m is that values increase as the suspended load increases. The usage of 1/m accounts for the path length of the instrument, thus making measurements from instruments of two different path lengths comparable.

All BBL transmissometer data were recorded by a Hydra data logger associated with an ADV or PCADP, except for the uppermost instruments on tripods at Sites B3 and B6, which were logged by a Brancker logger and a Seabird SeaCAT, respectively. Each large tripod had transmissometers at approximately 1 mab and 2.7 mab. The tripods at Sites B3 and B6 had additional sensors at ~0.4 mab and 1.7 mab. There were transmissometers on each subsurface array placed at 9 mab at Sites B3 and B6 (deep sites) and 5 mab at Site B7. Those data were logged by a SeaCAT CT logger. Each transmissometer was sampled at the native rate of the ADV, PCADP, or SeaCAT to which it was connected.

### Acoustic Backscatter Sensors (ABS)

The ABS is used to estimate concentrations of suspended particulate matter over short distances (~1-m-long profiles, usually oriented vertically in the BBL). The ABS emits pulses of high-frequency sound (typically 1 to 5 mHz) and records the reflected sound as a function of time, which can be converted to range using the speed of sound in water. Under ideal conditions, the ABS can be calibrated to convert backscattered acoustic intensity to estimates of suspended-sediment concentrations.

Each ABS instrument was set to record profiles of acoustic backscatter at 64 Hz, averaging 1 Hz per profile and recording 840 profiles per burst once every hour. Each profile consisted of 256 vertical bins, 5 mm in length.

### Conductivity-Temperature (CT) Recorders

CT recorders measure water temperature and conductivity at the sensor location and record the values at specified intervals. From these measurements, salinity can be calculated using the 1978 Practical Salinity Scale at http://www.seabird.com/application_notes/AN14.htm (IEEE, 1980).

Each large tripod had a Seabird Electronics T/S logger (either an SBE-37 MicroCAT or a SBE-16 SeaCAT) with sensors mounted at approximately 3 mab; in addition, the tripods at Sites B3 and B6 had a MicroCAT at 1.2 mab. The medium tripod at Site B2 had a SeaCAT at 1.48 mab.

Each shelf-break subsurface mooring had alternating T/S and T loggers spaced 5 m apart, and the subsurface mooring at Site B7 had alternating sensors 3 m apart. Each surface mooring had T/S loggers at 5-m depth and T loggers at 10-m depth to complete the water-column thermistor string.

### Temperature Loggers

A temperature logger measures temperature with a thermistor and records the data at programmed intervals. In this study, they were deployed to observe changes in profiles of water temperature associated with stratification and internal waves and tides. We deployed high accuracy (±0.002°C) fast-response RBR Ltd. Model TR-1050 oceanographic temperature loggers (Brancker loggers) on the subsurface moorings. The Brancker loggers were mounted every 5 or 10 m, interspersed with the MicroCATs.

### Laser In-situ Scattering and Transmissometry (LISST)

The LISST is an optical oceanographic instrument that is capable of making estimates of the suspended particulate size distribution (PSD) by measuring the diffraction of light through the water at multiple angles. From the PSD, one can estimate the total suspended solids concentration in the water at the sampling level.

We deployed a LISST-100X, type C, on the small tripod at Site B6, 0.31 mab, with a particle size range of 2.5 to 500 mm.

## Data Processing

### Data File Identifiers

A three-digit mooring identification number (mooring ID) is assigned to each mooring or tripod and is used to identify all files containing time-series data recorded by instruments mounted on that platform. The mooring ID is the key to identifying and (or) locating data records in the USGS Woods Hole Science Center (WHSC) time-series data management system

(Montgomery and others, 2007). Individual data files are labeled by four-digit numbers. The first three digits are the mooring ID and a fourth digit is assigned to individual data loggers on the mooring, usually numbered according to the vertical position on the mooring or tripod. For example, 5541 identifies the topmost instrument on mooring 554, 5542 the next instrument down on mooring 554, and so on. As data files are processed, additional identifiers are added to the four-digit identifier to indicate sensors, processing steps, and averaging. Table 3 summarizes the file-naming system.

Raw data files downloaded from each instrument were translated from the manufacturer-specific data format into the netCDF data-file format using toolboxes developed in Matlab software, specific to each instrument. The netCDF data file format, developed by the Unidata Corporation (http://www.unidata.ucar.edu/software/netcdf/), is a compact binary format compatible with most computer systems, that stores both the data and the metadata in the file. USGS uses the EPIC conventions (http://www.epic.noaa.gov/epic/document/convention.htm) for organizing and naming oceanographic data variables. These data were processed using quality-control procedures developed for all WHSC oceanographic data. Files generated during the first processing step (which involved conversion to engineering units and quality assurance calculations) were stored in netCDF format with .cdf suffixes. Final versions (after application of calibration coefficients, coordinate transformations, rotation to geographic coordinates, and averaging of good data) were stored in netCDF format with .nc extensions. All of the final statistics data are in EPIC-compliant netCDF format. Burst-data files are also in netCDF format, but are not EPIC-compliant, because they use an added dimension (sample number) not used by the EPIC convention.

**Table 3.** Summary of USGS netCDF file-naming conventions.

| USGS Mooring ID | Instrument Identifier | Sampling Scheme (optional) | Data Type (optional) | Version | File Extension | |
|---|---|---|---|---|---|---|
| USGS Mooring ID | First three digits identify mooring number. Fourth digit identifies datalogger location on the tripod. | | | | | |
| | mc | MicroCat temperature and salinity data | | | | |
| | adc | ADCP water flow data | | | | |
| | adv | ADV and accessory sensor data | | | | |
| | pca | PCADP and accessory sensor data | | | | |
| | abs | ABS statistics data | | | | |
| | bt | Brancker temperature data | | | | |
| | sc | Seacat temperature and salinity data | | | | |
| | att | Transmissometer data | | | | |
| | | 1 | First sampling scheme when multiple schemes are used | | | |
| | | 2 | Second sampling scheme when multiple scheme are used | | | |
| | | | b | Burst data for instruments with burst and statistics files | | |
| | | | q | Quality data for instruments with flagging recorded in separate files | | |
| | | | | -a | USGS best basic version | |
| | | | | | .nc | netCDF file extension |

**Example file names**

7582adv2b-a.nc

| Mooring ID | Instrument Identifier | Sampling Scheme (optional) | Data Type (optional) | Version | File Extension |
|---|---|---|---|---|---|
| 7582 | adv | 2 | b | -a | .nc |

7594mc-a.nc

| Mooring ID | Instrument Identifier | Sampling Scheme (optional) | Data Type (optional) | Version | File Extension |
|---|---|---|---|---|---|
| 7594 | mc | | | -a | .nc |

## Time

Times are reported in Universal Time (UT, equivalent to Greenwich Mean Time (GMT)). We checked for drift of instrument clocks by comparing instrument times with accurate times (from the GPS or clocks synchronized with the National Institute of Standards and Technology in Boulder, Colorado: http://tf.nist.gov/) before and after deployments. The observed offsets were small compared to the sample intervals (typically ~10 sec), so we did not adjust any instrument times in this data set.

Time is recorded in the netCDF files as two variables named time1 and time2 in compliance with EPIC standards to allow precise storage of time in integer format. Time1 is the Julian day, where midnight on May 23, 1968 = 2,440,000 and time2 is the elapsed time on that day, in milliseconds since midnight. Thus, time in Julian days is computed as time1+time2/(1,000 x 3,600 x 24).

## Current Meter Data

### Instrument Orientations

Each of the ADVs, PCADPs, and ADCPs had internally mounted flux-gate compasses. These were calibrated prior to deployment according to manufacturer's recommendations. Raw ADCP data were recorded in beam coordinates. Data from the ADVs were recorded in instrument coordinates (referred to as x, y, z coordinates here) and later rotated into geographic coordinates using burst-median values for heading, pitch, and roll. Data from the PCADP were recorded in beam coordinates and converted to geographic coordinates using burst-median heading, pitch, and roll values after correcting for velocity ambiguities.

All data were rotated to true geographic coordinates (positive toward east, north, and up) using instrument compasses and tilt sensors and correcting for local magnetic variation (13.8º E.).

For some of the results and discussions, we have rotated the horizontal components into alongshore and cross-shelf coordinates, with the positive alongshore axis oriented toward 300º true. Flow in the positive alongshore direction (toward Santa Monica Bay) is described as upcoast or poleward, whereas flow in the negative alongshore direction (toward San Diego) is described as downcoast or equatorward.

### Acoustic Doppler Current Meter (ADCP) Data

ADCP data were processed according to standard USGS procedures using ADCP Tools, a collection of Matlab routines written to read in and process raw ADCP data and create netCDF files of the raw and processed data. The toolbox is described by Côté and others (2000). Raw data files from the ADCPs were converted to netCDF format and checked for clock accuracy by comparing in and out-of-water times to the mooring log and checking for linear time progression. Data were despiked, with gaps replacing bad data points. We compared the clock, ADCP calibrations, and internal compass to nearby instruments for consistency. We compared data from the four beams in pairs for symmetry and checked for high-intensity reflection indicative of fish or other beam obstructions. Bad values were masked both manually and automatically and, where possible, a three-beam solution was used to fill in gaps caused by one compromised beam. Data above the water surface were masked; because the water depth at the site varies with the stage of the tide, there are periods when some bins above the water surface are retained within the file. We trimmed off data collected before the instrument was on bottom or after recovery. Finally, we rotated the data from beam coordinates into geographic coordinates. The final processed versions of these data were stored in EPIC-compliant format.

### Acoustic Doppler Velocimeter (ADV) Data

The ADVs were set to record velocities in instrument coordinates, which were rotated into Earth coordinates using data from the internal compass and tilt sensor. In addition to velocities, the ADV-logged data on the amplitude and correlation of the return signal, sound speed, range to boundary, compass and tilt, pressure (from an external Paroscientific Digiquartz pressure gauge connected to the ADV), and the external optical sensors. Data from each ADV (and the attached external sensors) was logged by an individual Sontek Hydra data logger and stored in binary format. The data in these files was processed using a series of Matlab routines in the Hydratools toolbox developed at USGS (Martini and others, 2005).

### Pulse-Coherent Acoustic Doppler Profiler (PCADP) Data

The processing of PCADP data is very similar to that of the ADV. The PCADP was also set to record velocities in instrument coordinates at several depths, amplitude, correlation, sound speed, and range to boundary. An internal compass recorded heading, pitch and roll, and pressure was recorded by an external Paros pressure gauge connected to the instrument. The PCADP stores data in a binary file, which was processed directly using the Hydratools toolbox.

## Optical Backscatter Sensor (OBS) Data

The Sontek Hydra data logger converts raw OBS voltage measurements to counts with a 14-bit analog-digital converter. We converted counts back to volts (a linear conversion) in our processing so that the data can be calibrated to sediment concentration using laboratory-derived calibration coefficients. The data are available in the .nc file for the instrument to which the OBS was connected (ADV or PCADP).

## Transmissometer Data

The Sontek Hydra data logger also logs transmissometer data in counts (in the raw data and .cdf files); a linear conversion is necessary to convert counts to volts. The Seabird SeaCAT and the RBR Brancker loggers, however, log the raw voltage. The transmissometer data can be presented either as percentage of light transmission (from 0 to 100, the former being completely occluded) or in terms of 1/m (utilizing another linear conversion). The advantage of presenting the data as 1/m is that values increase as the suspended load increases. The final data are available in the .nc file for the instrument with which the transmissometer was deployed (ADV, PCADP, or Seacat).

## Acoustic Backscatter Sensor (ABS) Data

We processed the raw binary ABS data with a Matlab-based toolbox that transformed the data to netCDF format, truncated files to include in-water times only, and flagged bad points. The ABS data were not subject to the normal conversion to scientific units and quality-control procedures, because calibration protocols are not in place. Thus it is preferable to retain all data rather than to potentially remove useful data.

### MicroCAT (MC) Data

We used software provided by SeaBird Electronics to convert the time series of raw conductivity measurements recorded by the MicroCATs into salinity. We also used the SeaBird software to calculate water density from the temperature and salinity measurements. The data were converted to ASCII format and then translated to netCDF. We verified clock accuracy by comparing in- and out-of-water times to the mooring log and noting that there was a linear time progression. Data were despiked and gaps were filled by interpolation where possible. The clock and calibrations were compared to nearby instruments for consistency. Processed versions of these data files are available in EPIC-compliant netCDF format.

### Meteorological Data

#### Site B6 Buoy Data

Meteorological data were recorded by an Airmar PB-100 meteorological sensor, logged by a USGS data logger custom designed for this sensor. The data received included wind speed and direction, air temperature, and atmospheric pressure. Data were logged at 1-sec intervals and averaged to a 5-min interval to remove variability associated with buoy motion. Atmospheric pressure data can be interpolated to hourly values and subtracted from the bottom pressure data to correct these measurements for changes in atmospheric pressure (Hasselmann and others, 1973).

#### NODC Buoy Data

Time series of wind speed, wind direction, atmospheric pressure, wave height, wave period, one-dimensional wave spectra, and other parameters were obtained from measurements taken at National Oceanographic Data Center (NODC) Buoy 46025, located at lat 33.745° N., and long 119.084° W., about 60 km west of the study area in 860-m water depth.

Meteorological and wave parameters from NODC Buoy 46025 are plotted in figure 3. Additional directional wave information was available from NODC Buoy 46222 on the edge of the San Pedro Shelf in 457-m water depth.

## Results

### Data QA/QC

All data are reviewed by senior oceanographers for completeness and quality in addition to automated Quality Assurance/Quality Control (QA/QC) procedures run in processing to netCDF. Data points flagged by automated procedures or USGS personnel are given fill values to retain a consistent time base. Because each current meter has its own internal compass to reference the current data to Earth coordinates, it is necessary to compare results from all instruments deployed at one site to ensure the data are consistent. A detailed examination of the current meter data that focuses on simultaneous measurements collected in the BBL suggests that the current measurements were internally consistent at all sites (appendix A).

### Online Data Access

Data used in this report is accessible via the Internet at *http://stellwagen.er.usgs.gov/pv_shelf07.html*. The EPIC-compliant netCDF files may be downloaded from the catalog displayed by the "Basic Sampling Interval" link at the bottom left of the page. The data may also be accessed directly via OPeNDAP server (*http://opendap.org*), where the URLs to use this data take the form *http://stellwagen.er.usgs.gov/opendap/PV_SHELF07//filename.nc/*. Information about the USGS Oceanographic Time-Series Management Database is provided in Montgomery and others (2007).

## Data Recovery

Data return from moored or tripod-mounted instruments on the Palos Verdes Shelf is summarized in table 2. This table also presents a detailed list of the instrument sensor depths (or heights), the various sampling schemes, and the filenames. Data recovery for each platform by general data type is also plotted in figure 4. There were particular difficulties with the Acoustic Backscatter Sensor Systems (ABSS), which is described in a separate section. Following is an overview of the data return and basic time-series plots according to platform.

### B1 Bottom Tripod—Near-bottom Currents and Suspended Sediment

The B1 bottom tripod was deployed in the shallowest water depth of 18.7 m. Complete records of current profile, waves (146 days), and near-bottom currents and suspended sediment (127 days) were acquired at this site. Fouling of the pressure sensor on the ADCP caused a significant drift in the pressure signal over the course of the deployment; however, good water-level data were recovered from the single-point current meter. Along- and cross-shore velocities at several depths from the ADCP and the near-bottom current meter at the basic time-step are plotted in figure 5. Directional wave parameters, determined by the RD Instruments processing software Wavesmon, are plotted in figure 6.

### B2 Bottom Tripod—Near-bottom Currents and Suspended Sediment

The B2 bottom tripod successfully collected 120 days of high-resolution data on the water-column currents and waves, near-bottom currents, and sediment resuspension. Along- and cross-shore velocities at several depths from the ADCP and the near-bottom current meter at the basic time-step are plotted in figure 7, and near-bottom temperature and suspended solids from the near-bottom current meter are plotted in figure 8. Directional wave parameters, determined by the RD Instruments processing software Wavesmon, are plotted in figure 9.

### B3 Large Bottom Tripod—Near-bottom Currents and Suspended Sediment

As mentioned previously, the tripod at Site B3 had to be recovered early and, therefore, recorded only 87 days of data. All instruments operated as expected and a full record of high-resolution data on the water-column currents, near-bottom currents, and sediment resuspension was acquired from multiple sensor packages. The overlap of near-bottom current data collected at the same depth by the PCADP and ADV allow for checks on instrument performance and data quality (appendix A). Along- and cross-shore velocities at several depths from the ADCP and the near-bottom current meters at the basic time step are plotted in figure 10. Near-bottom orbital wave velocity, temperature, salinity, and suspended solids from the near-bottom current meters and T/S recorders are plotted in figure 11.

### B3 Small Bottom Tripod—Bottom Boundary Layer Current Profile

The small tripod at Site B3 with an upward-facing 1,200-kHz ADCP had a broken leg upon recovery and the backup surface pickup float attached to the tripod frame was missing. It appeared that a vessel hit the surface pickup float, dragging the tripod and resulting in a broken tripod leg. The excessive tilt and roll due to the broken leg after being hit prevented the ADCP from accurately measuring currents. Thus, we only have a 22-day record with quality data. Although the data after the event looked reasonable upon initial examination, a plot of the principal component ellipses of the low-pass filtered data from this instrument combined with similar data from the upward-looking 300-kHz ADCP on the large tripod show that the excessive tilt and roll of the platform rendered the velocity data unusable. Plots of the along- and cross-shore velocities at several depths from the ADCP and a near-bottom current meter on the nearby large tripod at the basic time step show the data from this instrument to be of good quality (fig. 12).

### B3 Subsurface Taut-wire Mooring—Temperature and Salinity Profile

We obtained a complete record (118 days) of temperature and salinity from most of the instruments on the subsurface mooring at Site B3 in water depths from 14 m to 50 m, except the top T/S logger (53 days) and the lower T/S logger, which were also logging a transmissometer measuring suspended sediment at 9 mab (69 days). Raw and contoured low-pass filtered data from this mooring and the surface mooring (described below) are plotted in figures 13–15.

### B3 Surface Buoy

The surface buoy at Site B3 served as a guard buoy and supported three subsurface instruments—a MicroCAT at 1-m depth and Brancker temperature recorders at 5-m depth and 10-m depth. All three instruments acquired a complete record of 119 days.

### B5 Large Tripod—Near-bottom Currents and Suspended Sediment

The large tripod at Site B5 was deployed for 120 days, and most instruments operated as expected. A full record of high-resolution data on the water-column currents, near-bottom currents, and sediment resuspension was obtained from multiple sensor packages. The redundancy of near-bottom current data recorded by the PCADP and ADV allows for checks on instrument performance and data quality. Along- and cross-shore velocities at several depths from the ADCP and the near-bottom current meters at the basic time step are plotted in figure 16. Wave orbital velocities, temperature salinity, and suspended solids from the near-bottom instruments are plotted in figure 17.

### B6 Large Tripod—Near-bottom Currents and Suspended Sediment

As mentioned previously, the tripod at B6 had to be recovered by ROV and, therefore, recorded longer than planned. All instruments operated as expected (with the exception of the ABS, described below) and a full record of high-resolution data on the water-column currents, near-bottom currents, and sediment resuspension was collected from multiple sensor packages. The redundancy of near-bottom current data from the PCADP and ADV allow for checks on instrument performance and data quality. Along- and cross-shore velocities at several depths from the ADCP and the near-bottom current meters at the basic time step are plotted in figure 18.

Wave orbital velocities, temperature salinity, and suspended solids from the near-bottom instruments are plotted in figure 19.

### B6 Small Tripod—Bottom Boundary Layer Current Profile

It was necessary to use the backup recovery float to recover the small tripod at Site B6 with an upward-facing 1,200-kHz ADCP, because the primary recovery system did not return a pickup float. The tripod appeared to be upside down, because there was mud on the top of the tripod upon recovery. We suspect that a vessel hit and dragged the backup pickup float for this tripod, thereby dragging and flipping the tripod. The pitch-and-roll data from the ADCP showed that the tripod was flipped over on February 26, 2008, consistent with this scenario. Thus, there were 83 days of good data on the vertical profile of BBL currents at this site. Along- and cross-shore velocities at several depths from the ADCP and the near-bottom current meter on the adjacent tripod at the basic time step are plotted in figure 20.

### B6 Subsurface Taut-wire Mooring—Temperature and Salinity Profile

A complete record of temperature and salinity was obtained by the subsurface taut-wire mooring at Site B6 from 14-m to 42-m water depth (118 days). There were two additional Seabird SeaCAT T/S loggers at the bottom of the T/S string from which no data was recovered. One instrument failed to start recording; the second had communications problems and technicians were unable to recover data from the instrument. Two instruments were found to have slipped downwire from their initial positions upon recovery (8462 pr and 8464 bt). We were able to determine at what point during the deployment they slipped, and we cropped the data after this point. Raw and contoured low-pass filtered data from this mooring and the surface mooring (described below) are plotted in figures 21 to 23.

### B6 Surface Buoy

The surface buoy at Site B6 served as a guard buoy and supported a meteorological package and two subsurface instruments: a Brancker temperature recorder at 5-m water depth and a MicroCAT at 10-m water depth. The meteorological data include windspeed and direction, air temperature, and barometric pressure. All three instrument packages recorded data for the full deployment (120 days). Data from the meteorological station are plotted in figure 24.

### B7 Subsurface Taut-wire Mooring—Temperature and Salinity Profile

A complete record of 120 days of temperature and salinity was obtained by the subsurface taut-wire mooring at Site B7 from 14.4-m to 32-m water depth. In addition, there was a Seabird SBE-26 wave gauge at the bottom of the T/S string that recorded nondirectional wave parameters at 1-hr intervals for the full deployment. Raw and contoured low-pass filtered data from this mooring and the surface mooring (described below) are plotted in figures 25 to 27.

### B7 Surface Buoy

The surface buoy at Site B7 served as a guard buoy for the subsurface array and housed and supported three subsurface instruments: Brancker temperature recorders at 5.5-m, 8.5-m, and 11.5-m water depth. All three temperature loggers recorded data for the full deployment (119 days).

### ABSS

Data from the Aquatec acoustic backscatter systems (ABSS) were problematic. The systems were sent to the manufacturer for upgrades and then put through basic tank tests to ensure all channels were operational prior to deployment. Two systems had unusually low amplitudes in several channels upon retrieval. Subsequent tank tests with sediment showed similar results, and it was clear that there were wiring problems. Further diagnostics showed that the wiring for two of the channels on these two systems had been inadvertently swapped upon upgrade. Hence, the electronics board was receiving the incorrect pulse information for that frequency transducer. The data from these channels were not usable because they could not be corrected with post-processing procedures.

The system on the tripod at Site B5 had the correct wiring and recorded a full record of quality BBL suspended-sediment profiles. The system at Site B3 recorded quality data on the 2.5-mHz channel. The system at Site B6 did not record any quality data.

# Data Analyses

This section describes the quality of data collected in this program via combined analyses of data from various instruments and sources.

## Current Meter Data

### Tidal Currents

Harmonic tidal analysis was performed on the current data from each site with CMGTooL (Xu and others, 2002). This toolbox uses a slight modification of the TTIDE harmonic analysis routines (Pawlowicz and others, 2002) that are based on the Foreman (1977, 1978) procedures. We present analyses of the four major tidal constituents for this region of the California coast: the principal lunar semidiurnal ($M_2$; period of 12.42 h), principal solar semidiurnal ($S_2$; period of 12.00 h), lunisolar diurnal ($K_1$; period of 23.93 h), and principal solar diurnal ($O_1$; period of 25.82 h) constituents. It should be noted that these analyses were performed on the full-data record logged by each individual instrument; hence, some instruments such as the BBL ADCP at Site B3 had considerably shorter records than corresponding instruments at the site. The complete set of tidal analysis tables for each current meter at each depth level are presented in appendix B (tables B-1 to B-28). A comparison of the tidal currents from depth-averaged (barotropic) records and from all instruments on comparable timescales is presented here.

The barotropic tidal ellipses for the four major constituents at each site from the ADCP data and the corresponding LACSD data are plotted in figures 28 to 31. The $M_2$ semidiurnal tide is the largest constituent at the southeastern end of the shelf, whereas the principal lunisolar diurnal $K_1$ is more dominant on the northwestern end of the shelf. Both semidiurnal tides are oriented more across-shelf than are the diurnal tidal currents (figs. 28–31). This may be because the semidiurnal internal tides, which tend to be oriented mostly across- rather than along-shelf, are folded into and corrupt the barotropic signal, as has been previously noted on the Palos Verdes Shelf (Noble and others, 2003). There is good agreement in all constituents between the USGS ADCP at Site B5 and the LACSD ADCP at Site A5 for this deployment period, suggesting that the tidal-current characteristics do not change significantly over these small spatial scales. A comparison of the data showing $M_2$ characteristics from this deployment to the long-term LACSD data (2-yr record) reveals that the sites at the lower end of the shelf (A5 and B5) have tidal ellipses that are oriented slightly more offshore than the data from the long-term deployment shows (fig. 32). Also, the long-term results tend to average out the periodic internal tidal currents, which are usually oriented more perpendicular to the isobaths (Noble and others, 2002).

A look at the vertical structure of the tidal currents also demonstrates the variability along and across the shelf (figs. 33–37). In these figures, the time series from various instruments at a given site have been cropped to the timeframe of that instrument to create the shortest record for comparison purposes. As noted by Noble and others (2008), the determination of tidal parameters from current-meter records is highly dependent upon the length of the time series. Thus, the tidal parameters presented in these plots do not necessarily represent the long-term tidal characteristics, nor do they precisely match those presented in appendix B (tables 1–28). Along the 60-m isobath from Sites B3 to B6, $M_2$ amplitudes increase and $K_1$ amplitudes decrease, similar to the spatial patterns for tides in the long-term record (Noble and others, 2008). A bulge is noted in the amplitude of the $M_2$ tide near the seabed; the height of this bulge varies with site. At Sites B3 and B6 it is noted at approximately 5 mab, whereas at Site B5 it is higher in the water column at 20 mab. We do not have the high-resolution data for the bottom 10 m at Site B5, however, and while the profile appears to taper off below 10 mab, it is possible that we simply did not observe it here. No bulge in the tidal-amplitude profiles was observed inshore at Sites B1 and B2. A similar plot of the profile of tidal parameters from the long-term data at LACSD Site A5 (fig. 38) shows no bulge in the semidiurnal constituents either, suggesting that the observed bulges at Sites B3, B5, and B6 are due to the intensification of BBL flow from internal tidal bores.

Profiles of major axis orientation also vary according to site. Inshore at Sites B1 and B2, there is significant rotation of the semidiurnal constituents in the bottom 10 m (as much as 80° of rotation counterclockwise), causing the tidal ellipse orientations to become primarily cross-shelf. The orientations of the diurnal tidal ellipses are relatively constant with depth. Semidiurnal tidal ellipses at Sites B3 and B6 also rotate cross-shelf more in the bottom 10 m, albeit at only 20° counterclockwise, whereas Site B5 shows a flatter profile. The diurnal constituents rotate clockwise in the bottom 15 m at Site B3.

### Subtidal Flow

We used principal components analysis of the low-pass filtered vector-current data to assess the reliability of data obtained in this measurement program and to place these data in perspective of the long-term trends on the Palos Verdes Shelf. A 33-hr-cosine tapered low-pass filter was used to remove any fluctuations at timescales on the order of the tides or higher. Figure 39 depicts the principal component ellipses of subtidal data acquired by USGS and LACSD for the 2007 to 2008 field program on the Palos Verdes Shelf. The blue and red ellipses depict the data acquired by ADCPs in the near-bottom (bottom-most bin for that site) and near-surface layers (uppermost bin), respectively. The blue ellipses represent data from near-bottom ADVs, and the red ellipses represent data from near-bottom PCADPs at concurrent depth levels with the

ADVs. Similarly, the principal component ellipses from the 2007 measurement program were plotted against long-term data (2001–2003) from the LACSD array (fig. 40).

The characteristics of the subtidal ellipses show that the low-pass filtered flow from USGS 2007 data is congruent with the LACSD 2007 data and that this deployment period data displayed similar characteristics to the long-term data from the shelf. There is a slight discrepancy between the orientation of ellipses from near-surface data at USGS Site B5 and LACSD Site A5. This is not surprising, however, as the USGS data extended slightly farther into the water column than that of LACSD (that is, the top bin of the USGS ADCP was shallower). The subtidal ellipses suggest that the near-bottom currents tend to flow along-isobath, whereas the near-surface currents tend to follow the general trend of the coastline.

We examined the low-frequency flow vertically at each site by plotting vectors of the time-series data at several depth levels, then rotating them into alongshore coordinates using a static rotation angle of 60° (figs. 41–45). In general, the low-frequency flow is strongest near the surface and oriented primarily alongshore. The near-surface layers flow both upcoast and downcoast, while the near-bottom currents flow primarily upcoast, or poleward, as noted in previous studies (SAIC, 2004). Currents at Sites B3 and B5 exhibit more downcoast flow in the near-bottom layers than at Site B6. Currents at Sites B1 and B2 exhibit more across-shelf flow (primarily offshore) in the near-bottom layers than at the rest of the sites. Higher frequency fluctuations noted in the low-frequency-flow surface currents at the inshore sites (B1, B2) are consistent with the cross-shelf spatial pattern for subtidal currents seen in regions to the southeast off Huntington Beach (Hamilton and others, 2006).

## Near-Bottom Orbital Velocity Statistics from ADV Data

Near-bottom wave orbital velocities were estimated from hourly ADV burst measurements of velocity and pressure. The ADV recorded bursts of 7,200 velocity measurements at 10 Hz (12 min) every hour, centered 7.5 min after the hour. The three vector components of current velocities were recorded in instrument coordinates and rotated to u (eastward), v (northward), and w (upward) components using the local magnetic declination (13.8° E.) and the median heading, pitch, and roll data for each burst. Representative near-bottom wave orbital velocity $u_{br}$ (Madsen, 1994) was calculated as

$$u_{br} = \sqrt{2\int \left(S_{uu}(\omega) + S_{vv}(\omega)\right) d\omega} \tag{1}$$

where $S_{uu}$ and $S_{vv}$ are spectra of the horizontal components of near-bottom velocity as functions of angular wave frequency. The representative wave period Tr = 2p/*wr*, where *wr* is the weighted mean angular frequency,

$$\omega_r = \frac{\int \omega\left(S_{uu}(\omega) + S_{vv}(\omega)\right) d\omega}{\int \left(S_{uu}(\omega) + S_{vv}(\omega)\right) d\omega} \tag{2}$$

These calculations were performed in puv.m. Estimates of near-bottom orbital wave velocity are plotted along with the near-bottom suspended-sediment measurements in figures 8, 11, 17, and 19 for Sites B2, B3, B5, and B6, respectively.

### Water Column Temperature Characteristics

The raw temperature data from surface, subsurface, and bottom moorings show temporal changes in the stratification of the water column on many timescales. Diurnal fluctuations at all depth levels illustrate the passage of internal waves, fronts, or both through the area. This is particularly true in mid-December, the beginning of January, mid-February, and mid-March. These periods correspond to higher near-bottom velocities noted in the ADCP and ADVs. There are periods when these fluctuations exist throughout the water column or exclusively in the near-surface or near-bottom layers.

Low-frequency fluctuations in temperature and stratification are apparent in contour plots of low-pass filtered temperature data (figs. 15, 23, 26). Periods of cooler water (for example, December 26–January 5, February 3–5, March 1–3, and March 15–27) correspond with times of southward flow near the surface on the shelf break (figs. 43–45).

## Conclusions

The 2007–2008 Palos Verdes Shelf field program was successful in collecting 4 months of high-resolution near-bottom and water-column oceanographic data from 18-m to 60-m water depth. These extensive time-series data will enhance our understanding of the processes responsible for sediment transport on the Palo Verdes Shelf, as well as changes in the BBL due to the passage of internal tides and waves.

## Acknowledgments

The authors would like to thank the many people that made this field program a success. Jonathan Borden, Kevin O'Toole, David Gonzales, Rick Rendigs, Hal Williams, Jamie Grover, Benedicte Ferre, Brandi Armstrong, and Christine Sabens were instrumental in preparation, deployment, and recovery of the instrumentation, and Anne L. Gartner in editing this report. We would also like to thank the crews of the R/V *Robert Gordon Sproul* of the Scripps Institution of Oceanography and the R/V *Yellowfin* of the Southern California Marine Institute for the deployment and recovery of the instrumentation.

## References Cited

Côté, J.M., Hotchkiss, F.S., Martini, Marinna, and Denham, C.R., 2000, Accoustic Doppler Current Profiler (ADCP) data processing system manual: U.S. Geological Survey Open-File Report 00-458, available at *http://pubs.usgs.gov/of/2000/of00-458/*.

Foreman, M.G.G, 1977, Manual for tidal height analysis and prediction: Sidney, British Columbia, Institute of Ocean Sciences Technical Report, Pacific Marine Science Report 77-10.

Foreman, M.G.G., 1978, Manual for tidal current analysis and prediction: Sidney, British Columbia, Institute of Ocean Sciences Technical Report, Pacific Marine Science Report 78-6.

Hamilton, P., Noble, M.A., Largier, J., Rosenfeld, L.K., and Robertson, G., 2006, Cross-shelf subtidal variability in San Pedro Bay during summer, 2001: Continental Shelf Research, v. 26, p. 681–702.

Hasselmann, K., Barnett, T.P., Bouws, E., Carlson, H., Cartwright, D.E., Enke, K., Ewing, J.A., Gienapp, D.E., Hasselmann, P., Kruseman, A., Meerburg, P., Müller, D.J., Olbers, K., Richter, H., Sell, W., and Walden, H., 1973, Measurements of wind-wave growth and swell decay during the Joint North Sea Wave Project (JONSWAP): Ergnzungsheft zur Deutschen Hydrographischen Zeitschrift Reihe A, v. 8, no. 12, 95 p.

IEEE, 1980, 1978 practical salinity scale equations: Institute of Electrical and Electronics Engineers Journal of Oceanic Engineering, OE-5, no. 1, 14 p.

Lee, H.J., and Wiberg, P.L. (eds.), 2002, Sedimentation processes, DDT, and the Palos Verdes margin: Continental Shelf Research Special Issue, v. 22, no. 6–7.

Madsen, O.S.,1994, Spectral wave-current bottom boundary layer flows: Coastal Engineering, Proceedings, 1994, 24th International Conference Coastal Engineering Research Council, p. 384–398.

Martini, M.A., Lightsom, F.L., Sherwood, C.R., Xu, J.P., Lacy, J.R., Ramsey, A., and Horwitz, R., 2005, Hydratools, a Matlab-based data processing package for Sontek Hydra data: U.S. Geological Survey Open-File Report 2005-1026, available at *http://pubs.usgs.gov/of/2005/1026/*.

Montgomery, E.T., Martini, M.A., Lightsom, F.L., and Butman, B., 2007, Documentation of the U.S. Geological Survey oceanographic time-series measurement database, ver. 1.0: U.S. Geological Survey Open-File Report 2007-1194, available at *pubs.usgs.gov/of/2007/1194/*.

Noble, M.A., Ryan, H.F., and Wiberg, P.L., 2002, The dynamics of subtidal poleward flows over a narrow continental shelf, Palos Verdes, CA: Continental Shelf Research, v. 22, no. 6–7, p. 923–944.

Noble, M.A., and Xu, J.P., 2003, Observations of large-amplitude cross-shore internal bores near the shelf break, Santa Monica Bay, CA: Marine Environmental Research v. 56, no. 1–2, p. 127–149.

Noble, M.A., Rosenberger, K.J., Xu, J.P., Signell, R.P., and Steele, A., 2008, Connections among the spatial and temporal structures in tidal currents, internal bores, and surficial sediment distributions over the shelf off Palos Verdes, California: U.S. Geological Survey Scientific Investigations Report 2008-5094, available at *http://pubs.usgs.gov/sir/2008/5094*.

Pawlowicz, R., Beardsley, B., and Lentz, S., 2002, Classical tidal harmonic analysis including error estimates in Matlab using TTIDE: Computers and Geosciences, v. 28, p. 929–937.

Science Applications International Corporation (SAIC), 2004, Analysis of moored oceanographic data acquired on the Palos Verdes Shelf by the LACSD during the period from November 2000 to August 2003: Newport, Rhode Island , prepared by Science Applications International Corporation for U.S. Army Corps of Engineers, Santa Ana Dams Resident Office, and U.S. Environmental Protection Agency, Region IX, SAIC Report 659, 123 p.

Science Applications International Corporation (SAIC), 2005, Data report for the summer 2004 oceanographic measurement program conducted on the Palos Verdes Shelf: Newport, Rhode Island, prepared by Science Applications International Corporation for U.S. Environmental Protection Agency, Region IX, SAIC Report 694, 40 p.

Science Applications International Corporation (SAIC), 2009, Orange County Sanitation District ocean current studies: Analysis of inter- and intra-annual variability in coastal currents: San Diego, California, prepared by Science Applications International Corporation for Orange County Sanitation District, SAIC Report, 62 p.
Stull, J.K., Swift, D., Xu, J.P., and Niedoroda, A.W., 1996, Contaminant dispersal on the Palos Verdes continental margin I. Sediments and biota near a major California wastewater discharge: The Science of the Total Environment 179, p. 73–90.
Xu, J.P., Lightsom, F.L., Noble, M.A., and Denham, C., 2002, CMGTooL user's manual: U.S. Geological Survey Open-File Report 02-019, available at *http://geopubs.wr.usgs.gov/open-file/of02-19*.

# Figures 3-45

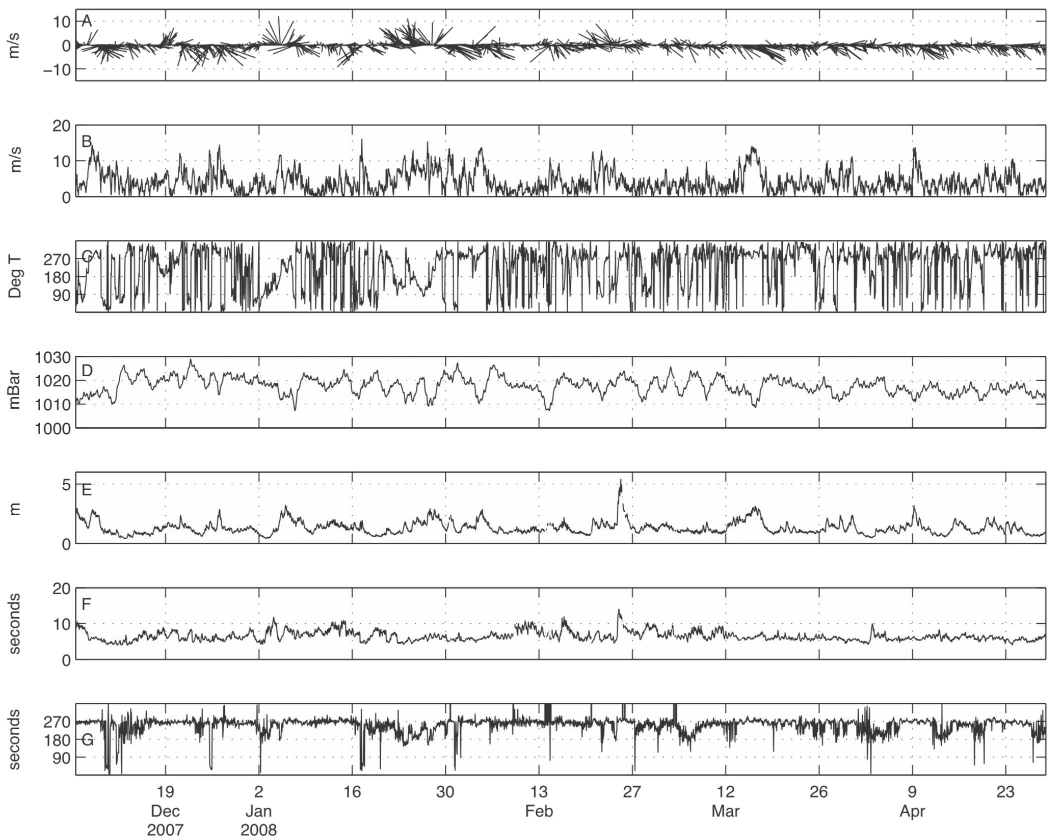


**Figure 3.** Meteorological and wave parameters from National Oceanographic Data Center (NDOC) Buoy 46025 for deployment period. Parameters plotted, from top panel down, include (A) low-pass filtered wind vectors, (B) Wind speed, (C) wind direction, (D) atmospheric pressure, (E) significant wave height, (F) mean wave period, and (G) mean wave direction.

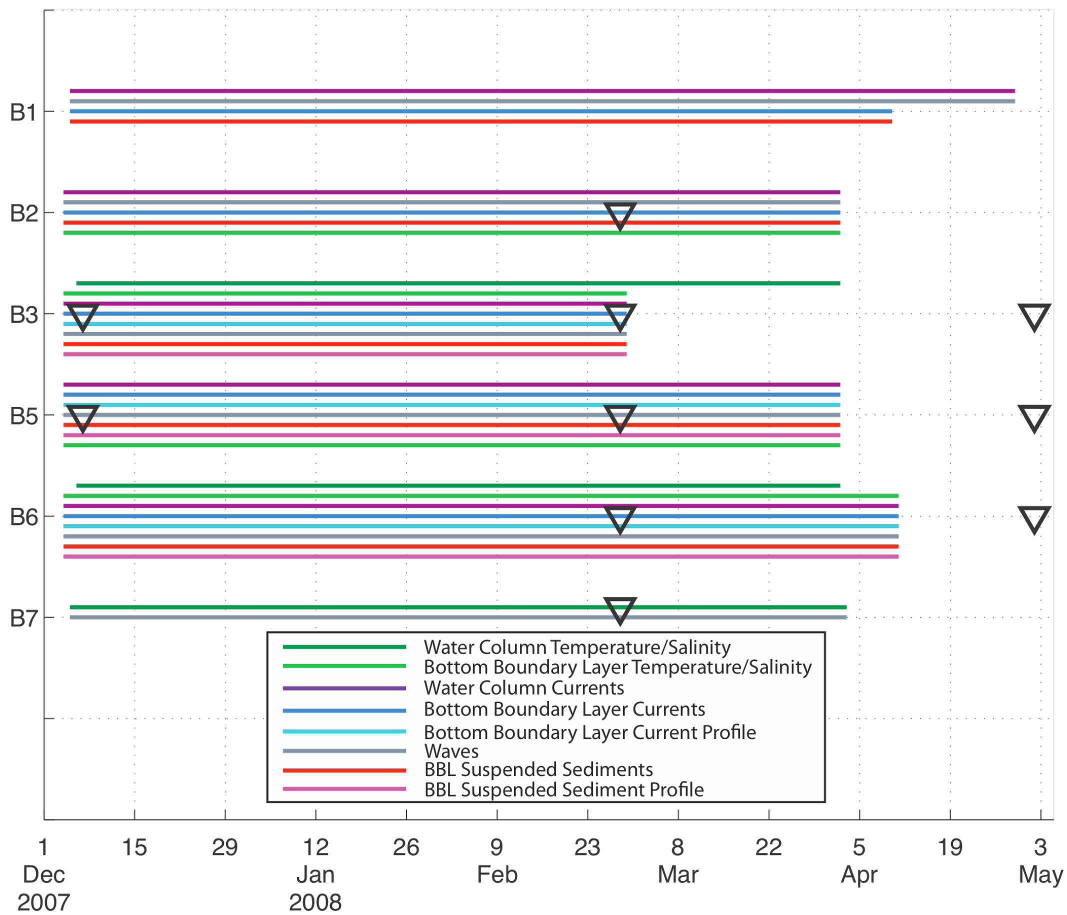


**Figure 4.** Data return for the 2007–2008 measurement program for each platform by data type. Black triangles represent coring surveys during the measurement program by hydraulically damped piston corer.

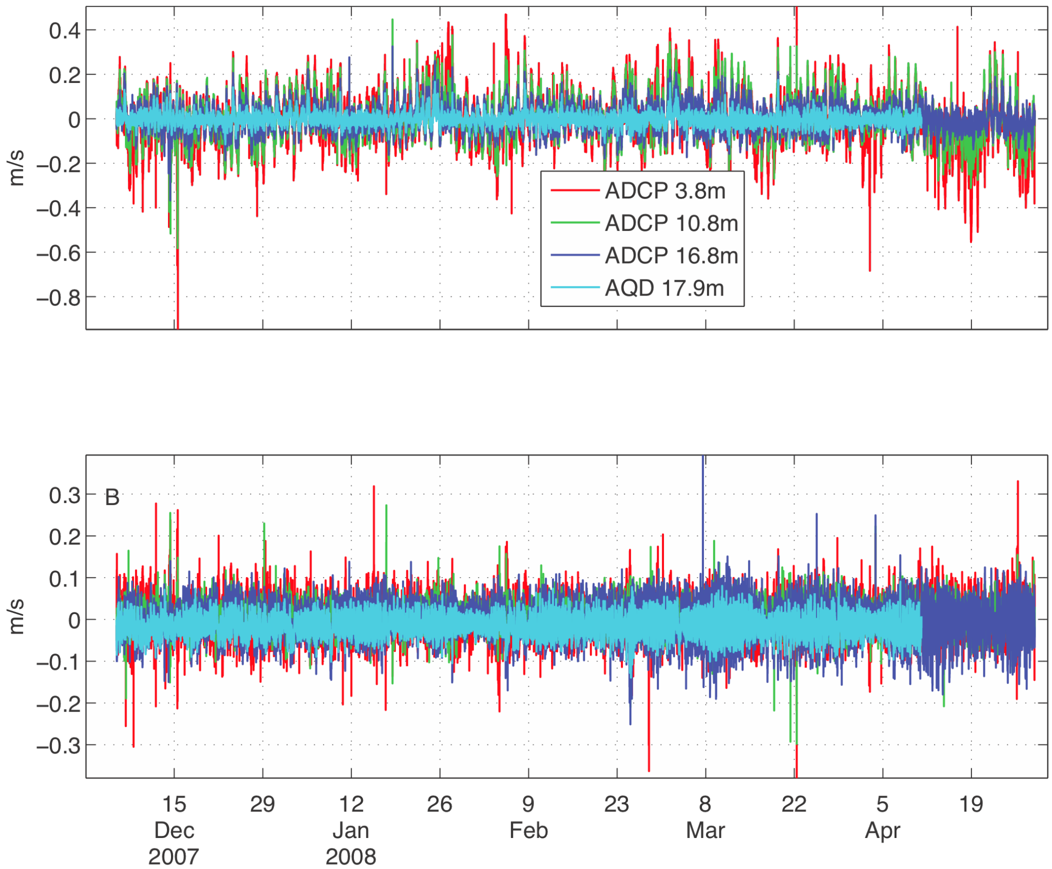


**Figure 5.** Along-shore (A) and cross-shore (B) currents at the basic time interval at several depth levels from Site B1 ADCP and Aquadopp current meters.

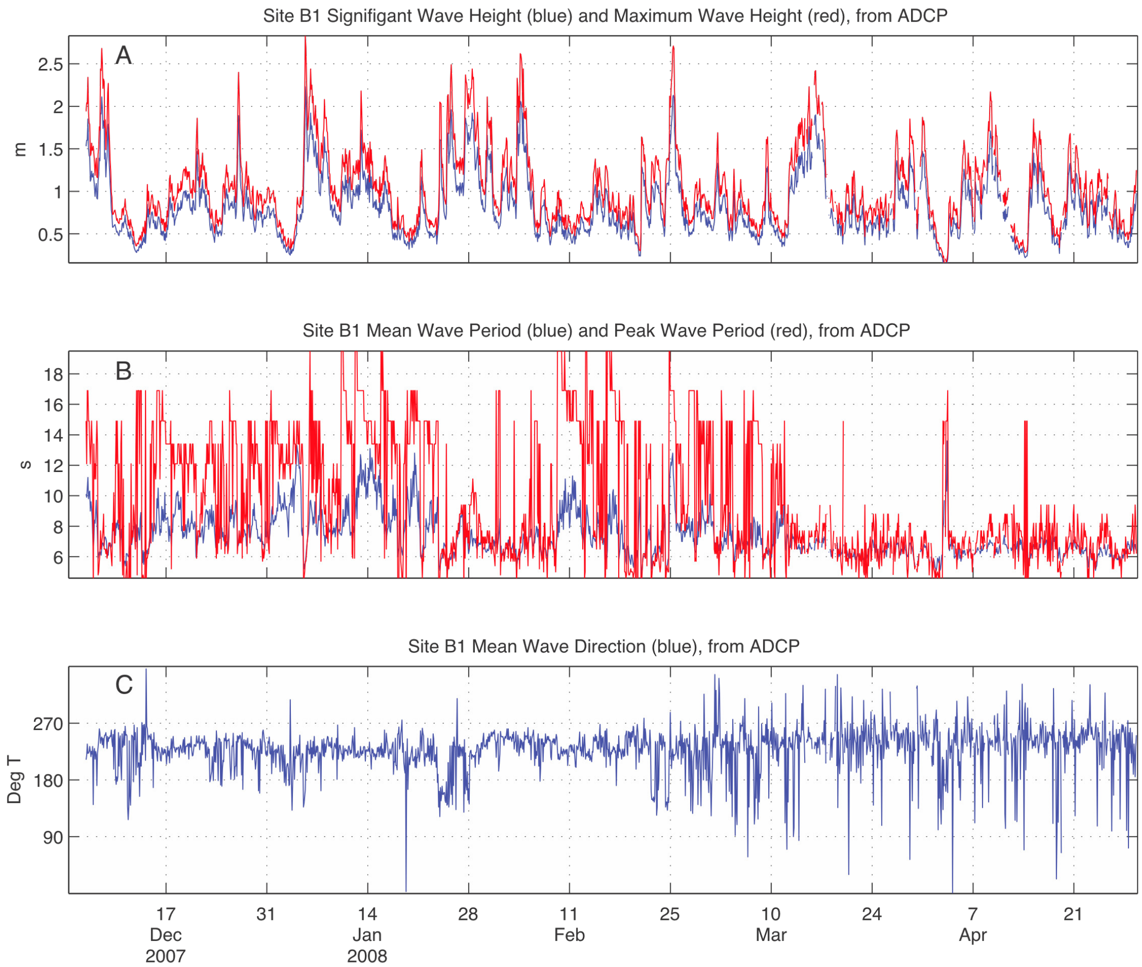


**Figure 6.** Directional wave parameters calculated from ADCP data at Site B1. Parameters plotted, from top down, include (A) significant wave height (blue) and maximum wave height (red), (B) mean wave period (blue) and peak wave period (red), and (C) mean wave direction (blue). Direction 30/210 degrees is cross-shelf.

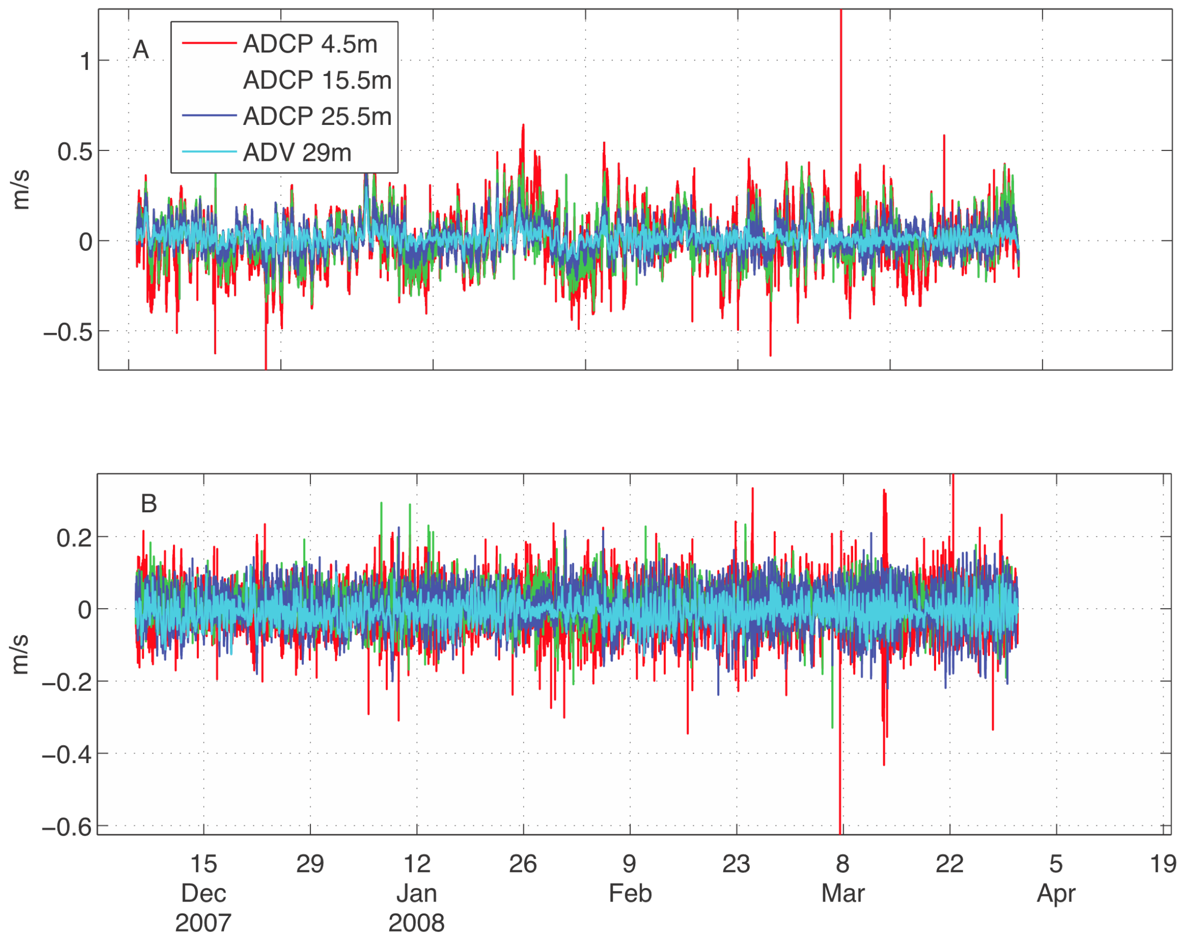


**Figure 7.** Along-shore (A) and cross-shore (B) currents at the basic time interval at several depth levels from Site B2 ADCP and Aquadopp current meters.

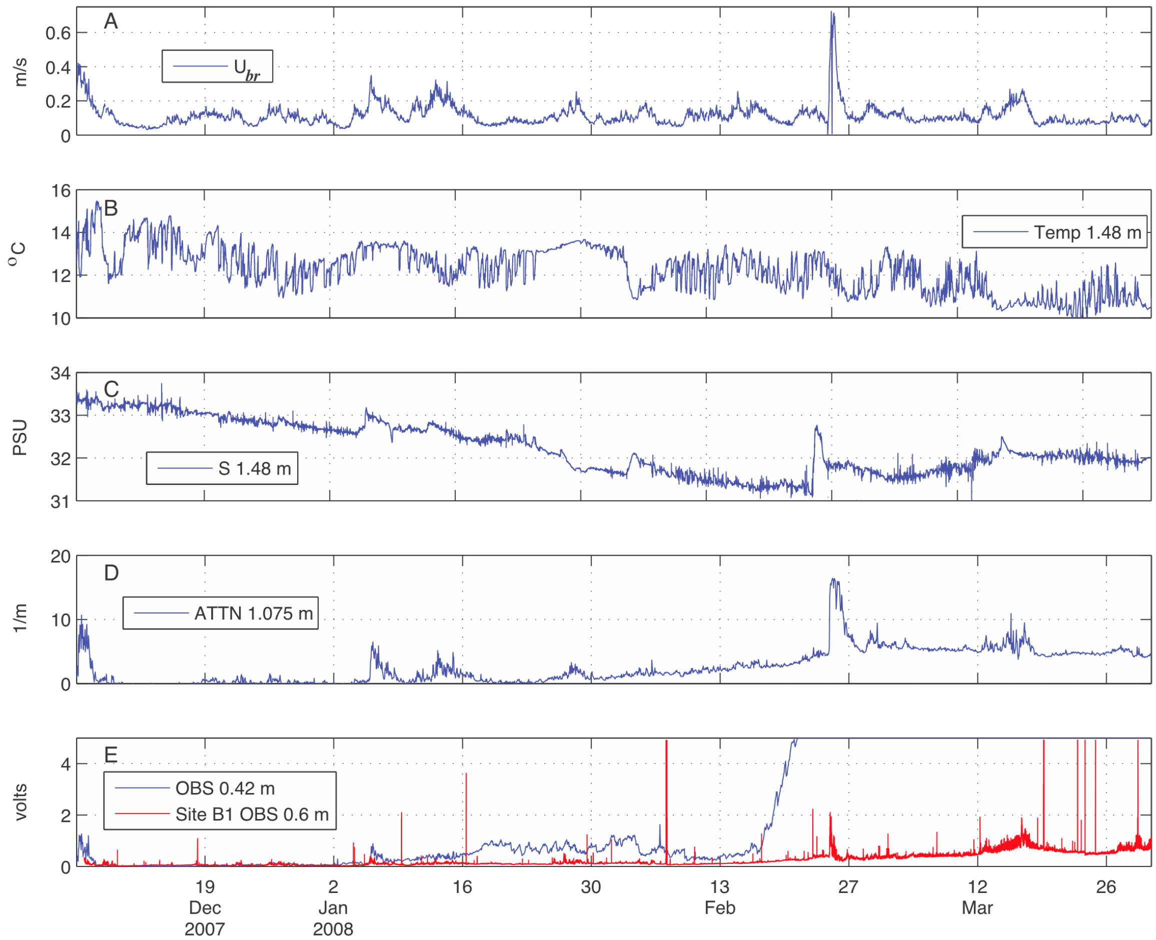


**Figure 8.** Near-bottom physical parameters from the large tripod at Site B2 including (A) orbital wave velocity ($U_{br}$), (B) temperature, (C) salinity (PSU), (D) beam attenuation (1/m), and (E) optical backscatter (OBS in volts), as well as OBS data from Site B1. Heights above bottom of the individual sensors are listed in meters.

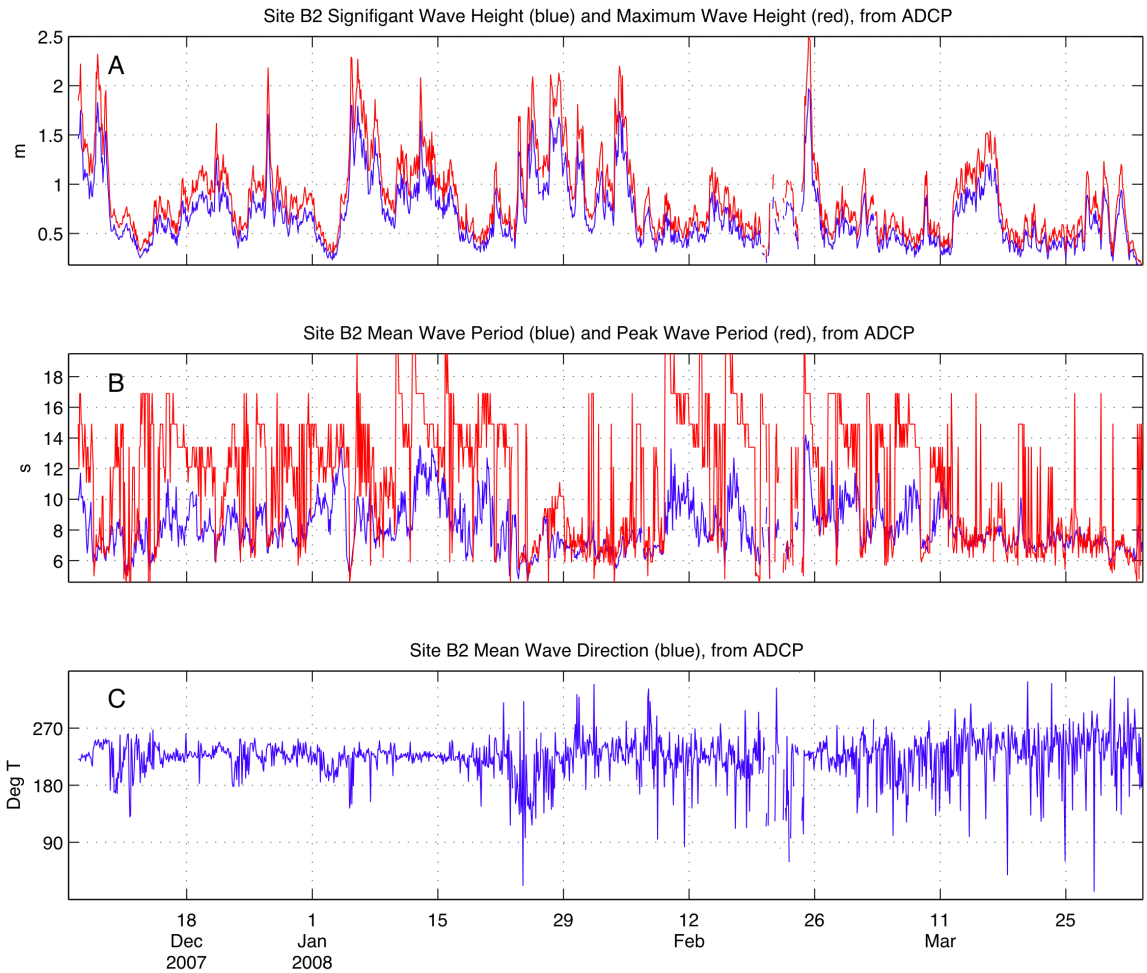


**Figure 9.** Directional wave parameters calculated from ADCP data at Site B2. Parameters plotted, from top down, include (A) significant wave height (blue) and maximum wave height (red), (B) mean wave period (blue) and peak wave period (red), and (C) mean wave direction (blue). Direction 30/210 degrees is cross-shelf.

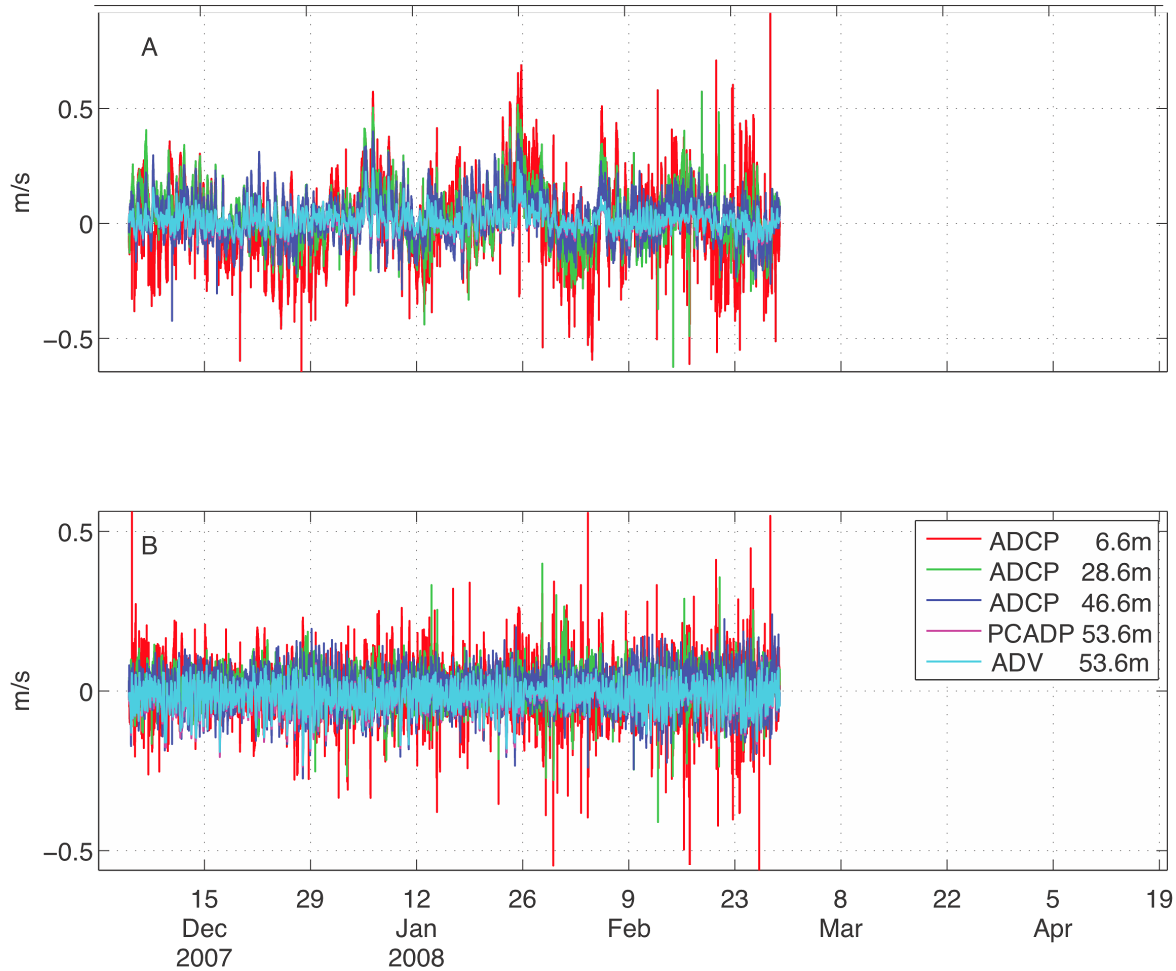


**Figure 10.** Along-shore (A) and cross-shore (B) currents at the basic time interval at several depth levels from Site B3 ADCP, ADV, and PCADP current meters.

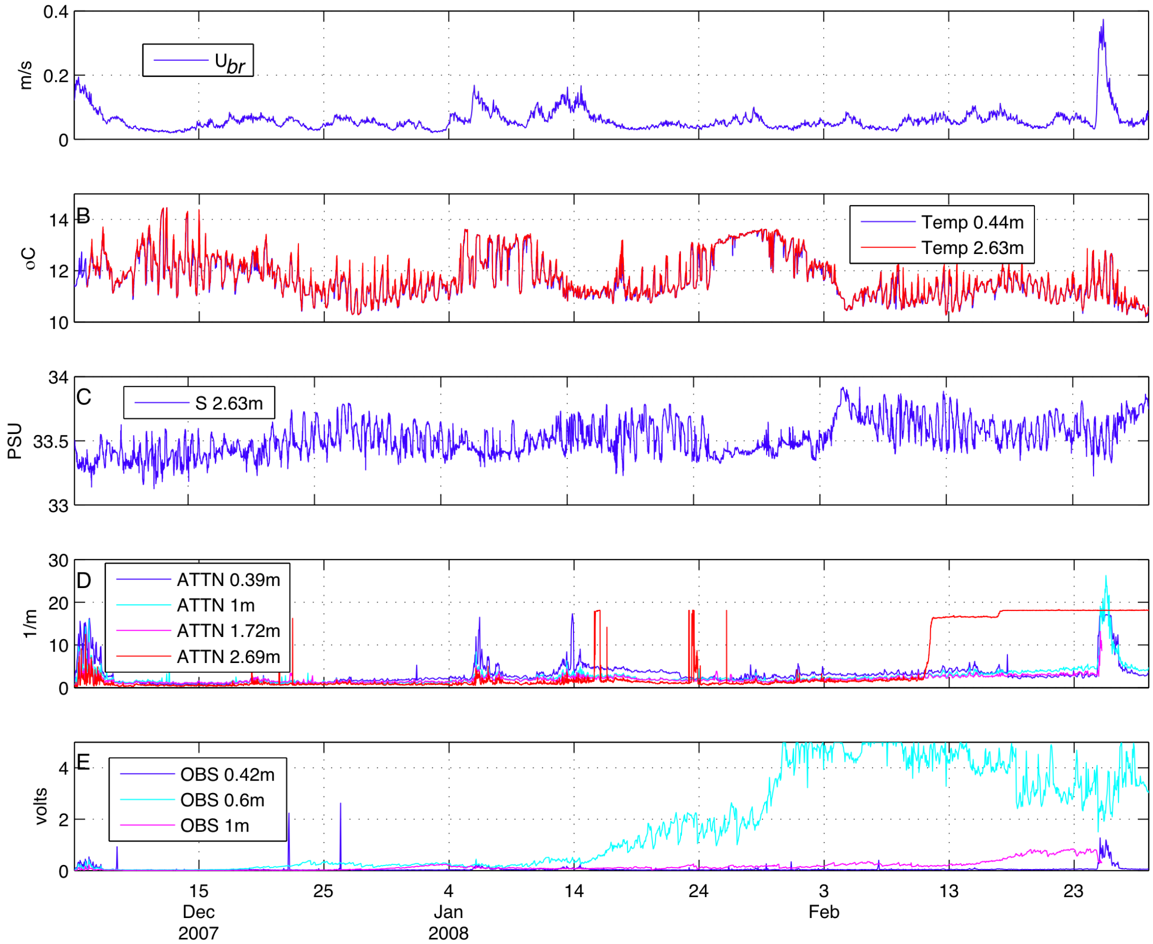


**Figure 11.** Near-bottom physical parameters from the large tripod at Site B3 including (A) orbital wave velocity ($U_{br}$), (B) temperature, (C) salinity (PSU), (D) beam attenuation (1/m), and (E) optical backscatter (OBS, in volts). Heights above bottom of the individual sensors are listed in meters.

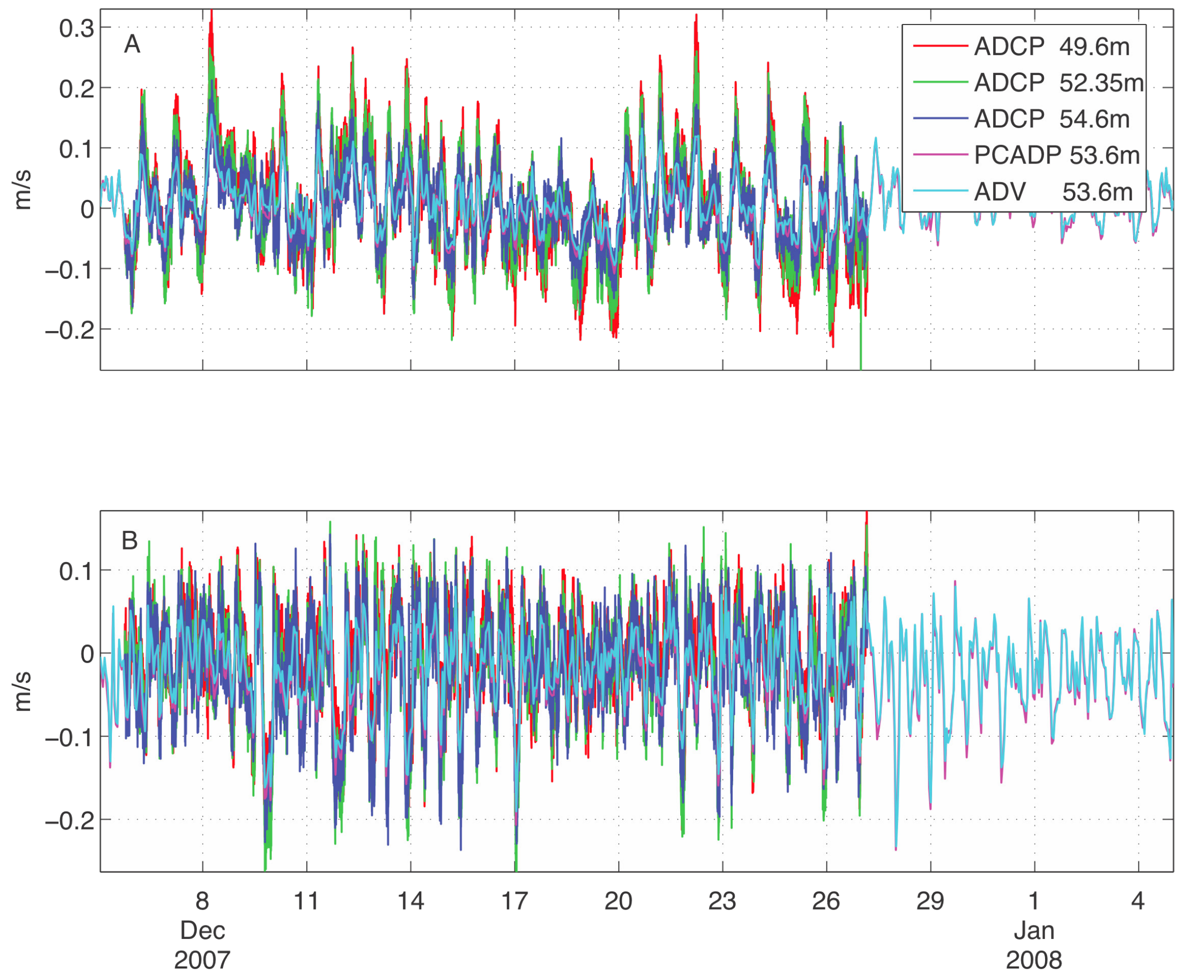


**Figure 12.** Along-shore (A) and cross-shore (B) currents at the basic time interval at several depth levels from Site B3 near-bottom 1200-kHz ADCP. Data from the near-bottom ADV on the large tripod are overplotted for comparison.

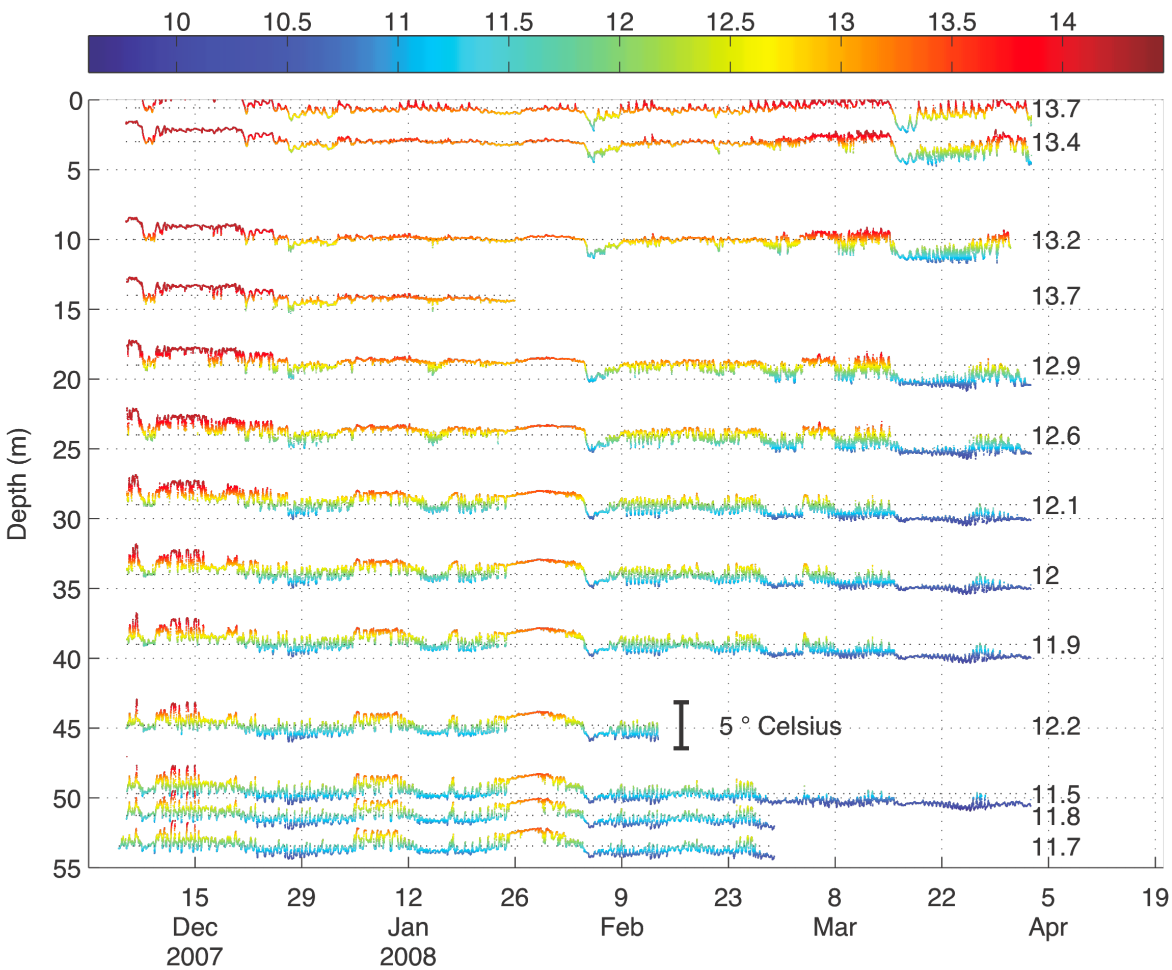


**Figure 13.** Temperature data at the basic time interval from surface and subsurface moorings at Site B3 plotted at the depth level of the instrument. Values to the right of the data indicate the mean temperature for the entire deployment for that instrument.

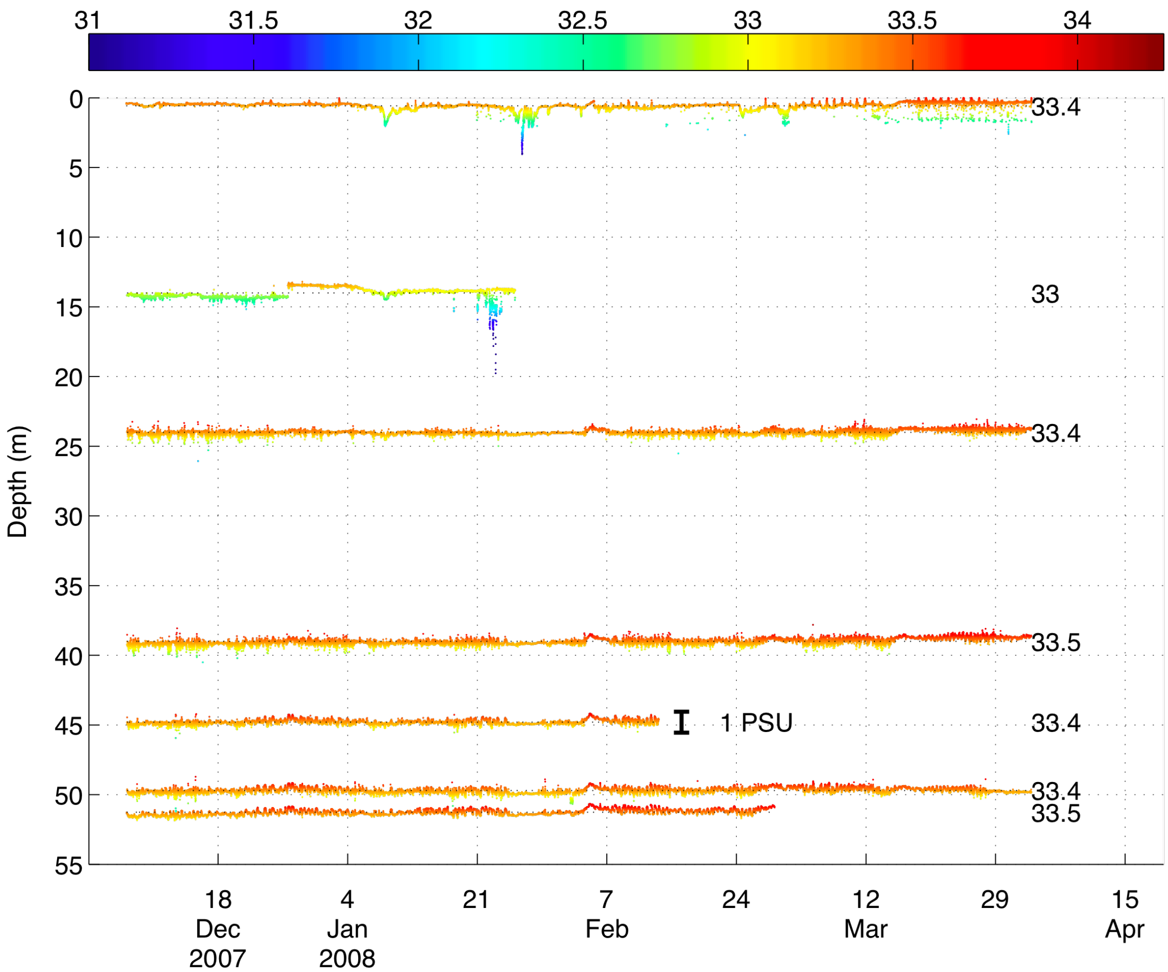


**Figure 14.** Salinity data at the basic time interval from surface and sub-surface moorings at Site B3 plotted at the depth level of the instrument. Values to the right of the data indicate the mean salinity for the entire deployment for that instrument.

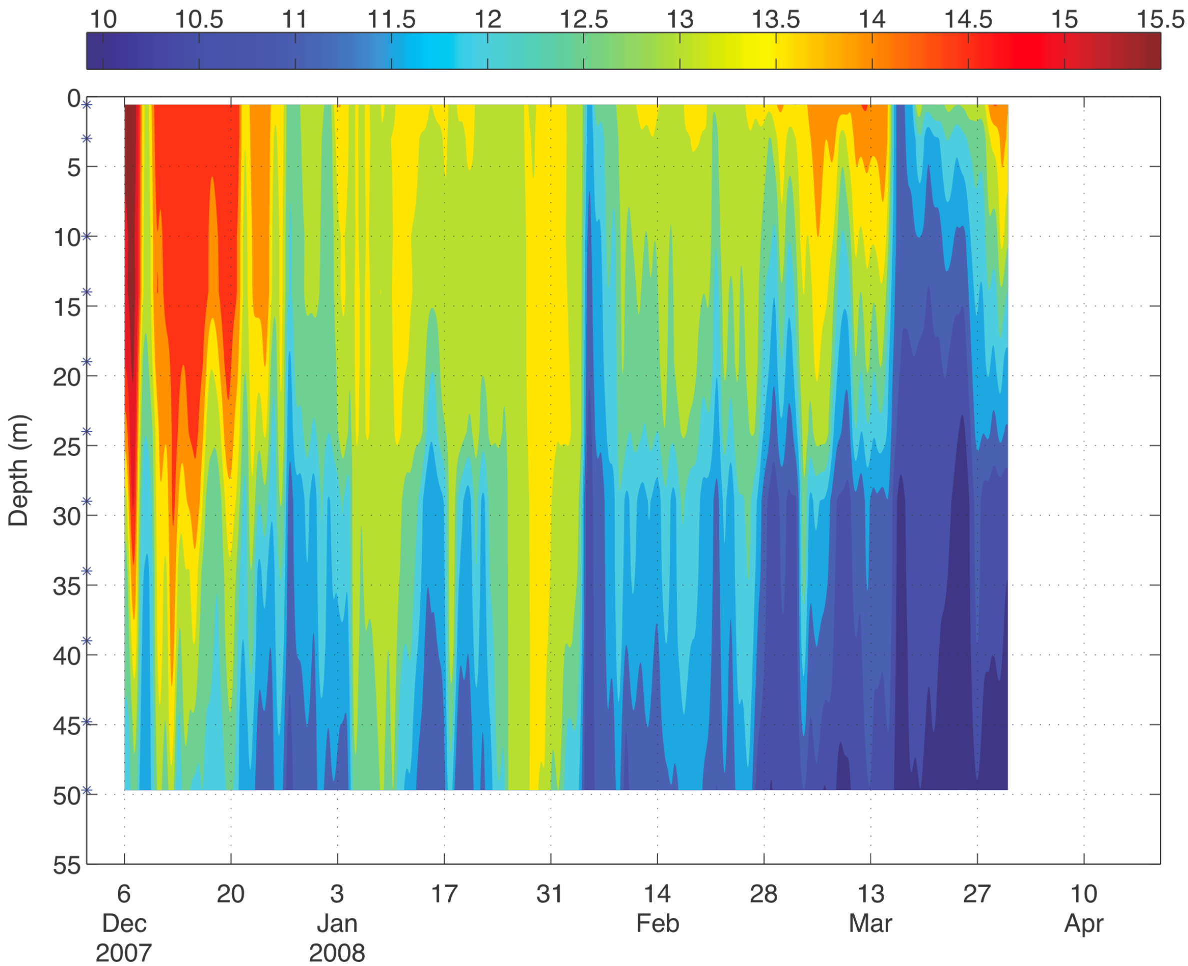


**Figure 15.** Contoured low-pass filtered temperature data from surface and subsurface moorings at Site B3.

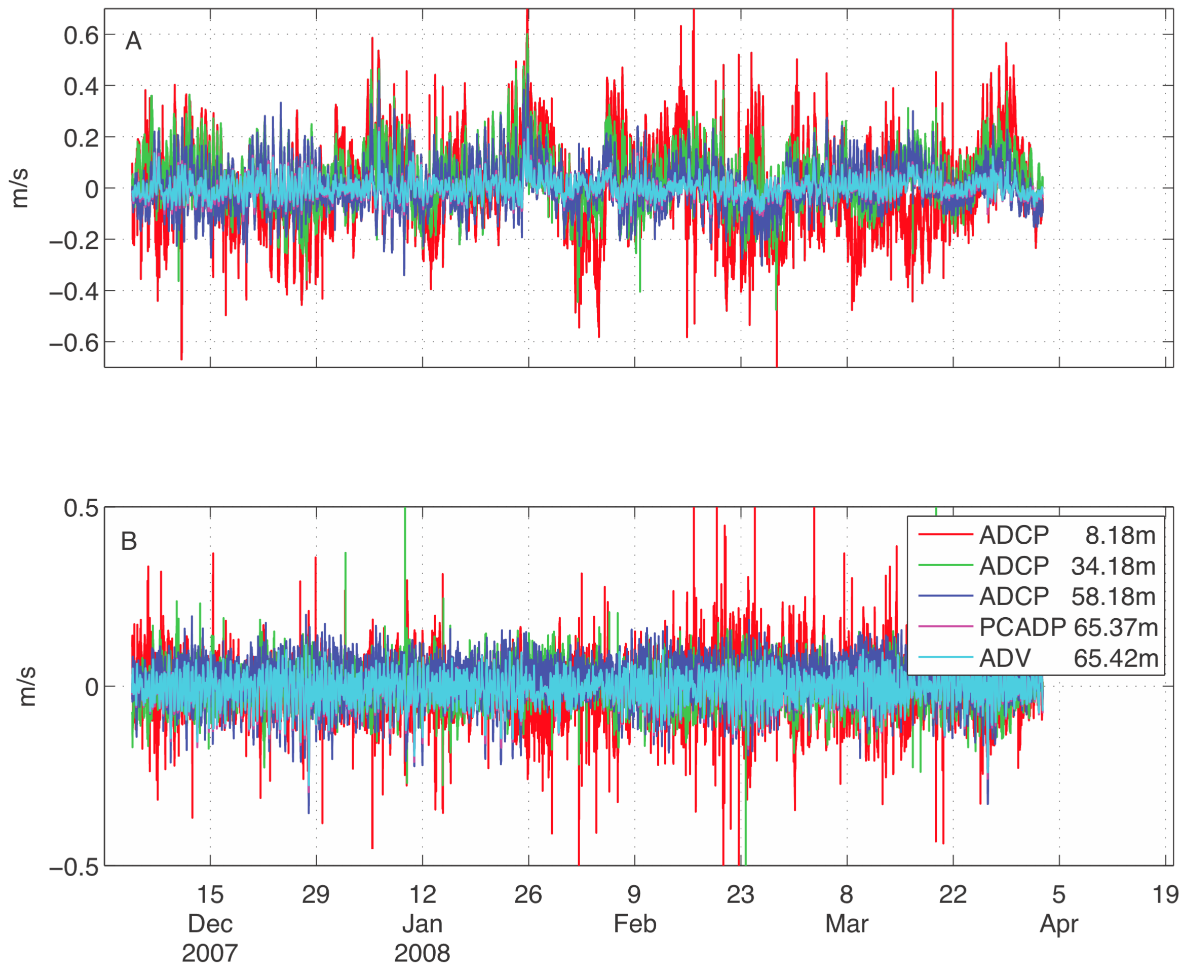


**Figure 16.** Along-shore (A) and cross-shore (B) currents at the basic time interval at several depth levels from Site B5 ADCP, ADV, and PCADP current meters.

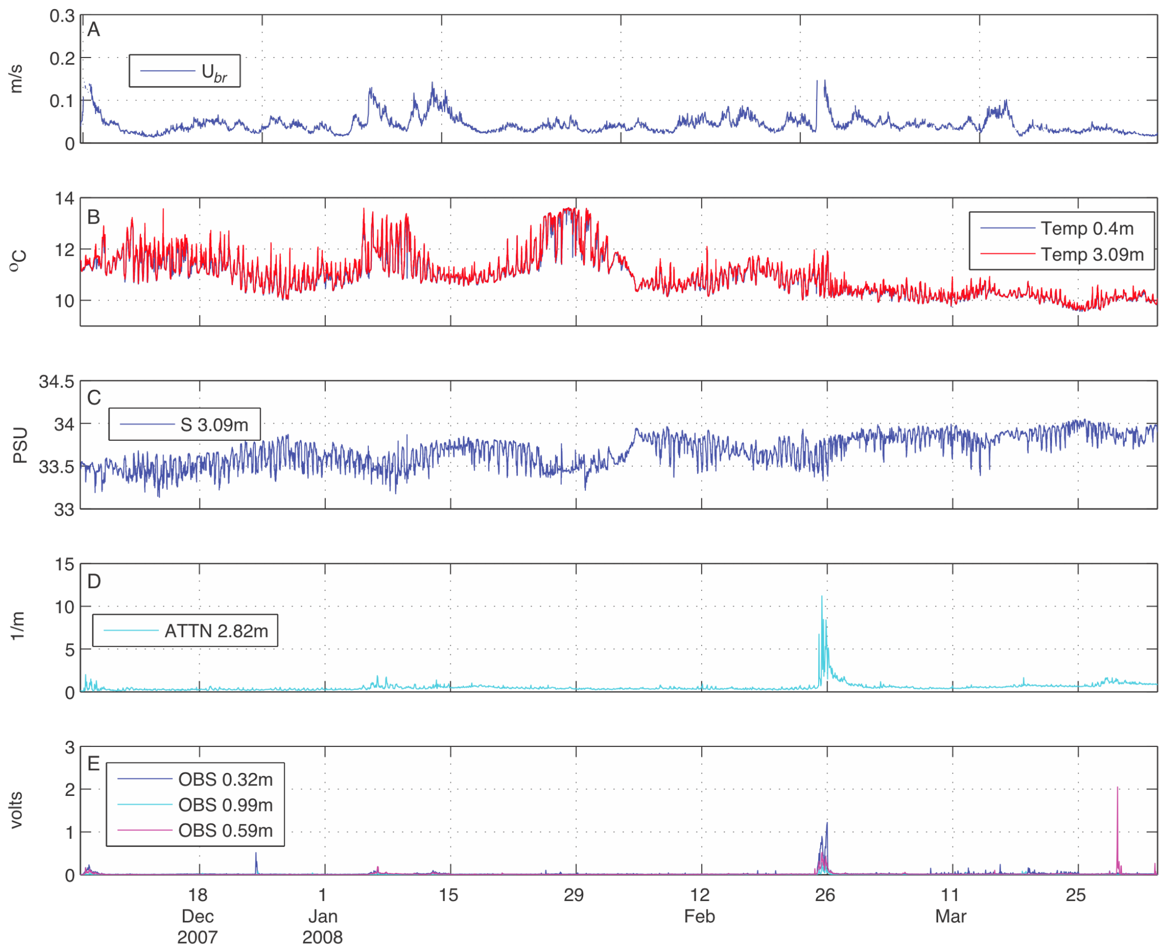


**Figure 17.** Near-bottom physical parameters from the large tripod at Site B5 including (A) orbital wave velocity ($U_{br}$), (B) temperature, (C) salinity (PSU), (D) beam attenuation (1/m), and (E) optical backscatter (OBS, in volts). Heights above bottom of the individual sensors are listed in meters.

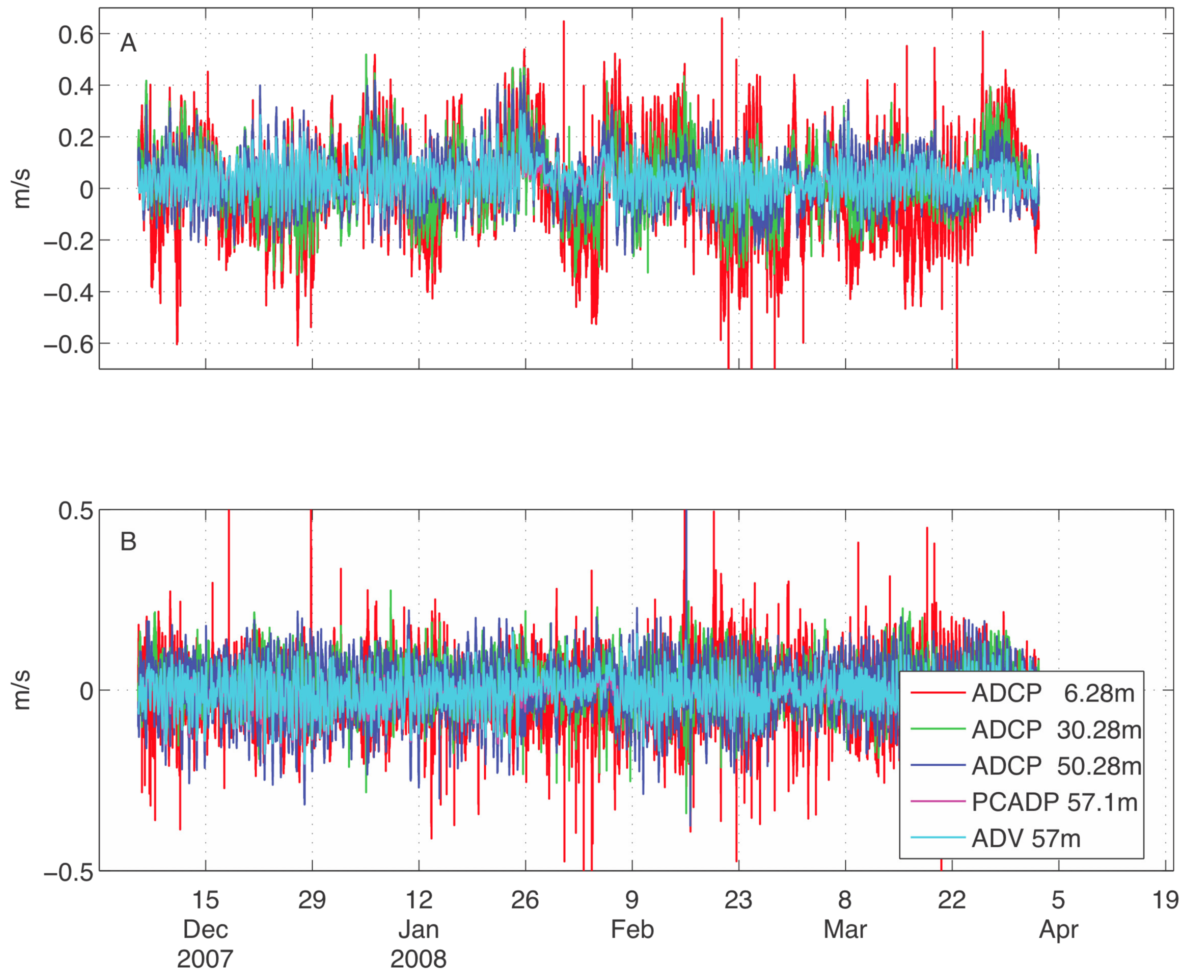


**Figure 18.** Along-shore (A) and cross-shore (B) currents at the basic time interval at several depth levels from Site B6 ADCP, ADV, and PCADP current meters.

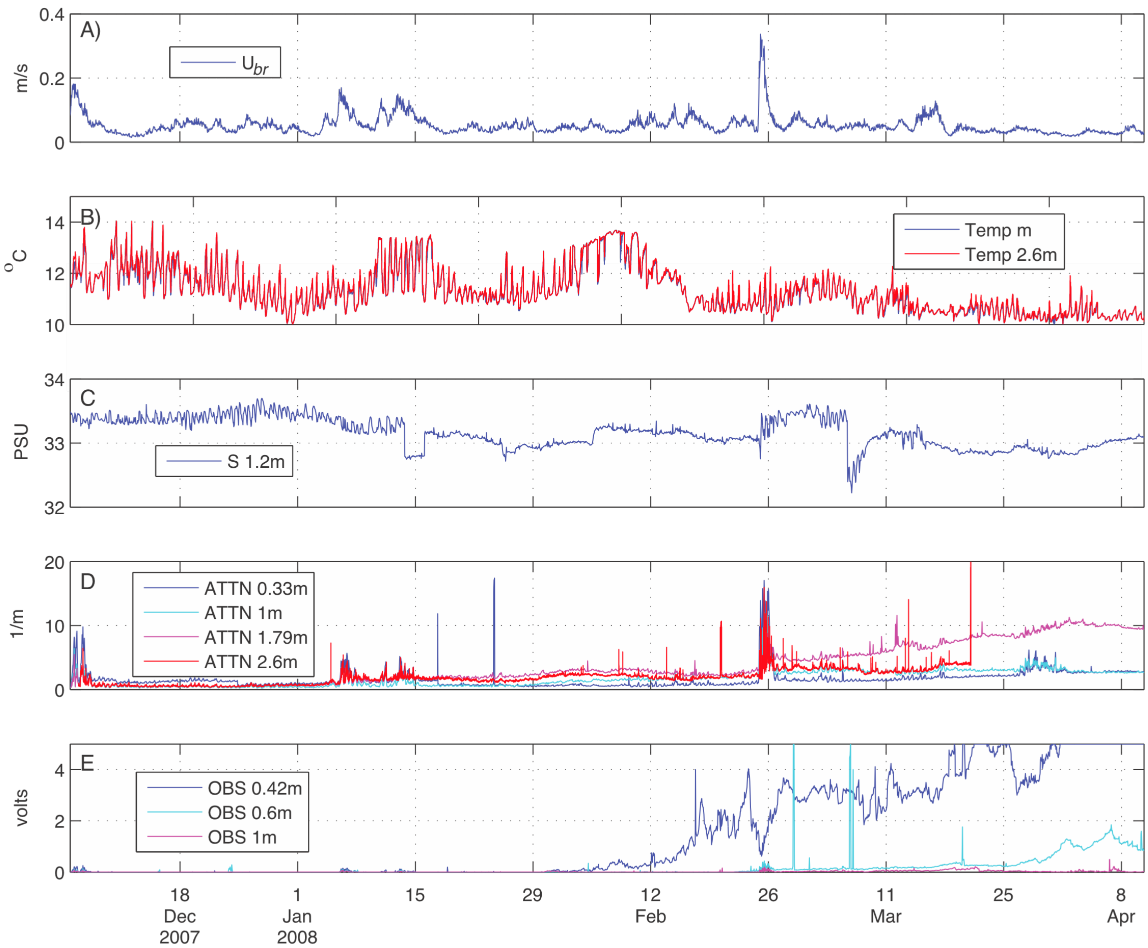


**Figure 19.** Near-bottom physical parameters from the large tripod at Site B6 including (A) orbital wave velocity ($U_{br}$), (B) temperature, (C) salinity (PSU), (D) beam attenuation (1/m), and (E) optical backscatter (OBS, in volts). Heights above bottom of the individual sensors are listed in meters.

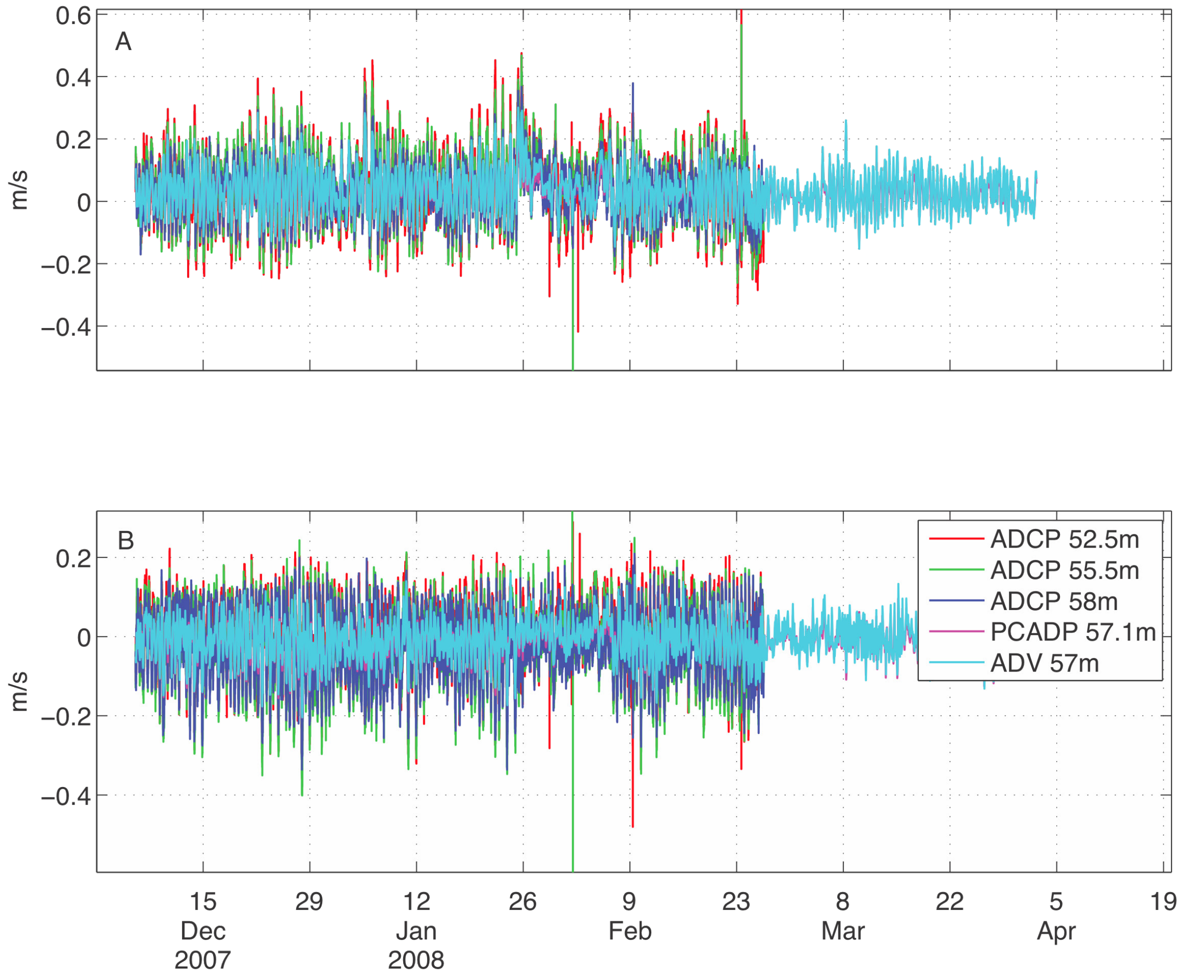


**Figure 20.** Along-shore (A) and cross-shore (B) currents at the basic time interval at several depth levels from Site B6 near-bottom 1200-kHz ADCP. Data from the near-bottom ADV on the large tripod are overplotted for comparison.

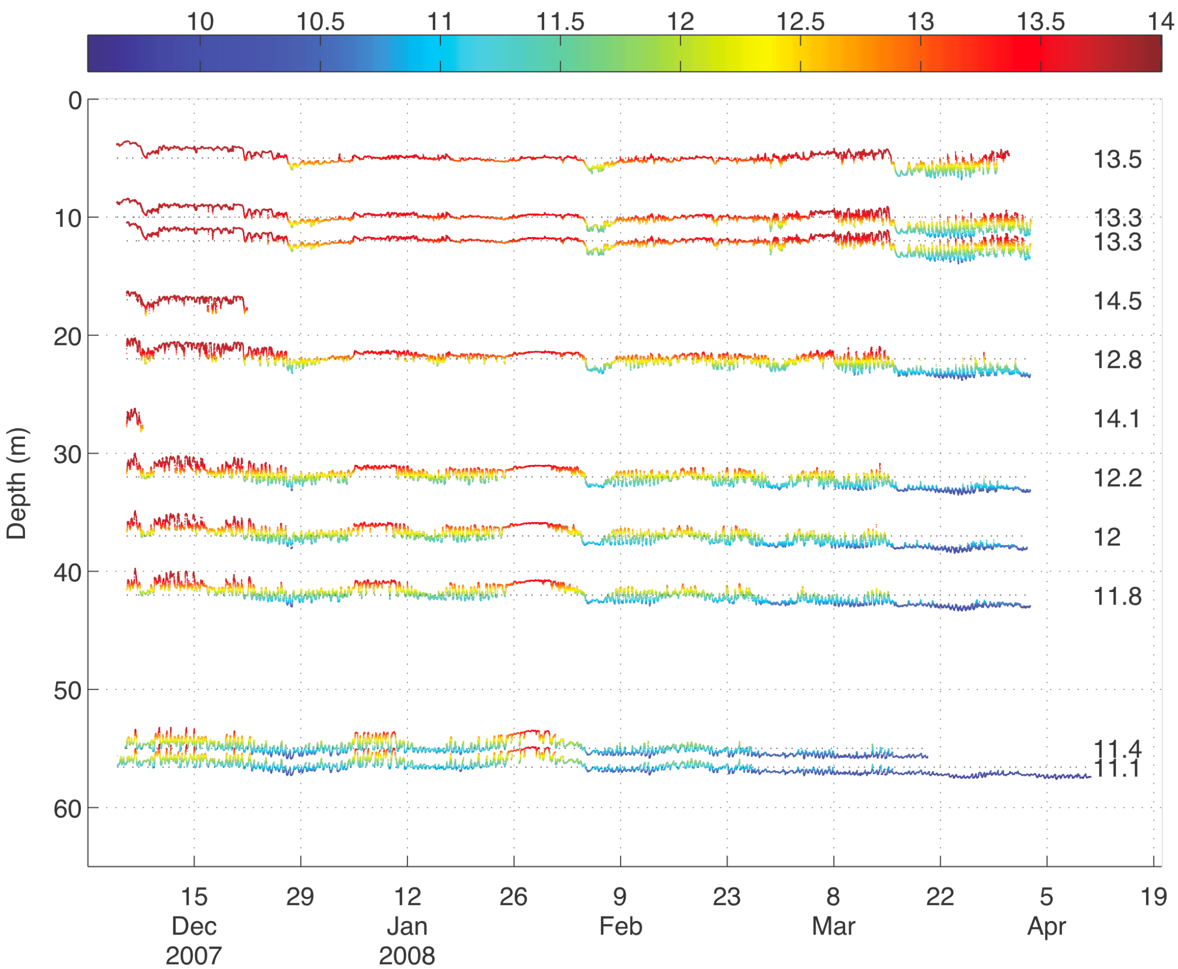


**Figure 21.** Temperature data at the basic time interval from surface and subsurface moorings at Site B6 plotted at the depth level of the instrument. Values to the right of the data indicate the mean temperature for the entire deployment for that instrument.

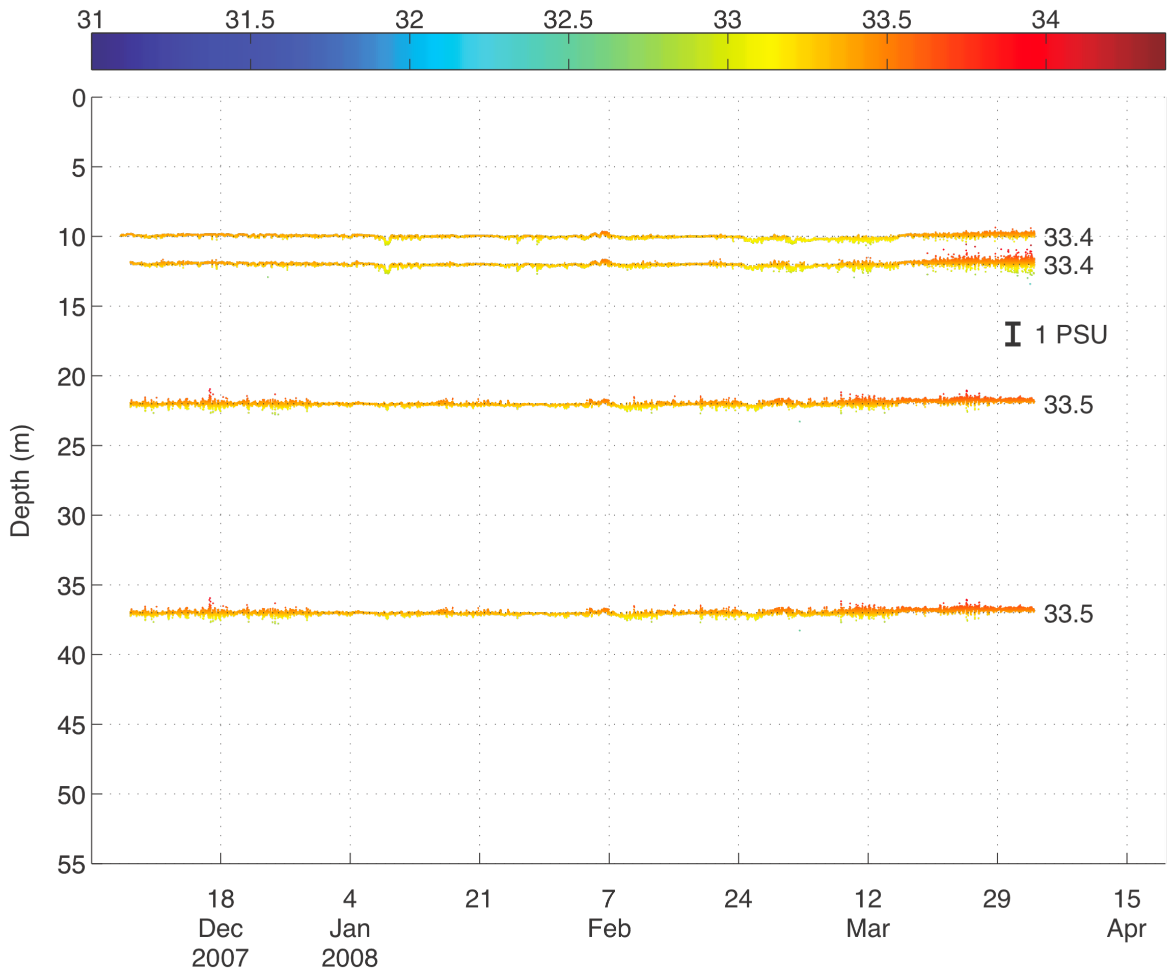


**Figure 22.** Salinity data at the basic time interval from surface and subsurface moorings at Site B6 plotted at the depth level of the instrument. Values to the right of the data indicate the mean salinity for the entire deployment for that instrument.

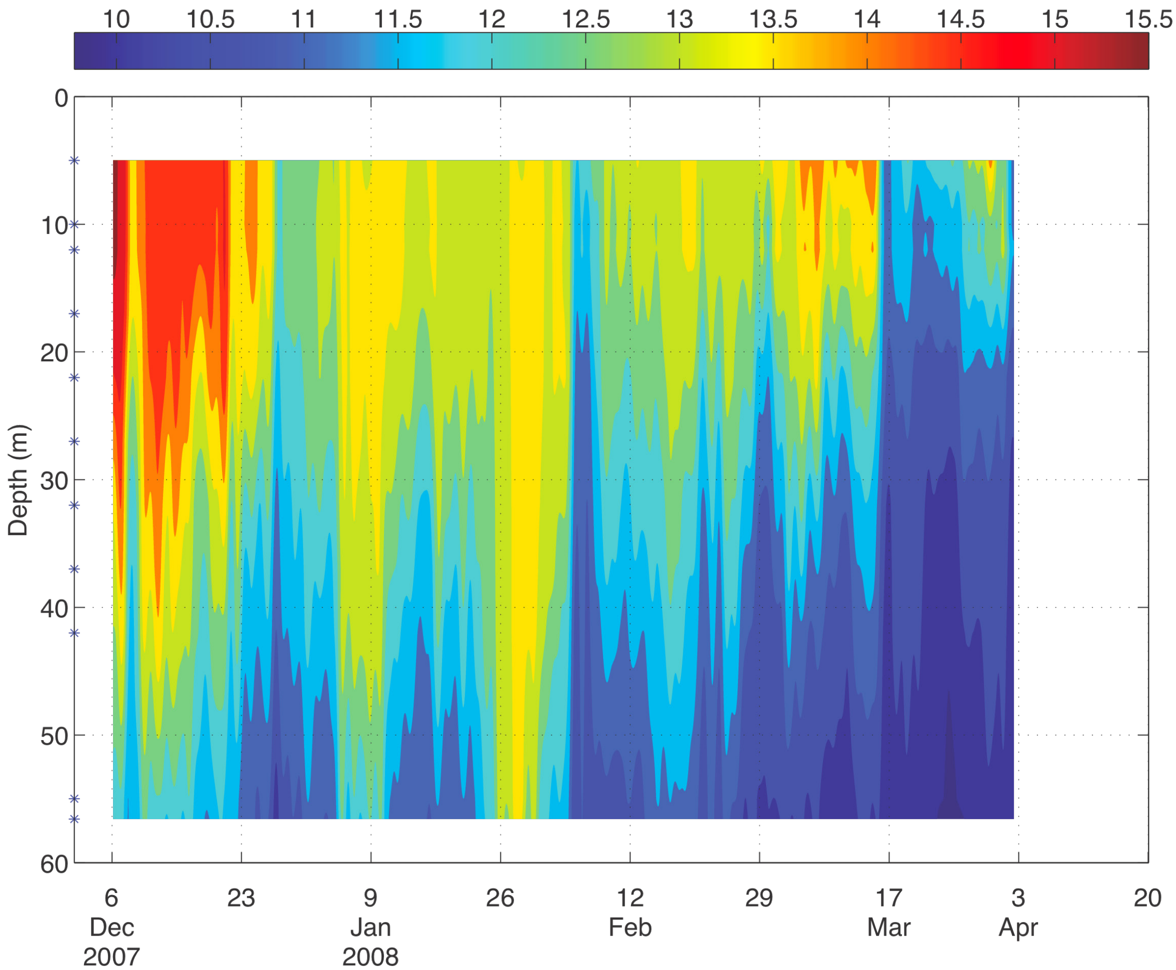


**Figure 23.** Contoured low-pass filtered temperature data from surface and subsurface moorings at Site B6.

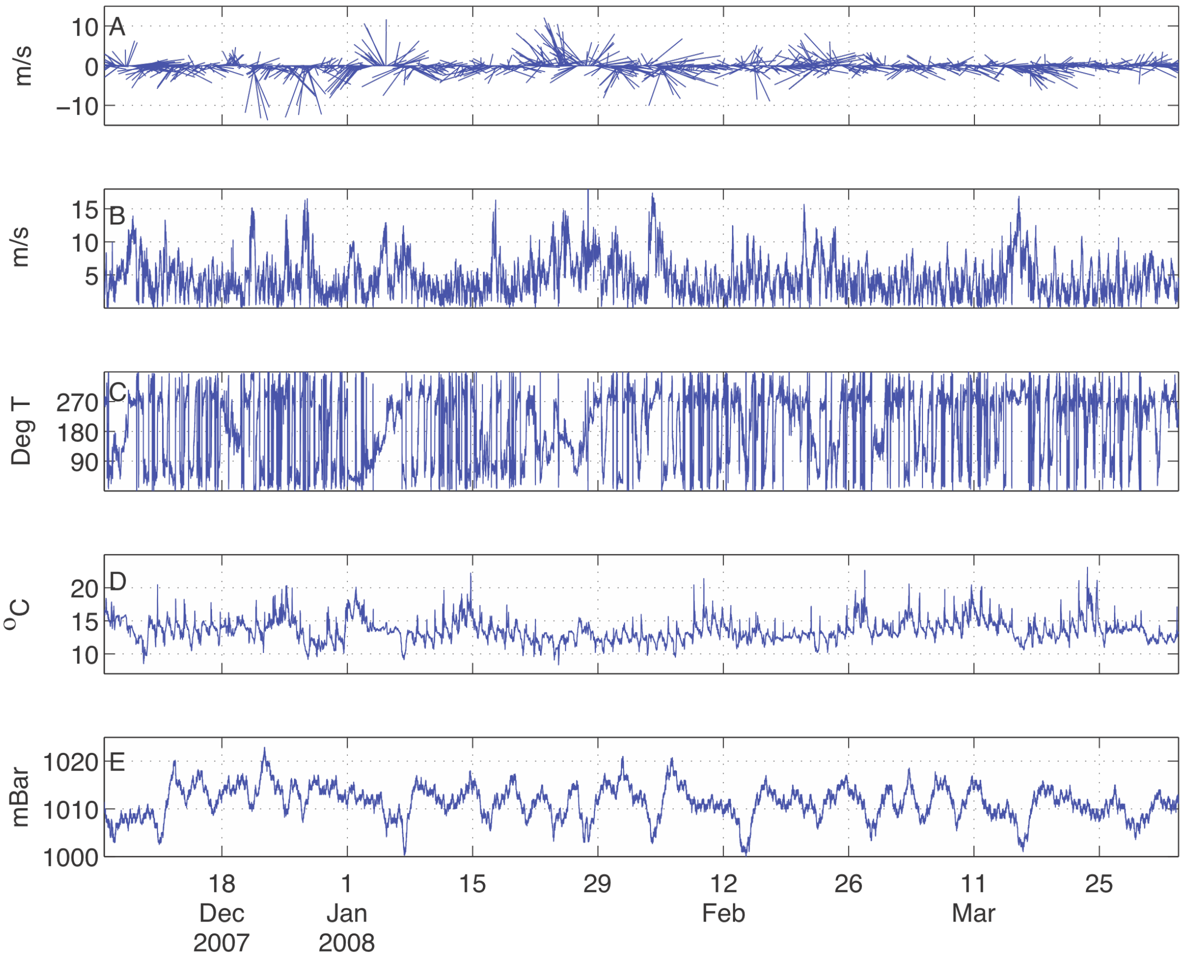


**Figure 24.** Meteorological data logged by the USGS meteorological station mounted on the surface buoy at Site B6. Parameters plotted, from top down, include (A) 6-hour low-pass filtered wind vectors, (B) wind speed, (C) wind direction, (D) atmospheric temperature, and (E) atmospheric pressure.

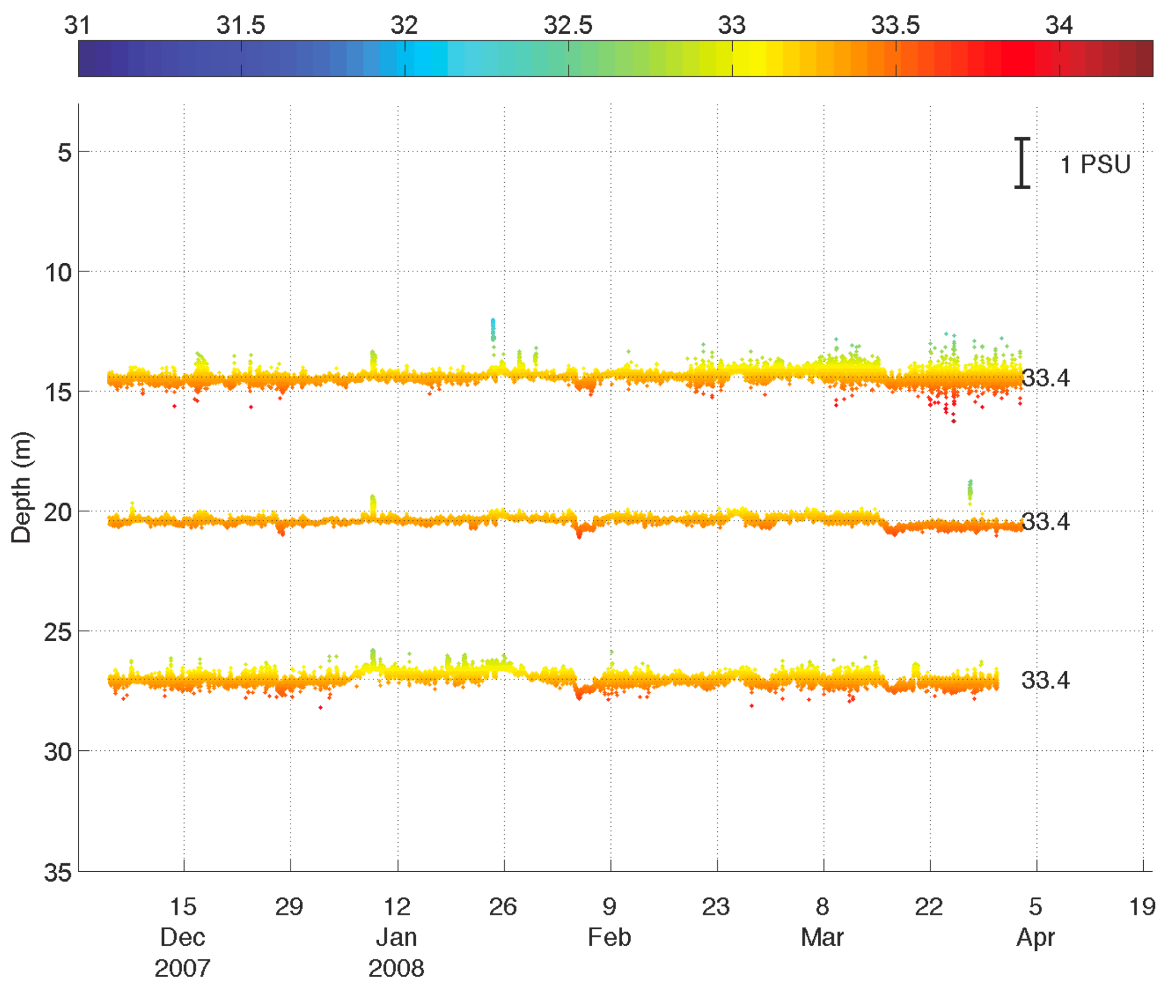


**Figure 25.** Salinity data at the basic time interval from surface and subsurface moorings at Site B7 plotted at the depth level of the instrument. Values to the right of the data indicate the mean salinity for the entire deployment for that instrument.

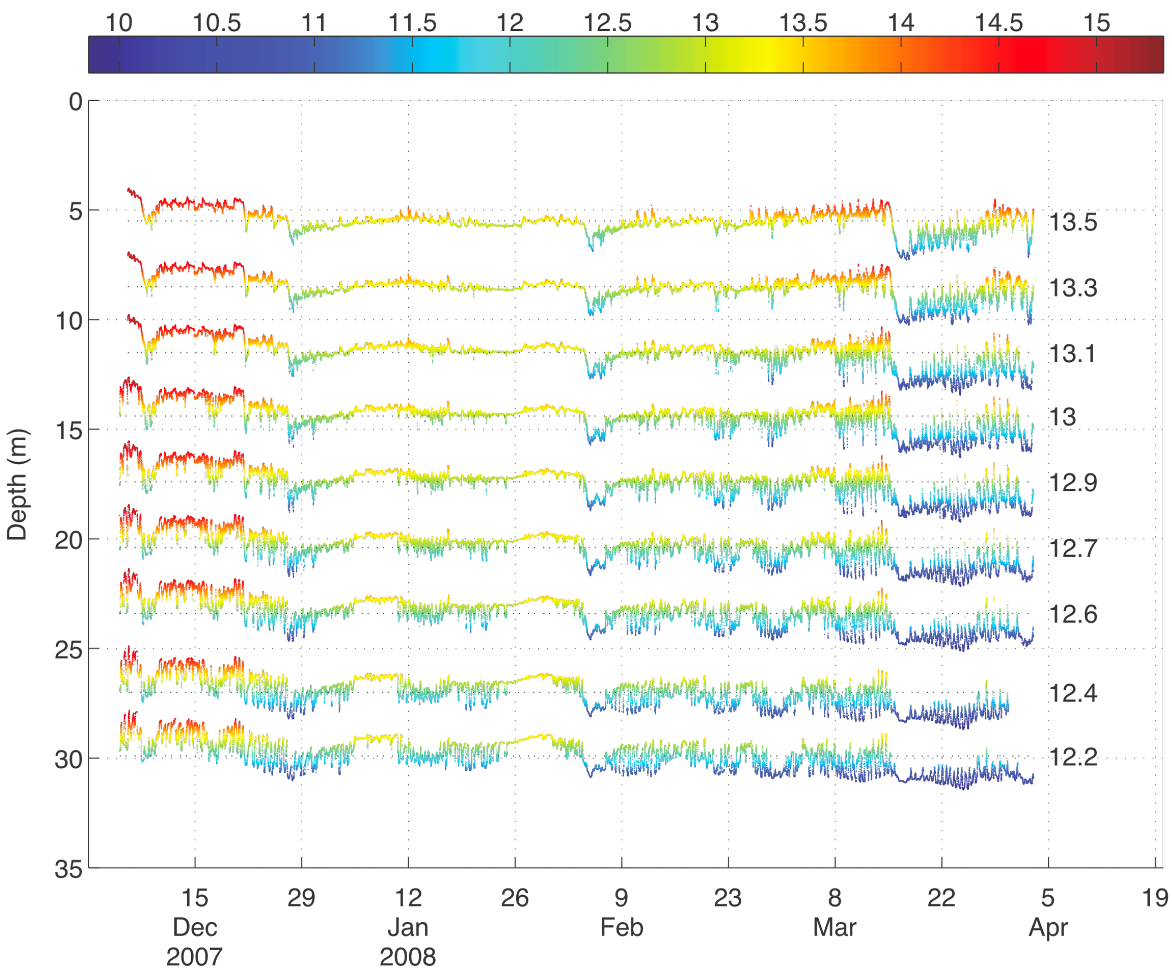


**Figure 26.** Temperature data at the basic time interval from surface and subsurface moorings at Site B7 plotted at the depth level of the instrument. Values to the right of the data indicate the mean temperature for the entire deployment for that instrument.

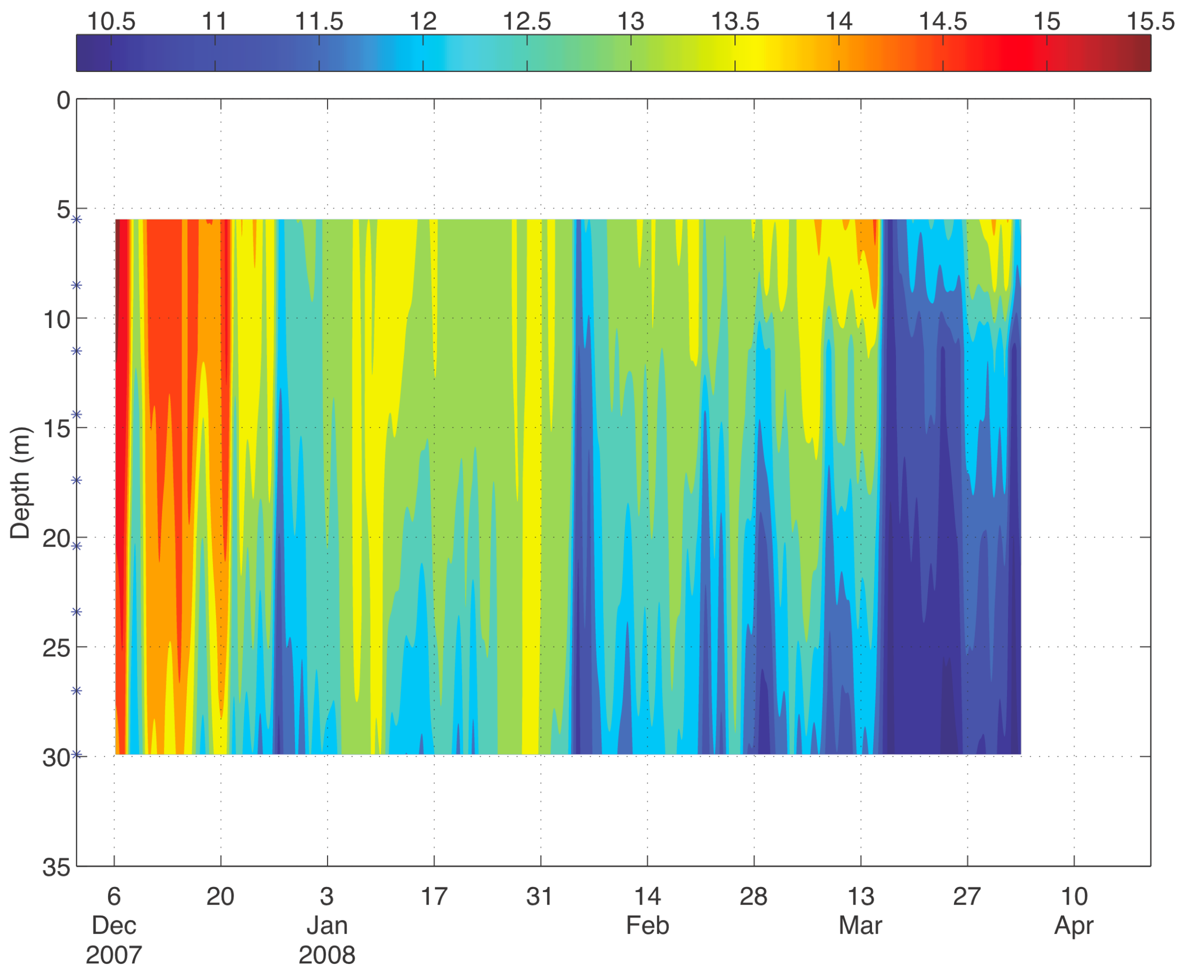


**Figure 27.** Contoured low-pass filtered temperature data from surface and subsurface moorings at Site B7.

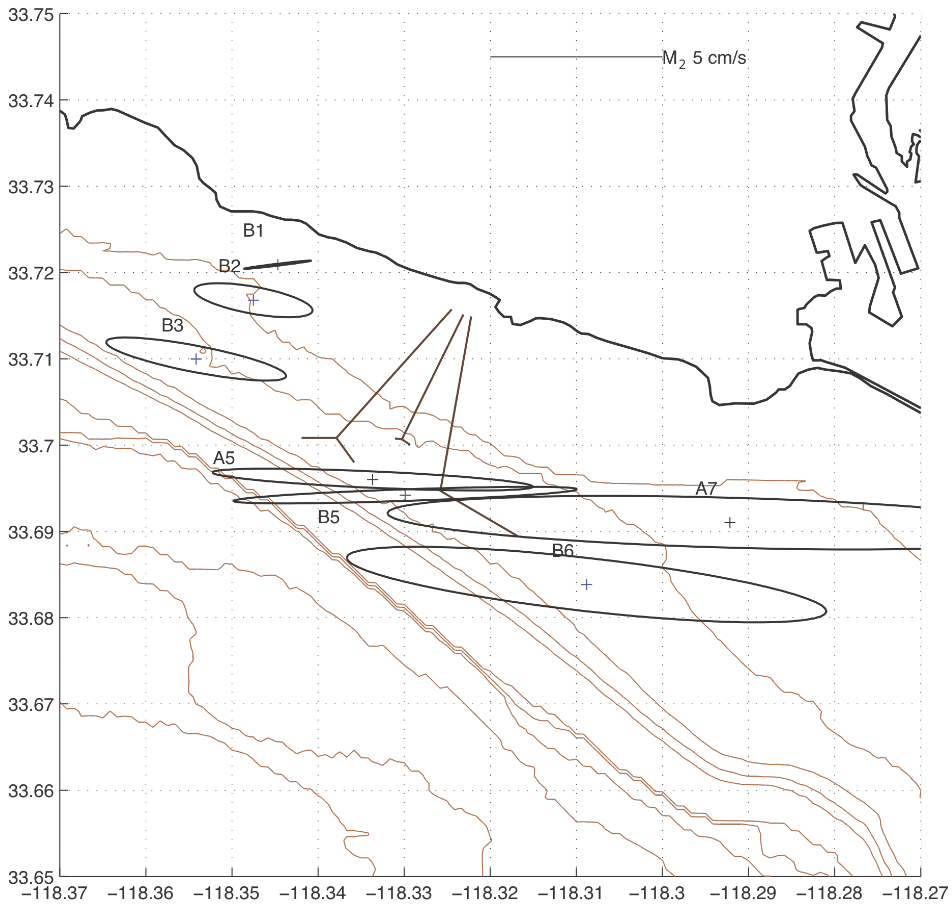


**Figure 28.** Depth-averaged $M_2$ tidal ellipses on the Palos Verdes Shelf from USGS and LACSD ADCP data for the 2007–2008 program. The scale bar denotes the amplitude of the semi-major axis.

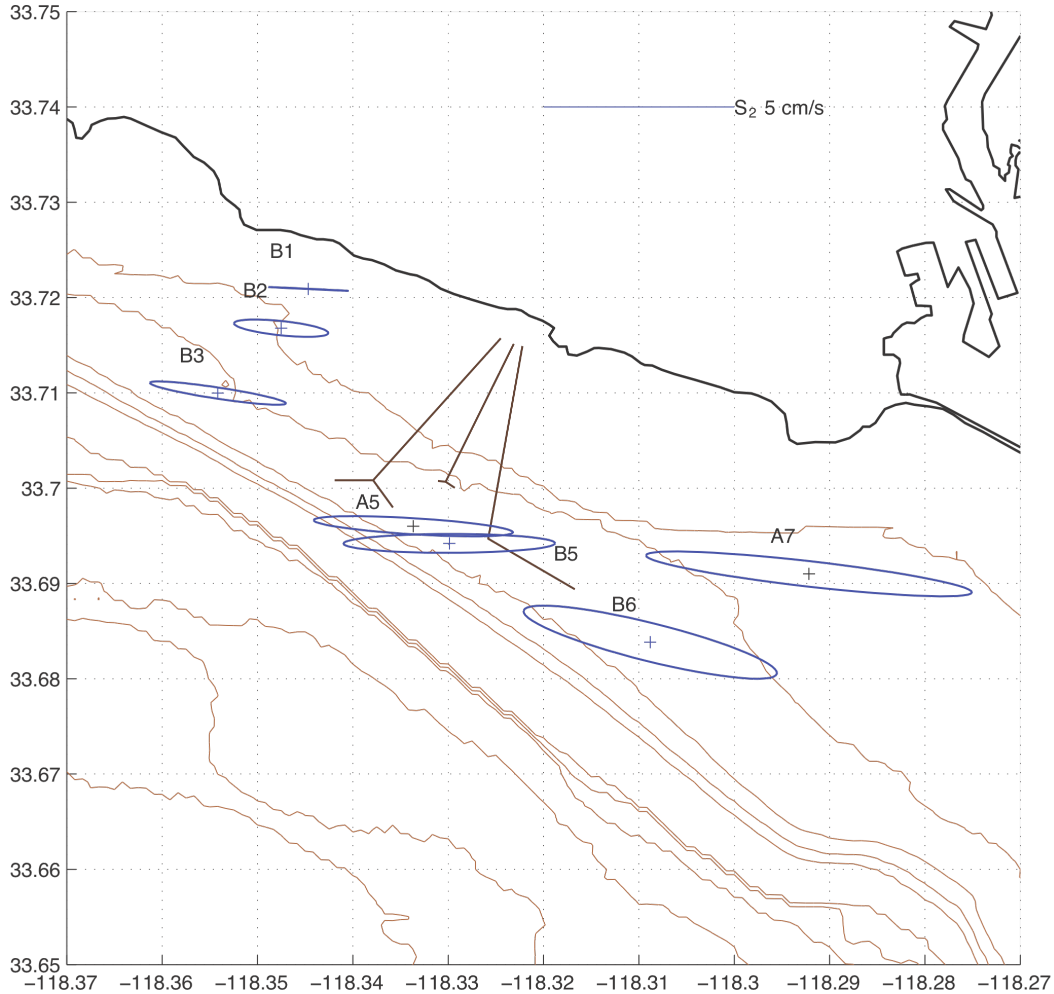


**Figure 29.** Depth-averaged $S_2$ tidal ellipses on the Palos Verdes Shelf from USGS and LACSD ADCP data for the 2007–2008 program. The scale bar denotes the amplitude of the semi-major axis.

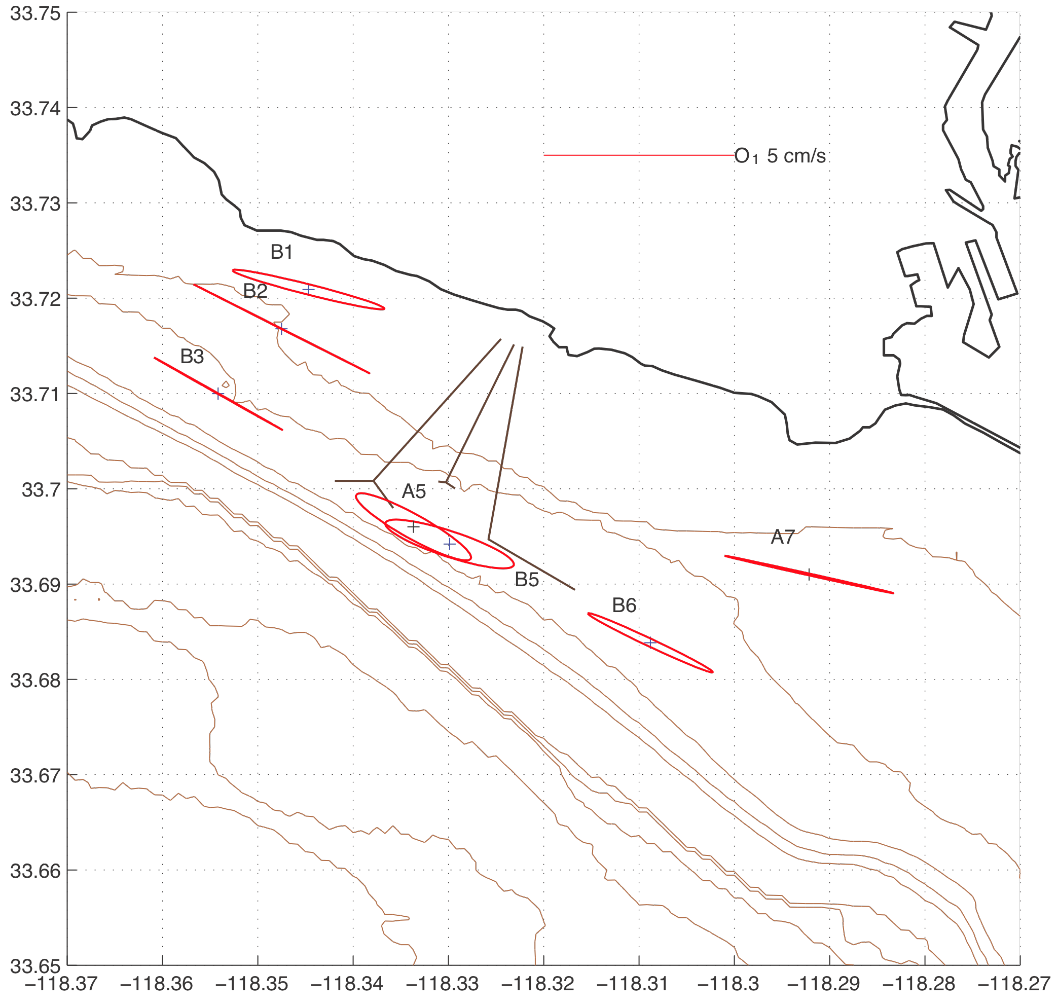


**Figure 30.** Depth-averaged $O_1$ tidal ellipses on the Palos Verdes Shelf from USGS and LACSD ADCP data for the 2007–2008 program. The scale bar denotes the amplitude of the semi-major axis.

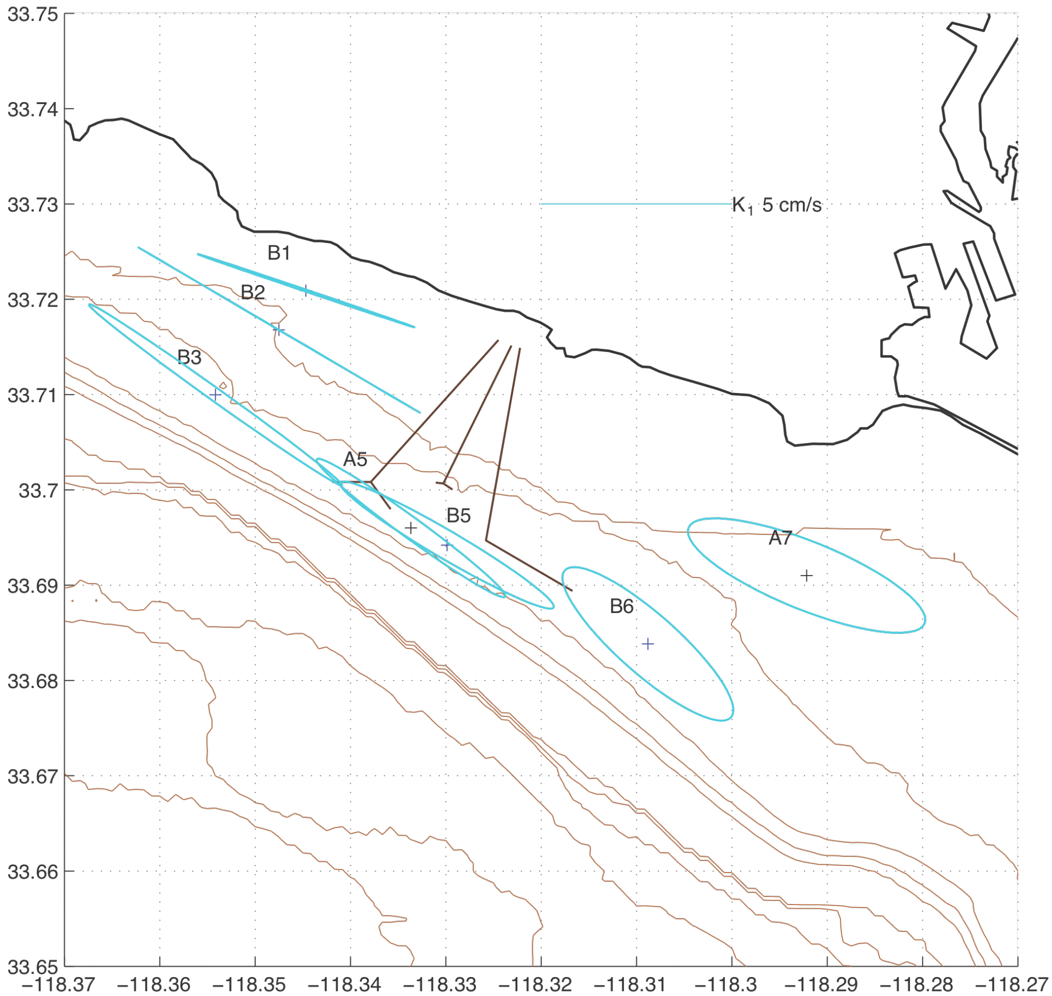


**Figure 31.** Depth-averaged $K_1$ tidal ellipses on the Palos Verdes Shelf from USGS and LACSD ADCP data for the 2007–2008 program. The scale bar denotes the amplitude of the semi-major axis.

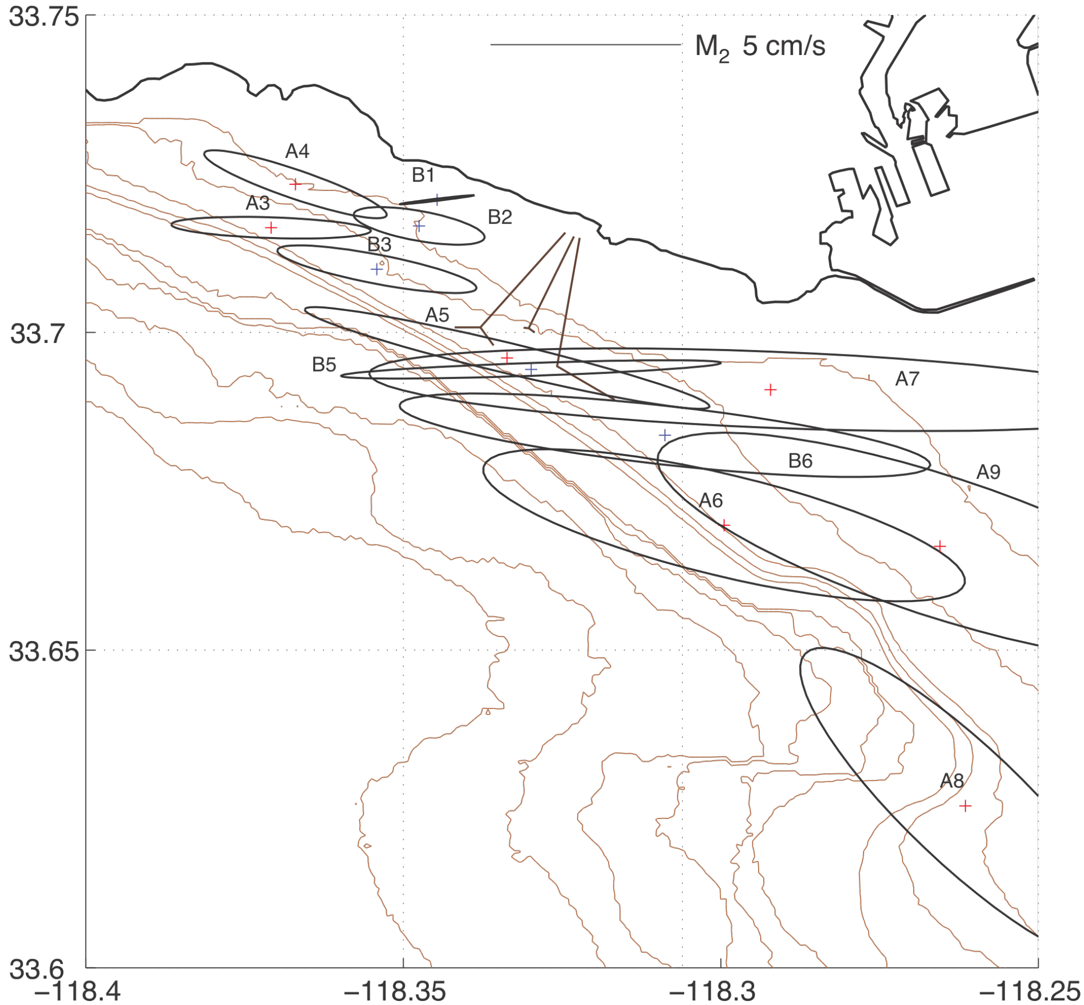


**Figure 32.** Depth-averaged $M_2$ tidal ellipses on the Palos Verdes Shelf from USGS ADCP data for the 2007–2008 program and LACSD long-term ADCP data (2001–2003). The scale bar denotes the amplitude of the semi-major axis.

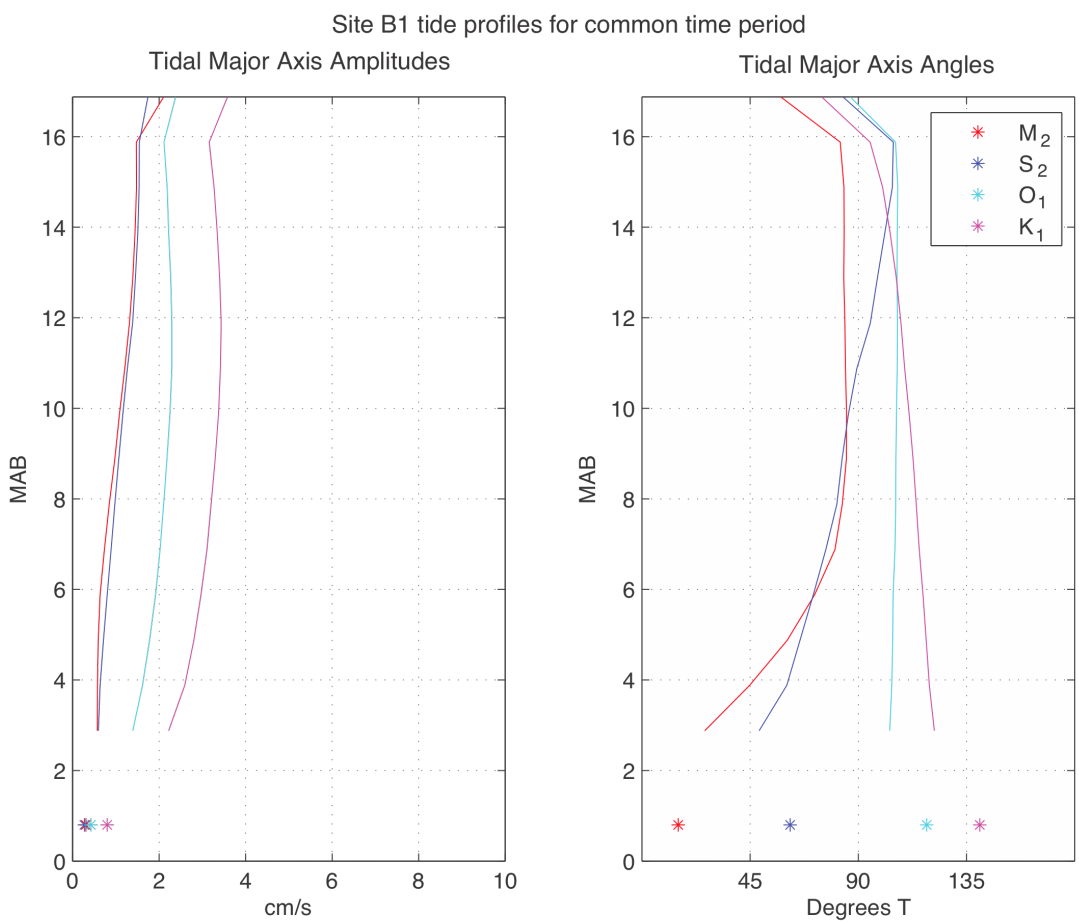


**Figure 33.** Vertical structure of the tidal ellipse major axis for the four major tidal constituents from the ADCP and near-bottom current meter at Site B1. The solid line represents data from the 600-kHz ADCP, and the asterisks represent data from the near-bottom current meter. Major axis angle orientation is listed as clockwise from True North.

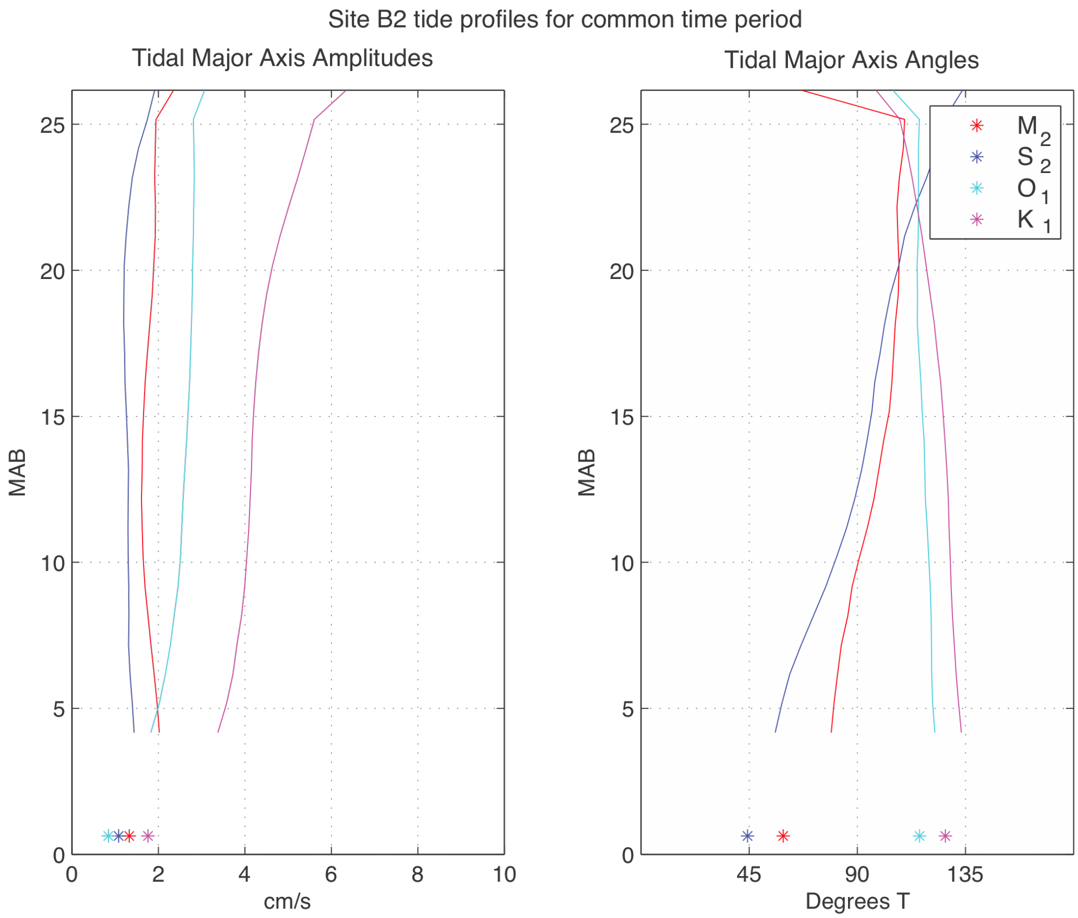


**Figure 34.** Vertical structure of the tidal ellipse major axis for the four major tidal constituents from the ADCP and near-bottom current meter at Site B2. The solid line represents data from the 600-kHz ADCP, and the asterisks represent data from the near-bottom current meter. Major axis angle orientation is listed as clockwise from True North.

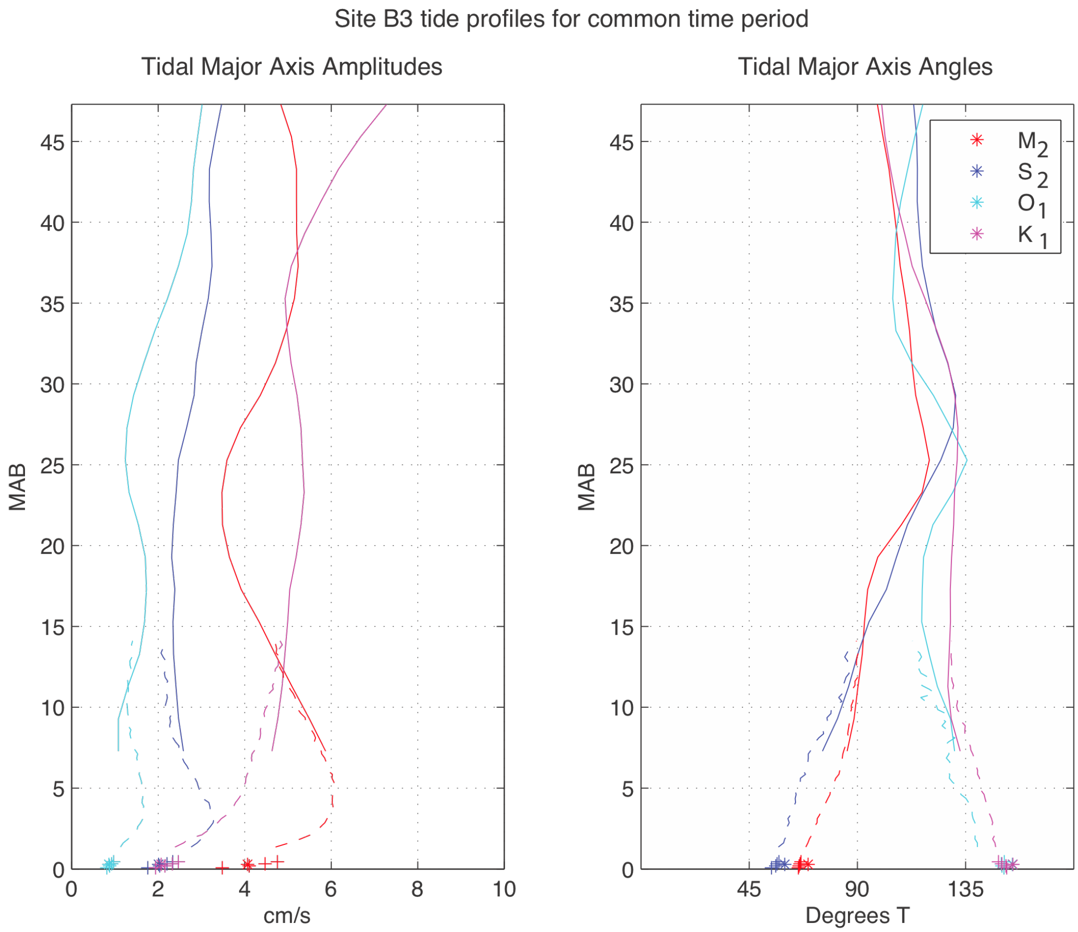


**Figure 35.** Vertical structure of the tidal ellipse major axis for the four major tidal constituents at Site B3 from the 300-kHz ADCP (solid line), near-bottom 1200-kHz ADCP (dashed line), ADV (asterisk), and PCADP (plus signs). Major axis angle orientation is listed as clockwise from True North.

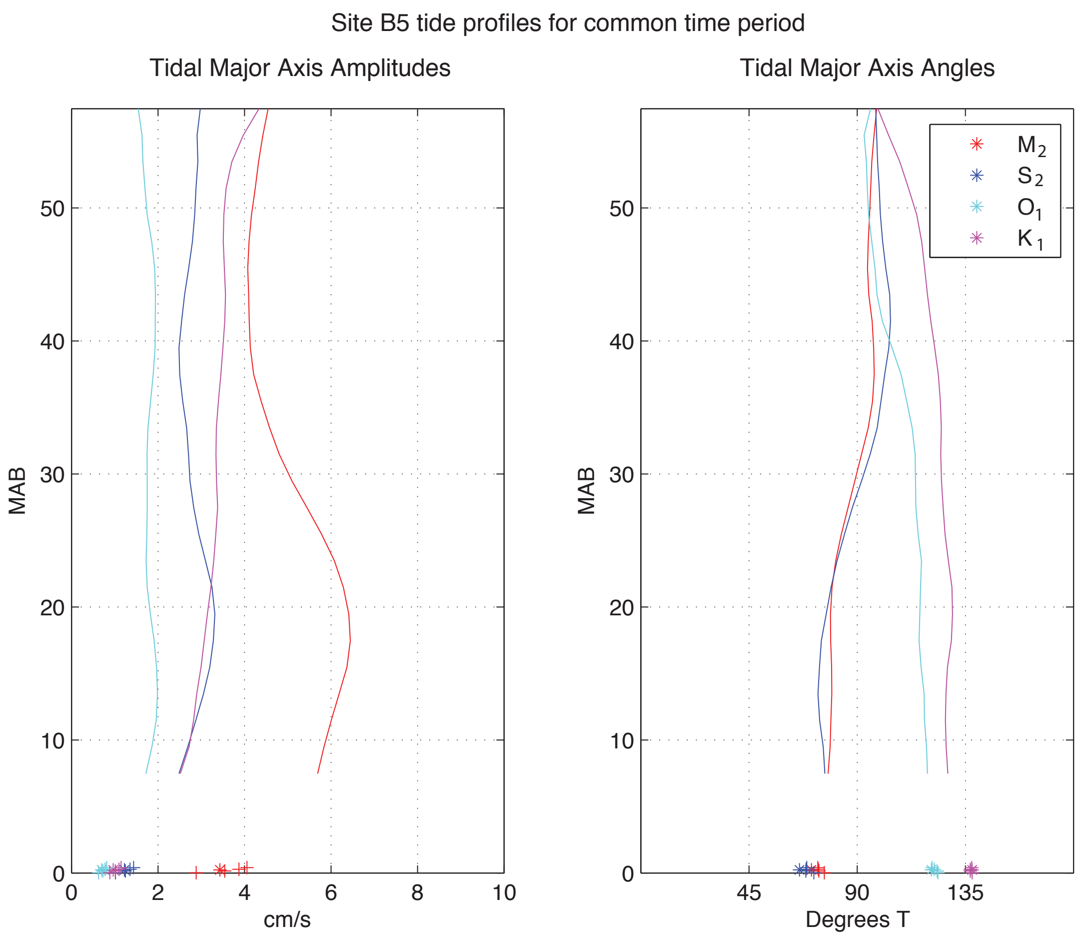


**Figure 36.** Vertical structure of the tidal ellipse major axis for the 4 major tidal constituents at Site B5 from the 300-kHz ADCP (solid line), near-bottom ADV (asterisk), and PCADP (plus signs). Major axis angle orientation is listed as clockwise from True North.

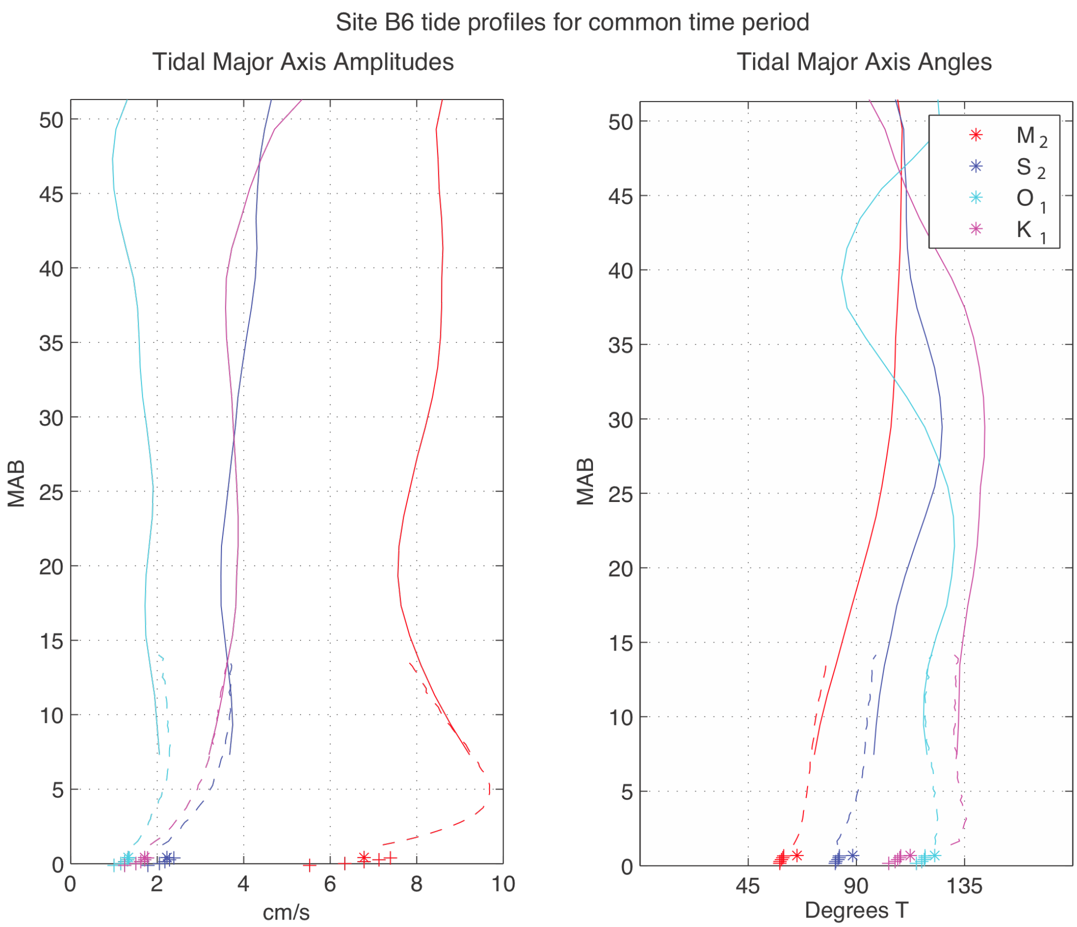


**Figure 37.** Vertical structure of the tidal ellipse major axis for the four major tidal constituents at Site B6 from the 300-kHz ADCP (solid line), near-bottom 1200-kHz ADCP (dashed line), ADV (asterisk), and PCADP (plus signs). Major axis angle orientation is listed as clockwise from True North.

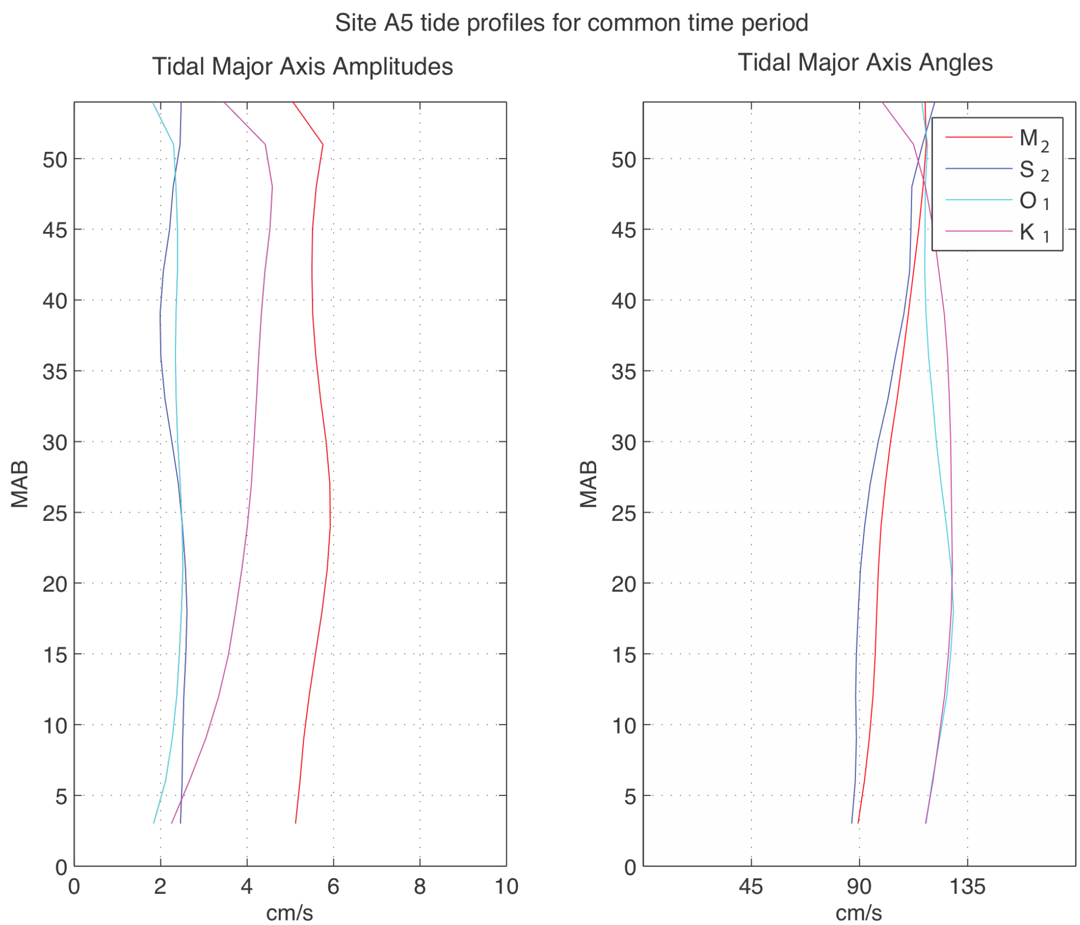


**Figure 38.** Vertical structure of the tidal ellipse major axis for the fourmajor tidal constituents from the long-term LACSD ADCP record (2001–2003) at Site A5. Major axis angle orientation is listed as clockwise from True North.

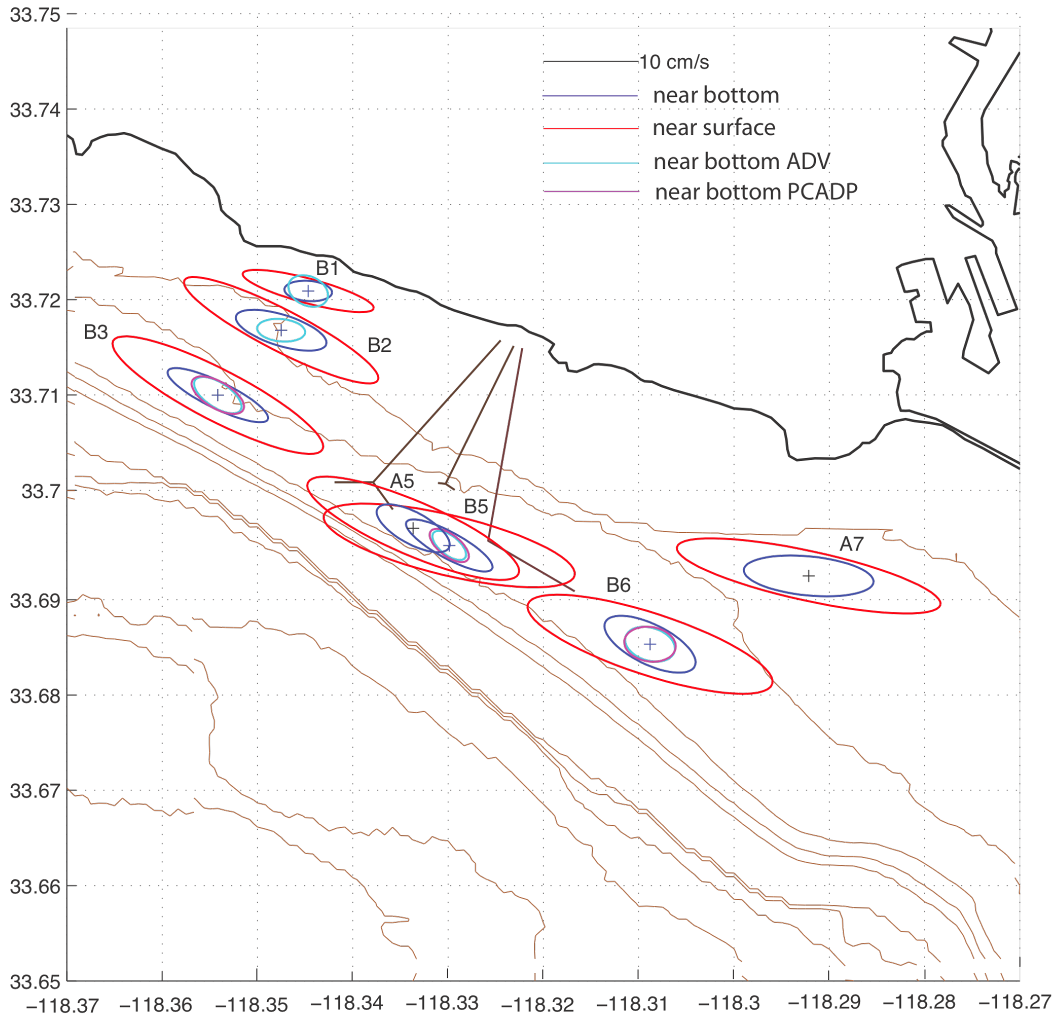


**Figure 39.** Principal component ellipses from depth-averaged, low-pass filtered USGS and LACSD ADCP data for the 2007–2008 measurement program.

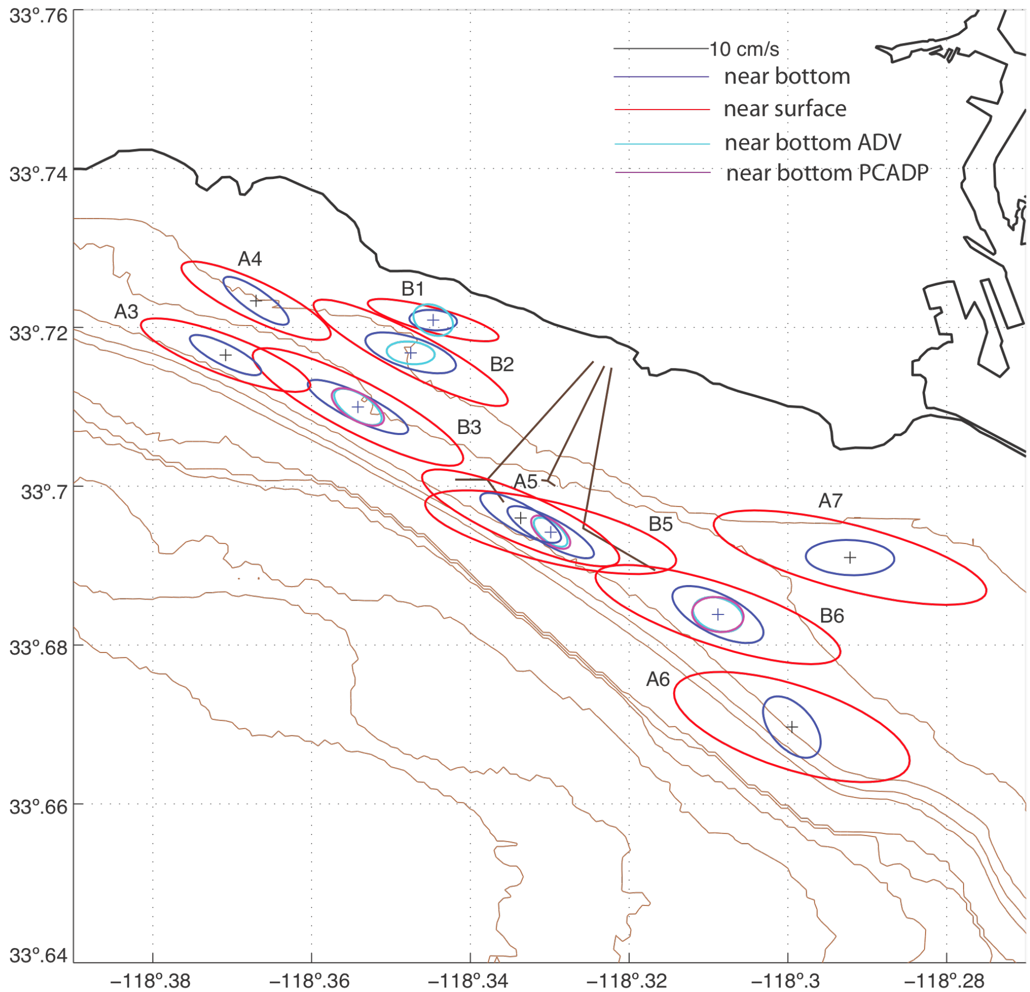


**Figure 40.** Principal component ellipses from depth-averaged, low-pass filtered USGS ADCP data for the 2007–2008 measurement program and the long-term LACSD ADCP data.

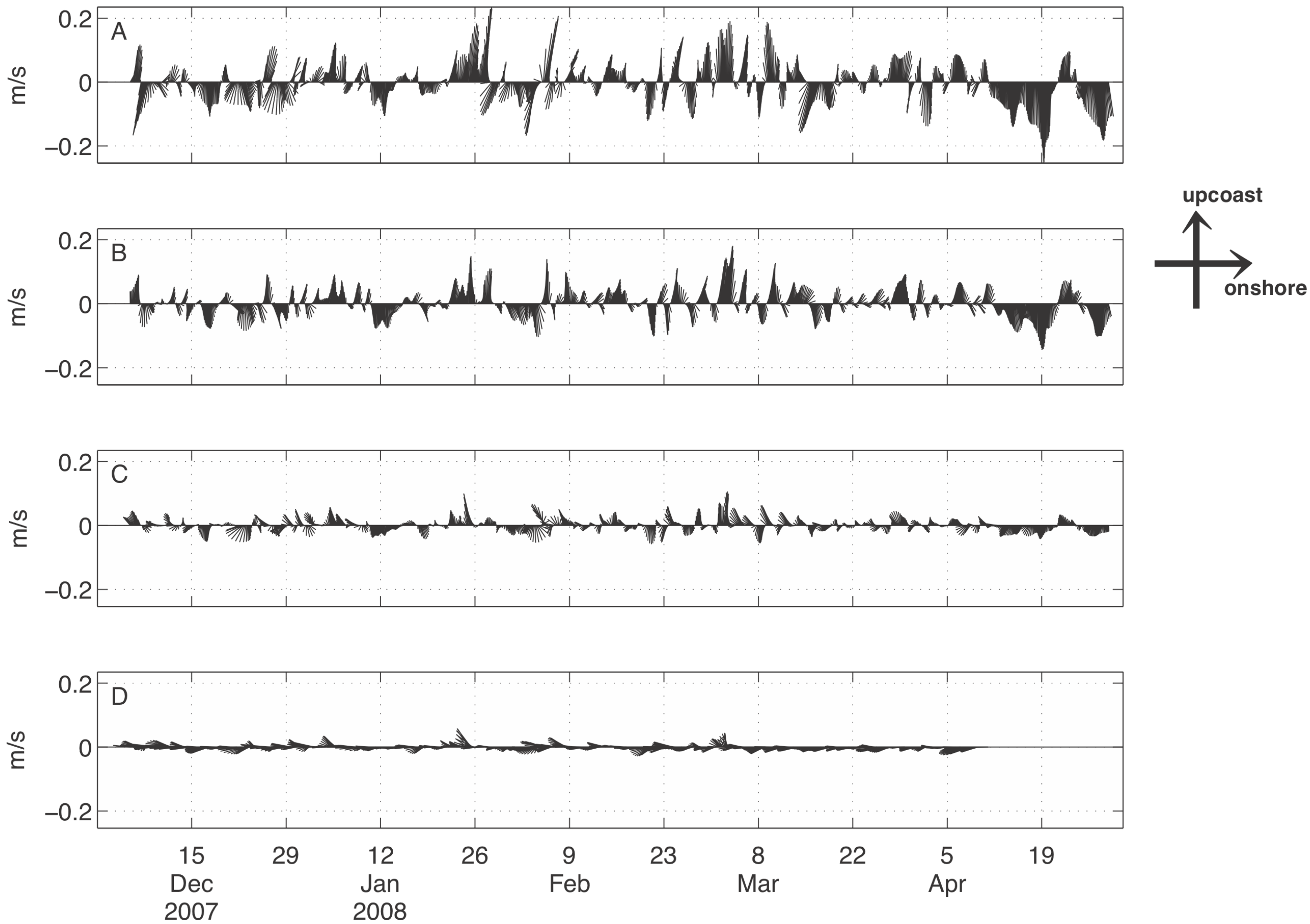


**Figure 41.** Vector plots of low-pass filtered current meter data rotated into along-shore coordinates at (A) the near-surface, (B) mid-water column, (C) near-bottom from the ADCP record, and (D) the near-bottom Aquadopp at Site B1.

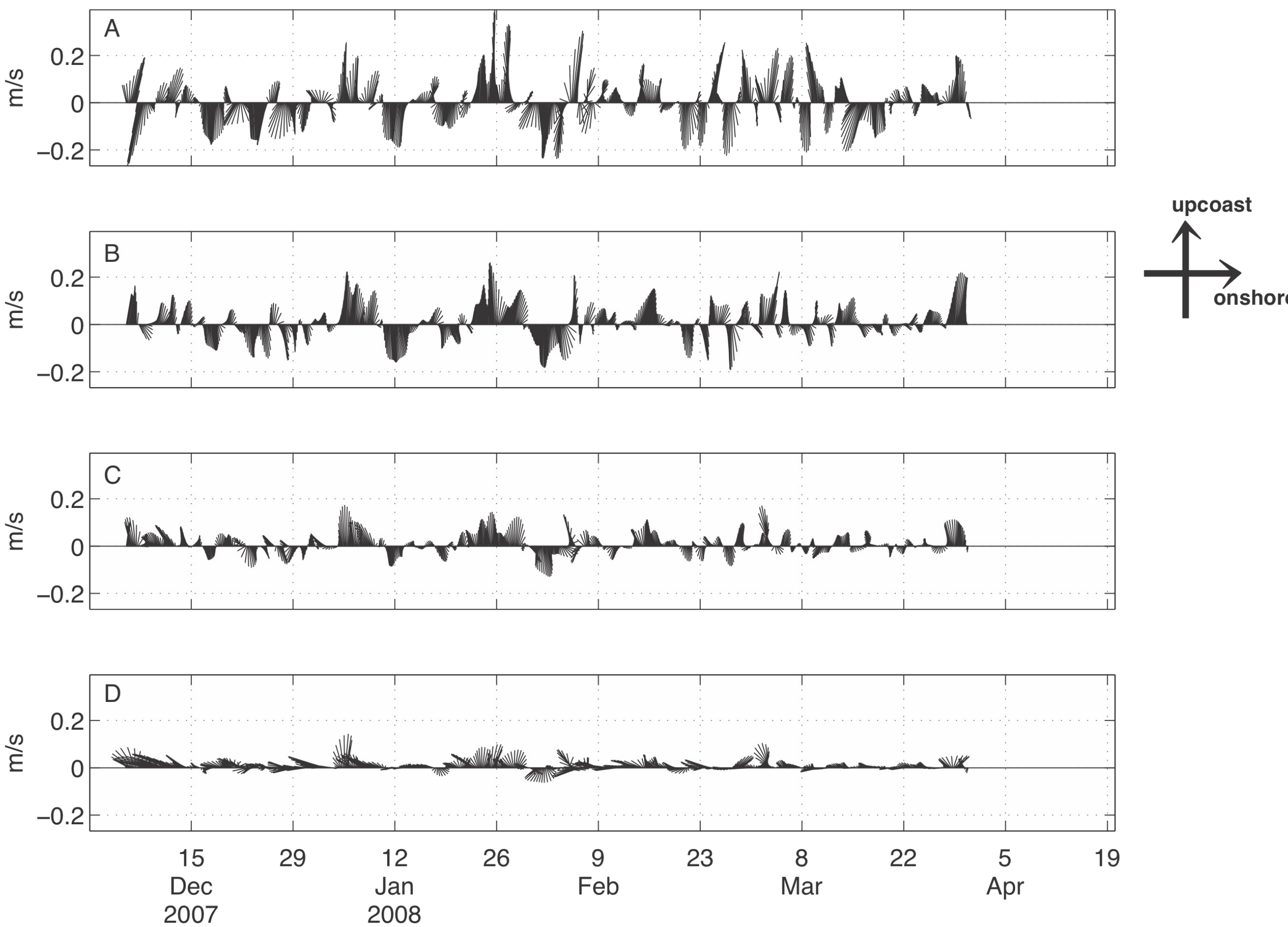


**Figure 42.** Vector plots of low-pass filtered current meter data rotated into along-shore coordinates at (A) the near-surface, (B) mid-water column, (C) near-bottom from the ADCP record, and (D) the near-bottom ADV at Site B2.

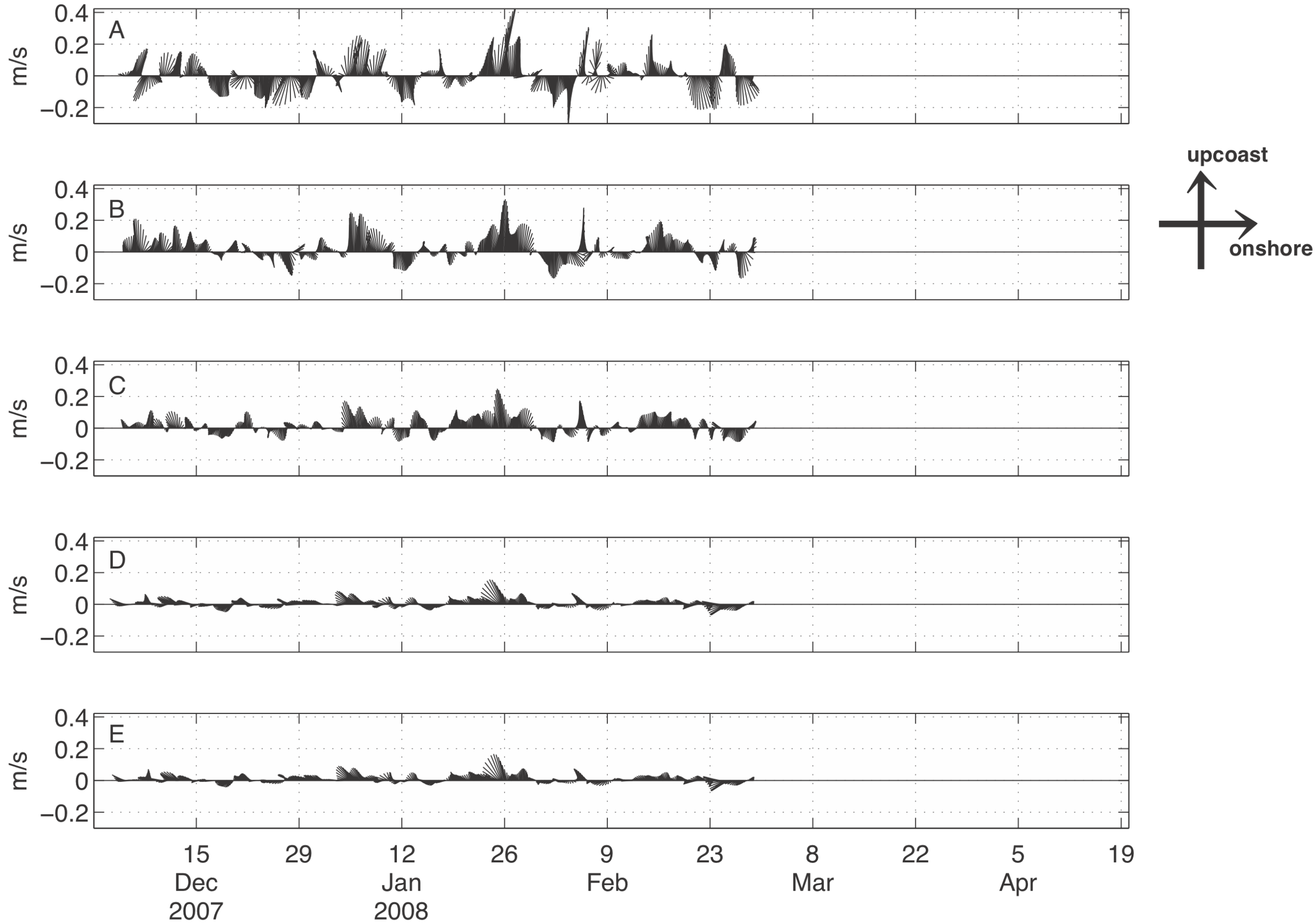


**Figure 43.** Vector plots of low-pass filtered current meter data rotated into along-shore coordinates at (A) the near-surface, (B) mid-water column, C) near-bottom from the ADCP record, (D) the near-bottom PCADP, and (E) the near-bottom ADV at Sit(C B3.

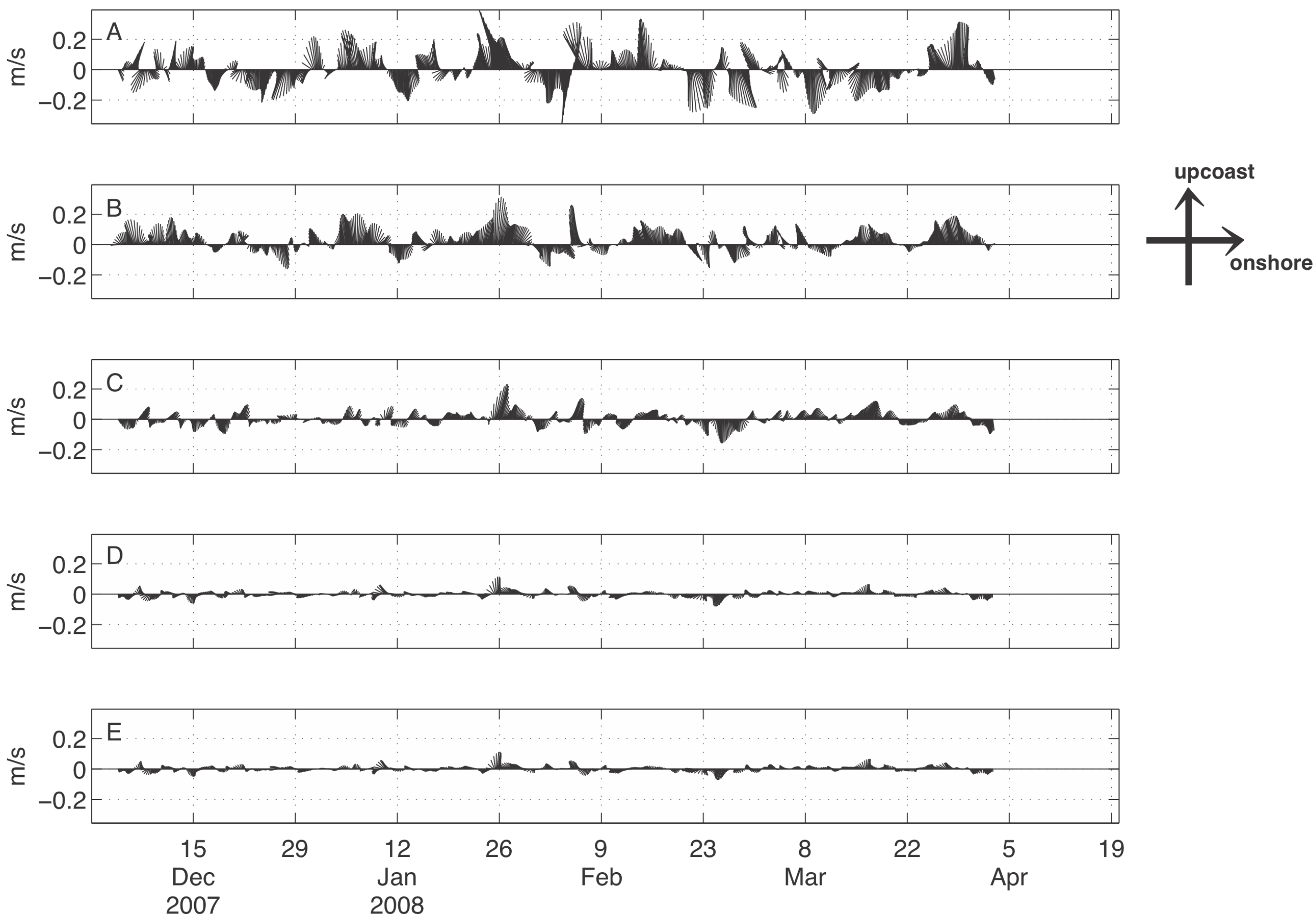


**Figure 44.** Vector plots of low-pass filtered current meter data rotated into along-shore coordinates at (A) the near-surface, (B) mid-water column, (C) near-bottom from the ADCP record,( D) the near-bottom PCADP, and (E) the near-bottom ADV at Site B5.

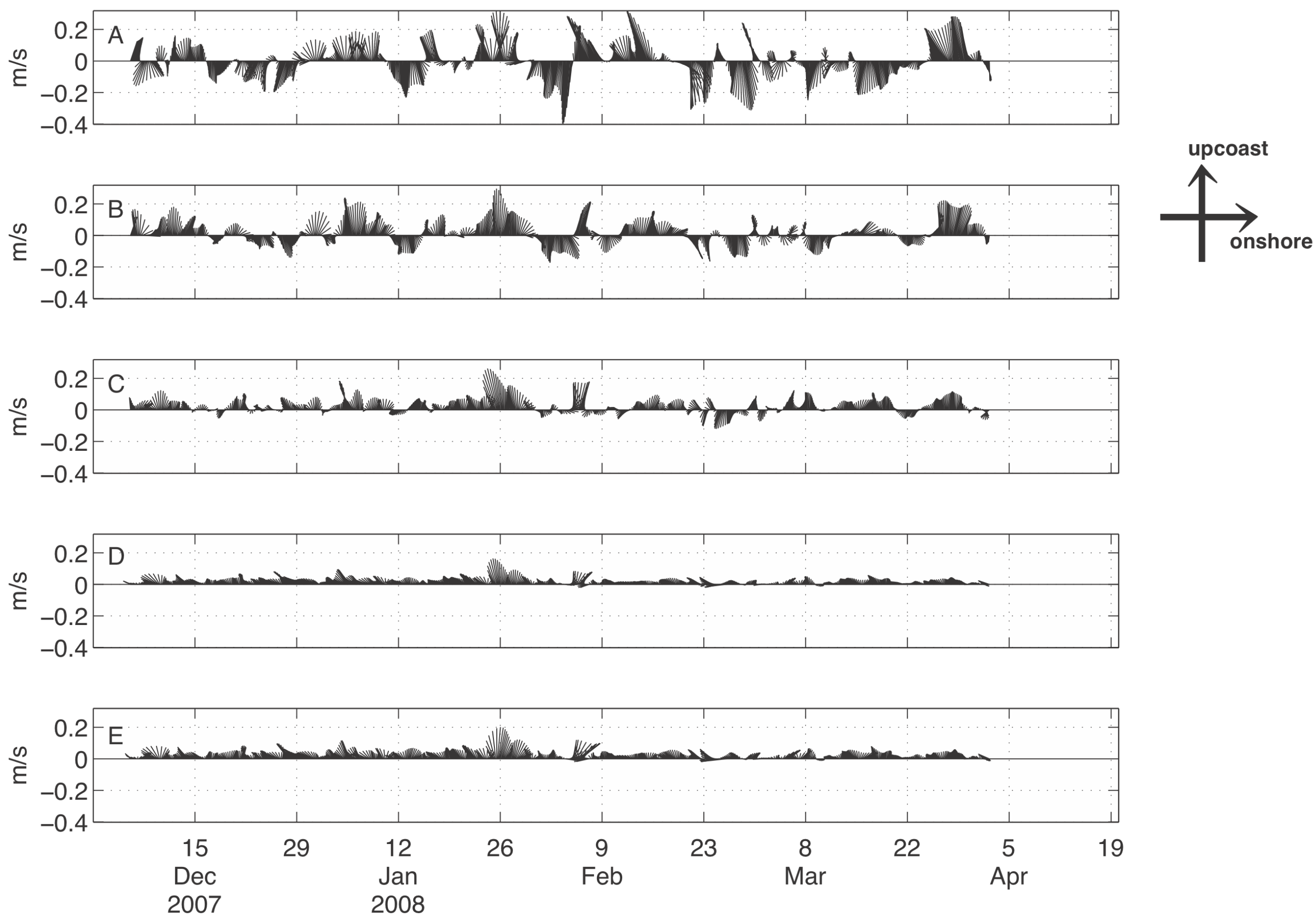


**Figure 45.** Vector plots of low-pass filtered current meter data rotated into along-shore coordinates at (A) the near-surface, (B) mid-water column, (C) near-bottom from the ADCP record, (D) the near-bottom PCADP, and (E) the near-bottom ADV at Site B6.

# Appendix A

## Detailed Examination of Current-meter Data Quality

*Assessment of the accuracy of the amplitude, orientation, and time base for currents measured near the bed by several different instruments deployed in the Palos Verdes Shelf 2007–2008 field program*

A major goal of the USGS field program conducted on the Palos Verdes Shelf in the winter of 2007–2008 was to determine the structure of the velocity profile for currents in the bottom 10 m of the water column. Hence, several types of sensors that monitored near-bottom currents were deployed at five sites on the Palos Verdes Shelf (Sites B1, B2, B3, B5, and B6; fig. 1). Most of the current records were 3–4 months long (fig. 4). A few sensors were damaged after deployment; hence, their records were less than 2 months long. Details on the current sensors are given in tables A-1 and A-2. The types of current sensors follow:

300-kHz ADCP

Currents measured every 2 m from 7 mab to within 7 m of the sea surface. Upward-looking current sensor.

600-kHz ADCP

Currents measured every meter from 2 mab to within 3 m of the sea surface. Upward-looking current sensor.

1,200-kHz ADCP

Currents measured every 0.25 m from 1.4 mab to 15 mab. Upward-looking current sensor.

PCADP

Currents measured every 0.125 m within 0.5 mab.

Downward-looking current sensor.

ADV

Currents measured at one level within 0.6 mab

AQD

Currents measured at one level within 1 mab

Two to four of these current sensors were deployed at each site. Several of the sensors monitored currents in very similar water depths. These measurements were compared in order to determine if there was any error in the amplitude, orientation, or time base in the data gathered by the different sensors.

There was no overlap in the depths of currents measured at Sites B1 and B2 (table A-1). At Site B1, an AQD measured currents 0.8 mab, which was 2.1 m below the lowest current site for the 600-kHz ADCP. At Site B2, an ADV measured currents 0.6 mab, which was 3.6 m below the lowest bin of the 600-kHz ADCP.

Near-bottom currents were measured by different instruments at several common depths at the other sites (table A-1). Four sensors were deployed at Sites B3 and B6. The four lowest bins of the 300-kHz ADCP overlapped the upper bins of the 1,200-kHz ADCP (bins 25–49). The lowest bin of the 1,200-kHz ADCP was located about a meter above the highest bin of the PCADP. The middle bins of the PCADP overlapped the ADV measurement. Only three sensors were deployed at Site B5. The lower bins in the 300-kHz ADV deployed did not overlap any other measurement depth. The middle bins of the PCADP overlapped the ADV, similar to the instrument setups at Sites B3 and B6.

Note that the several instruments measured currents over different vertical depth ranges. The 300-kHz bins were 2 m wide. The bins for the 600-kHz ADCP were 1 m wide. The bin widths for the 1,200-kHz ADCP and the PCADP were 25 and 12.5 cm, respectively. The single-point current meters usually had small measurement volumes.

The general trend of the coastline along the Palos Verdes Shelf was oriented along 295° true (table A-2). The isobaths at the five current measurement sites were generally oriented within 15–20° of the coastline. The subtidal mid-depth current ellipses were generally narrow and oriented between 284° and 295°. Hence the alongshelf /cross-shelf orientation is chosen as 295°/65°. A positive alongshelf current flows toward the northwest. Positive cross-shelf currents flow toward the coast.

## Characteristics of the Measured Near-bottom Currents

The diurnal and semidiurnal tidal currents tended to dominate the near-bottom currents on the Palos Verdes Shelf (fig. A-1). Semidiurnal tidal currents were oriented more across- than along-shelf in shallow water and tended to dominate the near-bottom, cross-shelf current field (table A-3). The diurnal currents were oriented generally along the shelf and were stronger than semidiurnal currents at depths greater than 7 mab (table A-4). Because the tidal currents were strong, their characteristics, calculated using the Foreman tidal programs (Foreman, 1978), were used to compare currents at each site for the several depth levels (fig. A-1).

## Net Current Characteristics

*Site B1:*

The speed, direction, and time base of the two current sensors are too far apart to determine details of the current field, but the measured parameters seem reasonable. All current sensors recorded accurate data.

*Site B2:*

The speed, direction, and time base of the two current sensors are too far apart to determine details of the current field, but the measured parameters seem reasonable. All current sensors recorded accurate data.

*Site B3:*

The speed, direction, and time base of all current sensors are within error bars for the near-bed currents. The measured tidal characteristics suggest that the time base for the PCADP could be 1 h earlier than the real time, but correlation analysis does not support this suggestion. Hence, all current sensors recorded accurate data.

*Site B5:*

The speed, direction, and time base of all current sensors are within error bars for the near-bed currents. All current sensors recorded accurate data.

*Site B6:*

The speeds and time bases for all four current sensors are similar. There is a possibility that the orientation of the PCADP is 5°–9° counterclockwise from the other instruments. The orientations measured by the other sensors are within the error bars of each other. In general, all current sensors recorded accurate data except for a possible direction offset for the PCADP.

## Measurement Details

*Site B1:*

There were no overlapping current measurements. The AQD measured currents at 0.8 mab, with 2.1 m below currents measured by the 600-kHz ADCP. The current measurements are consistent with each other, but too far apart to determine details.

*Site B2:*

There were no overlapping current measurements. The ADV measures currents at 0.6 mab, with 3.6 m below currents measured by the 600-kHz ADCP. The current measurements are consistent with each other, but too far apart to determine details.

*Site B3:*

Three of the four current sensors measured currents from the beginning to nearly the end of the deployment period at Site B3 (fig. 4). The 1,200-kHz ADCP sensor was hit near the end of December. Hence, its record is only 21 days long. The current characteristics were calculated for all instruments during the common December time period. The characteristics were also calculated for the three instruments that lasted for the entire deployment period.

The comparison among the near-bed semidiurnal and diurnal tidal currents indicated that all sensors reported similar speeds and current orientations at the many common measurement depths for the December time period. There is a suggestion that the currents measured by the PCADP exceed currents measured by the other sensors by an hour (tables A-3 and A-4). However, the tides calculated using the Foreman tidal programs accounted for less than 35 percent of the energy in the major tidal bands. The coherence among the records at the diurnal and semidiurnal tidal frequencies show no significant phase shift, nor was there any significant lag in the correlations among the records. Hence, it is probable that there is no error in the time bases of the PCADP.

Overlapping current measurements over the entire time period were obtained from the PCADP and the ADV, which have current sensors within 1 m of the bed. The tidal characteristics observed during this period were very similar to those measured in December. There were no significant differences in either the speed, orientation, or phase of the tidal currents. In addition, the orientations of the subtidal ellipses were similar in magnitude and direction.

*Site B5:*

The only instruments that measured currents at similar vertical locations were the ADV and PCADP. The tidal-current characteristics suggested that the ADV measured the same current field as bin 3 of the PCADP. This is only one bin (12 cm) lower than the predicted bin. Tidal currents in the ADCP were a bit larger than, but had a similar orientation to, those measured by the PCADP. The subtidal ellipses for the PCADP and the ADV had the same orientation, and speeds were within 0.4 cm/s. This suggests all instruments had good speed, direction, and time bases.

*Site B6:*

Three of the four current sensors measured currents from the beginning to nearly the end of the deployment period at Site B3 (fig. 4). The 1,200-kHz ADCP sensor was either hit or damaged in a major storm near the end of February. Hence, its record is short, but not nearly as short as the 1,200-kHz ADCP record at Site B3. The characteristics of the currents are calculated for the common time period between December and March and for the full time period.

The comparison among the near-bed semidiurnal and diurnal tidal currents indicated that all sensors recorded similar speeds and had the same time base at the many common measurement depths for the December through March time period. However, the currents measured by the PCADP seem to be rotated about 5° counterclockwise of currents measured by the other sensors. The rotation angle seems constant over the small depth range of the PCADP. This rotation angle is on the edge of the error bars, but might be significant.

The subtidal current ellipses measured at the overlapped bins on the 1,200- and 300-kHz ADCPs have very similar major axis amplitudes and orientations. The speeds seem to be within 0.5 cm/s, and the orientations within 1° of each other. The subtidal ellipses for the ADV and PCADP have similar amplitudes, but the PCADP is 10° counterclockwise of the ADV (similar to the tidal offset).

The tidal characteristics measured over the full record are similar to those measured in the slightly shorter record.

**Table A-1.** Depth above the seabed for currents measured at five sites on the Palos Verdes Shelf during the winter of 2007–2008.

| **Site B1 (19.7 m)** | | | |
|---|---|---|---|
| 600-kHz ADCP | | Aquadopp | |
| Bin | Depth above the seabed (m) | Bin | Depth above the seabed (m) |
| 1 | 2.9 | | |
| | | 1 | 0.8 |

| **Site B2 (29.6 m)** | | | |
|---|---|---|---|
| 600-kHz ADCP | | ADV | |
| Bin | Depth above the seabed (m) | Bin | Depth above the seabed (m) |
| 1 | 4.2 | | |
| | | 1 | 0.6 |

**Table A-1, cont.**

| **Site B3 (53.9 m and 56.0 m (1200-kHz ADCP))** | | | |
|---|---|---|---|
| 300-kHz ADCP | | 1200-kHz ADCP | |
| Bin | Depth above the seabed (m) | Bin | Depth above the seabed (m) |
| 4 | 13.3 | 49 | 13.4 |
| | | 48 | 13.1 |
| 3 | 11.3 | 41 | 11.4 |
| | | 40 | 11.1 |
| 2 | 9.3 | 33 | 9.4 |
| | | 32 | 9.1 |
| 1 | 7.3 | 25 | 7.4 |
| | | 24 | 7.1 |
| 1200-kHz ADCP | | PCADP | |
| 1 | 1.4 | | |
| | | 1 | 0.4 |
| PCADP | | ADV | |
| 2 | 0.32 | 1 | 0.28 |
| 3 | 0.19 | | |

| **Site B5 (66.7 m)** | | | |
|---|---|---|---|
| 300-kHz ADCP | | | |
| Bin | Depth above the seabed (m) | Bin | Depth above the seabed (m) |
| 1 | 7.3 | | |
| PCADP | | ADV | |
| 2 | 0.28 | 1 | 0.23 |
| 3 | 0.15 | | |

**Table A-1, cont.**

| **Site B6<br>(57.59 m and 59.26 m (1200-kHz ADCP))** | | | |
|---|---|---|---|
| 300-kHz ADCP | | 1200-kHz ADCP | |
| Bin | Depth above the seabed (m) | Bin | Depth above the seabed (m) |
| 4 | 13.3 | 49 | 13.4 |
| | | 48 | 13.0 |
| 3 | 11.3 | 41 | 11.3 |
| | | 40 | 11.0 |
| 2 | 9.3 | 33 | 9.3 |
| | | 32 | 9.0 |
| 1 | 7.3 | 25 | 7.3 |
| | | 24 | 7.0 |
| 1200-kHz ADCP | | PCADP | |
| 1 | 1.25 | | |
| | | 1 | 0.53 |
| PCADP | | ADV | |
| 1 | 0.53 | 1 | 0.55 |

**Table A-2.** Topographic characteristics, subtidal mid-water-column current orientation, and measurement depths for instruments deployed on the Palos Verdes Shelf in the winter of 2007–2008. The alongshelf orientation for currents is 295°. Positive currents flow toward the northwest. Current measurements were collected by 600- and 300-kHz ADCPs.

| Site | Water depth (m) | Isobath angle (rotation angle) (deg) | ADCP subtidal mid-depth angle (deg) | Depth Bin 1 (mab)<br>Depth (top bin)<br>Bin width |
|---|---|---|---|---|
| Coastline | 0 | 295 (65) | | |
| B1 | 19.7 | 298 (62) | 285 | 16.8 (2.9 mab)<br>1.8 (16)<br>1 m |
| B2 | 29.6 | 300 (60) | 295 | 25.45 (4.2 mab)<br>3.45 (23)<br>1 m |
| B3 | 53.9 | 302 (58) | 294 | 46.6 (7.3 mab)<br>6.6 (21)<br>2 m |
| B5 | 65.7 | 302 (58) | 284 | 58.2 (7.5 mab)<br>6.2 (27)<br>2 m |
| B6 | 57.6 | 315 (45) | 293 | 50.3 (7.3 mab)<br>6.3 (23)<br>2 m |

**Table A-3.** Semidiurnal tidal characteristics for near-bed currents at Sites B1–B6. Orientation is counterclockwise from alongshore (115°/295°). Hence an orientation of 90° is cross-shelf. The site with the smaller phase leads the site with the larger.

**Site B1**

There were no overlapping current measurements. The current measurements are consistent with each other, but too far apart to determine details.

**AQD vs 600-kHz ADCP**

**Whole record**

$M_2$ tidal component

| AQD | MJ (cm/s) | Inc (deg) | Phase (deg) | ADCP (bin) | MJ ((cm/s)) | Inc (deg) | Phase (deg) |
|---|---|---|---|---|---|---|---|
| | | | | 3 | 0.6 | 54 | 102 |
| | | | | 2 | 0.6 | 69 | 119 |
| 1* | 0.3 | -81 | 155 | 1 | 0.6 | 88 | 137 |

*AQD measurement is 2.1 m below first ADCP bin.

**Site B2**

There were no overlapping current measurements. The current measurements are consistent with each other, but too far apart to determine details.

**ADV vs 600-kHz ADCP**

**Whole record**

$M_2$ tidal component

| ADV | MJ ((cm/s)) | Inc (deg) | Phase (deg) | ADCP (bin) | MJ ((cm/s)) | Inc (deg) | Phase (deg) |
|---|---|---|---|---|---|---|---|
| | | | | 3 | 1.8 | 33 | 89 |
| | | | | 2 | 1.9 | 35 | 91 |
| 1* | 1.3 | 56 | 93 | 1 | 2.0 | 36 | 92 |

*The ADV measures 3.6 m below the first bin of the ADCP.

**Table A-3, cont.**

**Site B3**

During December time period when the 1200-kHz ADCP data is good. In general, the error bars are 1 cm/s for speed, 10° for inclination and 15–20° for phase.

**1200-kHz ADP vs 300-kHz ADCP**

**December time period**

$M_2$ tidal currents

| 1200-kHz ADCP (bin) | MJ (cm/s) | Inc (deg) | Phase (deg) | 300-kHz ADCP (bin) | MJ (cm/s) | Inc (deg) | Phase (deg) |
|---|---|---|---|---|---|---|---|
| 41 | 4.74 | 26 | 45 | 3 | 4.82 | 25 | 41 |
| 33 | 5.11 | 28 | 43 | 2 | 5.19 | 26 | 41 |
| 25 | 5.46 | 30 | 41 | 1 | 5.54 | 29 | 38 |

**PCADP vs 1200-kHz ADCP**

$M_2$ tidal component

| PCADP (bin) | MJ (cm/s) | Inc (deg) | Phase (deg) | ADCP (bin) | MJ (cm/s) | Inc (deg) | Phase (deg) |
|---|---|---|---|---|---|---|---|
| | | | | 2 | 4.80 | 45 | 26 |
| 1 * | 4.74 | 49 | 0 | 1 | 4.50 | 46 | 25 |
| 2 | 4.45 | 49 | 0 | | | | |
| 3 | 4.09 | 49 | 0 | | | | |

*Bin 1 m deeper than first bin of the ADCP

**ADV vs PCADP**

$M_2$ tidal component

| ADV | MJ (cm/s) | Inc (deg) | Phase (deg) | PCADP (bin) | MJ (cm/s) | Inc (deg) | Phase (deg) |
|---|---|---|---|---|---|---|---|
| | | | | 2 | 4.45 | 49 | 0 |
| 1 | 4.04 | 45 | 29 | 3 | 4.09 | 49 | 0 |
| | | | | 4 | 3.47 | 49 | 0 |

**Table A-3, cont.**

**PCADP vs 300-kHz ADCP**

**Full Record**

$M_2$ tidal component

| PCADP (bin) | MJ (cm/s) | Inc (deg) | Phase (deg) | ADCP (bin) | MJ (cm/s) | Inc (deg) | Phase (deg) |
|---|---|---|---|---|---|---|---|
| | | | | 2 | 4.17 | 36 | 56 |
| 1 * | 3.89 | 47 | 20 | 1 | 4.52 | 33 | 58 |
| 2 | 3.65 | 47 | 3.65 | | | | |
| 3 | 3.34 | 47 | 3.34 | | | | |

*Bn 6.9 m deeper than first bin of the ADCP

**ADV vs PCADP**

$M_2$ tidal component

| ADV | MJ (cm/s) | Inc (deg) | Phase (deg) | PCADP (bin) | MJ (cm/s) | Inc (deg) | Phase (deg) |
|---|---|---|---|---|---|---|---|
| | | | | 2 | 3.65 | 47 | 20 |
| 1 | 3.36 | 43 | 50 | 3 | 3.34 | 47 | 20 |
| | | | | 4 | 2.79 | 47 | 20 |

**Site B5**

**PCADP vs 300-kHz ADCP**

**Whole record**

$M_2$ tidal component

| PCADP (bin) | MJ (cm/s) | Inc (deg) | Phase (deg) | ADCP (bin) | MJ (cm/s) | Inc (deg) | Phase (deg) |
|---|---|---|---|---|---|---|---|
| | | | | 3 | 5.9 | 36 | 32 |
| | | | | 2 | 5.7 | 36 | 28 |
| | | | | 1 | 5.6 | 37 | 24 |
| 1* | 4.0 | 41 | 346 | | | | |
| 2 | 3.9 | 41 | 345 | | | | |
| 3 | 3.5 | 41 | 345 | | | | |

*PCADP bin 1 is 6.9 m below the ADCP

**Table A-3, cont.**

**ADV vs PCADP**

$M_2$ tidal component

| ADV | MJ (cm/s) | Inc (deg) | Phase (deg) | PCADP (bin) | MJ (cm/s) | Inc (deg) | Phase (deg) |
|---|---|---|---|---|---|---|---|
| | | | | 2 | 3.9 | 41 | 345 |
| 1 | 3.4 | 44 | 347 | 3 | 3.5 | 41 | 345 |
| | | | | 4 | 2.9 | 39 | 344 |

**Site B6**

Tidal characteristics calculated for the December to March and the December to April time periods. In general the error bars are less than 1 cm/s on speed, 6° on inclination and 10° on phase.

**1200-kHz ADP vs 300-kHz ADCP**

**December–March**

$M_2$ tidal currents

| 1200-kHz ADCP (bin) | MJ (cm/s) | Inc (deg) | Phase (deg) | 300-kHz ADCP (bin) | MJ (cm/s) | Inc (deg) | Phase (deg) |
|---|---|---|---|---|---|---|---|
| 41 | 8.0 | 40 | 29 | 3 | 8.1 | 37 | 28 |
| 33 | 8.4 | 42 | 29 | 2 | 8.4 | 40 | 29 |
| 25 | 8.9 | 44 | 28 | 1 | 8.9 | 42 | 30 |

**PCADP vs 1200-kHz ADCP**

$M_2$ tidal component

| PCADP (bin) | MJ (cm/s) | Inc (deg) | Phase (deg) | ADCP (bin) | MJ (cm/s) | Inc (deg) | Phase (deg) |
|---|---|---|---|---|---|---|---|
| | | | | 2 | 7.3 | 50 | 26 |
| | | | | 1 | 6.9 | 51 | 26 |
| 1* | 7.4 | 55 | 1 | | | | |
| 2 | 7.1 | 56 | 2 | | | | |
| 3 | 6.8 | 56 | 2 | | | | |

*Bin 1.7 m deeper than first bin of the ADCP.

**Table A-4.** Diurnal tidal characteristics for near-bed currents at Sites B1–B6. Orientation is counterclockwise from alongshore (115/295°). Hence an orientation of 90° is cross-shelf. The site with the smaller phase leads the site with the larger.

**Site B1**

There were no overlapping current measurements. The current measurements are consistent with each other, but too far apart to determine details.

**AQD vs 600-kHz ADCP**

**Whole record**

$K_1$ tidal component

| AQD | MJ (cm/s) | Inc (deg) | Phase (deg) | ADCP (bin) | MJ (cm/s) | Inc (deg) | Phase (deg) |
|---|---|---|---|---|---|---|---|
| | | | | 3 | 2.8 | -3 | 136 |
| | | | | 2 | 2.6 | -5 | 134 |
| 1* | 0.8 | -26 | 132 | 1 | 2.2 | -7 | 132 |

*AQD measurement is 2.1 m below first ADCP bin.

**Site B2**

There were no overlapping current measurements. The current measurements are consistent with each other, but too far apart to determine details.

**ADV vs 600-kHz ADCP**

**Whole record**

$K_1$ tidal component

| ADV | MJ (cm/s) | Inc (deg) | Phase (deg) | ADCP (bin) | MJ (cm/s) | Inc (deg) | Phase (deg) |
|---|---|---|---|---|---|---|---|
| | | | | 3 | 3.7 | -16 | 166 |
| | | | | 2 | 3.6 | -17 | 165 |
| 1* | 1.8 | -12 | 149 | 1 | 3.3 | -18 | 162 |

*The ADV measures 3.6 m below the first bin of the ADCP.

**Table A-4, cont.**

**Site B3**

During December time period when the 1200-kHz ADCP data is good. In general the error bars are less than 1 cm/s for speed, 10° for inclination, and 15–20° for phase.

**1200-kHz ADCP vs 300-kHz ADCP**

**December time period**

$K_1$ tidal currents

| 1200-kHz ADCP (bin) | MJ (cm/s) | Inc (deg) | Phase (deg) | 300-kHz ADCP (bin) | MJ (cm/s) | Inc (deg) | Phase (deg) |
|---|---|---|---|---|---|---|---|
| 41 | 4.61 | -15 | 138 | 3 | 4.84 | 143 | -19 |
| 33 | 4.43 | -17 | 139 | 2 | 4.74 | 141 | -17 |
| 25 | 4.20 | -22 | 142 | 1 | 4.60 | 138 | -16 |

**PCADP vs 1200-kHz ADCP**

$K_1$ tidal component

| PCADP (bin) | MJ (cm/s) | Inc (deg) | Phase (deg) | ADCP (bin) | MJ (cm/s) | Inc (deg) | Phase (deg) |
|---|---|---|---|---|---|---|---|
| | | | | 2 | 2.55 | -32 | 148 |
| 1 * | 2.46 | -34 | 127 | 1 | 2.35 | -33 | 149 |
| 2 | 2.32 | -35 | 129 | | | | |
| 3 | 2.14 | -37 | 130 | | | | |

* Bin 1 m deeper than the ADCP bin 1.

**ADV vs PCADP**

| ADV | MJ (cm/s) | Inc (deg) | Phase (deg) | PCADP (bin) | MJ (cm/s) | Inc (deg) | Phase (deg) |
|---|---|---|---|---|---|---|---|
| | | | | 2 | 2.32 | -35 | 129 |
| 1 | 2.06 | -40 | 144 | 3 | 2.14 | -37 | 130 |
| | | | | 4 | 1.93 | -37 | 130 |

**PCADP vs 300-kHz ADCP**

**Whole record**

$K_1$ tidal component

| PCADP (bin) | MJ (cm/s) | Inc (deg) | Phase (deg) | ADCP (bin) | MJ (cm/s) | Inc (deg) | Phase (deg) |
|---|---|---|---|---|---|---|---|
| | | | | 2 | 3.68 | -14 | 166 |
| 1 * | 2.2 | -20 | 148 | 1 | 3.56 | -16 | 166 |
| 2 | 2.1 | -20 | 148 | | | | |
| 3 | 1.9 | -21 | 148 | | | | |

*Bin 6.9 m deeper than the ADCP bin 1.

**Table A-4, cont.**

**ADV vs PCADP**

$K_1$ tidal component

| ADV | MJ (cm/s) | Inc (deg) | Phase (deg) | PCADP (bin) | MJ (cm/s) | Inc (deg) | Phase (deg) |
|---|---|---|---|---|---|---|---|
| | | | | 2 | 2.1 | -20 | 148 |
| 1 | 1.9 | -24 | 164 | 3 | 1.9 | -21 | 148 |
| | | | | 4 | 1.7 | -22 | 149 |

**Site B5**

**PDADP vs 300-kHz ADCP**

$K_1$ tidal component

| PCADP (bin) | MJ (cm/s) | Inc (deg) | Phase (deg) | ADCP (bin) | MJ (cm/s) | Inc (deg) | Phase (deg) |
|---|---|---|---|---|---|---|---|
| | | | | 3 | 2.8 | -12 | 169 |
| | | | | 2 | 2.7 | -12 | 172 |
| | | | | 1 | 2.5 | -13 | 175 |
| 1* | 1.1 | -22 | 164 | | | | |
| 2 | 1.1 | -22 | 164 | | | | |
| 3 | 1.0 | -22 | 164 | | | | |

*PCADP bin 1 is 6.9 m below the ADCP.

**ADV vs PCADP**

$K_1$ tidal component

| ADV | MJ (cm/s) | Inc (deg) | Phase (deg) | PCADP (bin) | MJ (cm/s) | Inc (deg) | Phase (deg) |
|---|---|---|---|---|---|---|---|
| | | | | 2 | 1.1 | -22 | 164 |
| 1 | 1.0 | 132 | 166 | 3 | 1.0 | -22 | 164 |
| | | | | 4 | 0.9 | -22 | 165 |

**Table A-4, cont.**

**Site B6**

Note: K1 ellipse is round; hence we will use $O_1$.

**December–March**

**1200-kHz ADP vs 300-kHz ADCP**

$O_1$ tidal currents

| 1200-kHz ACDP (bin) | MJ (cm/s) | Inc (deg) | Phase (deg) | 300-kHz ADCP (bin) | MJ (cm/s) | Inc (deg) | Phase (deg) |
|---|---|---|---|---|---|---|---|
| 41 | 2.2 | -4 | 134 | 3 | 1.9 | -3 | 130 |
| 33 | 2.2 | -4 | 134 | 2 | 2.0 | -3 | 131 |
| 25 | 2.2 | -6 | 135 | 1 | 2.0 | -3 | 131 |
| | | | | | | | |

**PCADP vs. 1200-kHz ADCP**

$O_1$ tidal component

| PCADP (bin) | MJ (cm/s) | Inc (deg) | Phase (deg) | ADCP (bin) | MJ (cm/s) | Inc (deg) | Phase (deg) |
|---|---|---|---|---|---|---|---|
| | | | | 2 | 1.5 | -8 | 129 |
| | | | | 1 | 1.4 | -8 | 128 |
| 1* | 1.4 | -4 | 105 | | | | |
| 2 | 1.3 | -4 | 105 | | | | |
| 3 | 1.2 | -3 | 105 | | | | |

*Bin 1.7 m deeper than first bin of the ADCP.

**ADV vs. PCADP**

$O_1$ tidal component

| ADV | MJ (cm/s) | Inc (deg) | Phase (deg) | PCADP (bin) | MJ (cm/s) | Inc (deg) | Phase (deg) |
|---|---|---|---|---|---|---|---|
| | | | | 2 | 1.3 | -4 | 105 |
| 1 | 1.3 | -8 | 105 | 3 | 1.2 | -3 | 105 |
| | | | | 4 | 1.2 | -3 | 104 |

**ADV vs PCADP**

**Full record**

$O_1$ tidal component

| ADV | MJ (cm/s) | Inc (deg) | Phase (deg) | PCADP (bin) | MJ (cm/s) | Inc (deg) | Phase (deg) |
|---|---|---|---|---|---|---|---|
| | | | | 2 | 1.3 | 0 | 102 |
| 1 | 1.3 | -4 | 102 | 3 | 1.2 | 0 | 102 |
| | | | | 4 | 1.2 | 2 | 101 |

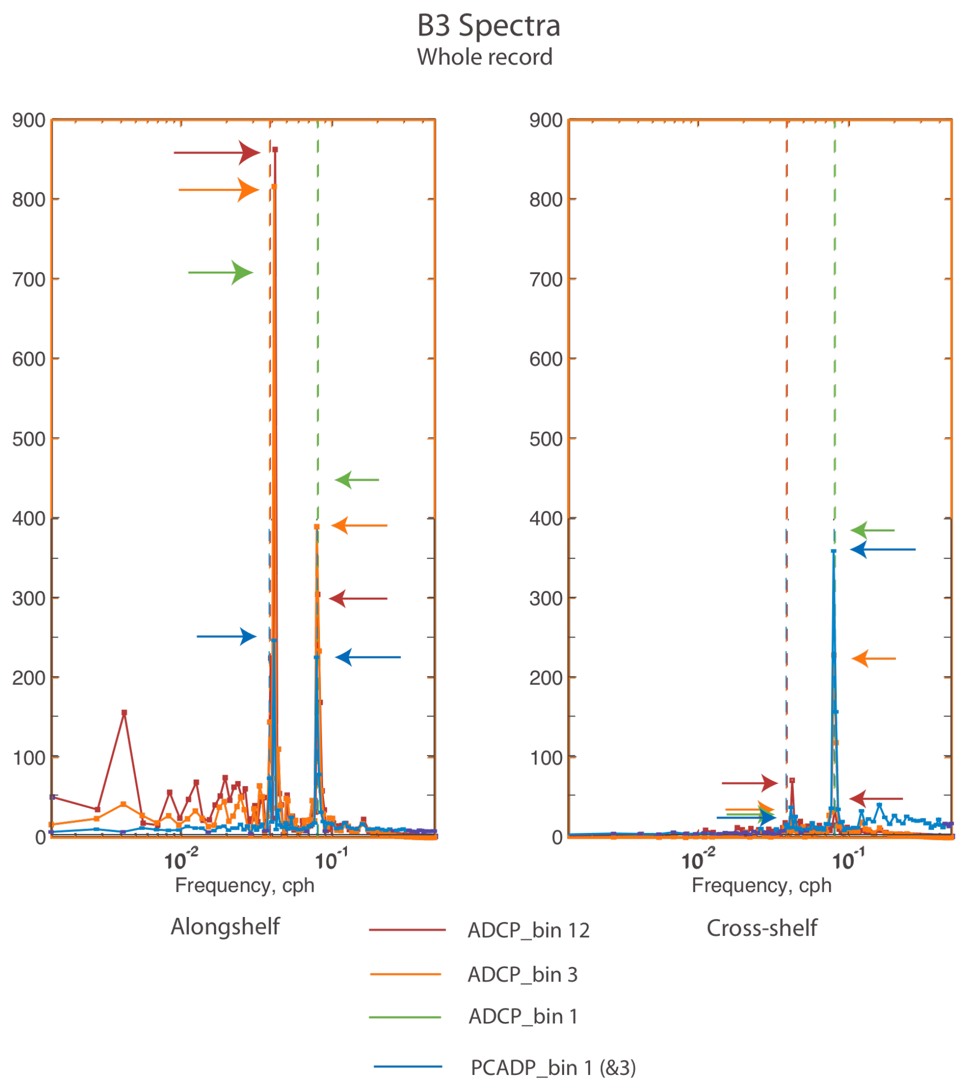


**Figure A-1.** Variance-conserving spectra of along- and cross-shelf currents at Site B3. The vertical dashed lines denote the diurnal and semidiurnal tidal bands. A piece length of 720 hwas used in this analysis.

# Appendix B

## Tidal Currents Measured over the Palos Verdes Shelf

The characteristics for the principal tidal currents were

> $M_2$ (period 12.42 hours), $S_2$ (period 12.00 hours),
> $O_1$ (period 25.82 hours) and $K_1$ (period 23.93 hours)

at the five mooring sites (B1, B2, B3, B5, and B6) occupied in the winter of 2007–2008.

The tidal characteristics at each site are listed for all depth currents measured in the water column.

The columns:

Major: The semi-major axis of the tidal ellipse in cm/s.

Minor: The semi-minor axis of the tidal ellipse in cm/s.

Inclination: Inclination of the major axis of the tidal ellipse in degrees. The major axis is oriented east-west if the inclination is 90° or 270°.

Phase: Phase, in degrees, when the currents flow parallel to the positive major axis of the tidal ellipse. The positive major axis of the ellipse is defined as having an orientation either between 270° and 0° or between 0° and 90°.

The tidal parameters are calculated using a version of the Foreman tidal programs (Foreman, 1978), as converted into the MATLAB programming language by Pawlowicz and others (2002).

**Table B-1.** $M_2$ tidal characteristics from current meter records at Site B1. [cph, cycles per hour; SNR, signal-to-noise ratio]

| Site B1–$M_2$–0.08051 cph | | | | | | | | | | | |
|---|---|---|---|---|---|---|---|---|---|---|---|
| **Depth*** | **Elevation** | **Bin#** | **Major** | **error** | **Minor** | **error** | **Inclination** | **error** | **Phase** | **error** | **SNR** |
| 2.8 | 16.88 | 15 | 2.1 | 0.5 | -0.3 | 0.6 | 219.7 | 16.8 | 359.5 | 14.8 | 17 |
| 3.8 | 15.88 | 14 | 1.5 | 0.8 | -0.2 | 0.4 | 249.6 | 15.0 | 37.6 | 31.1 | 4 |
| 4.8 | 14.88 | 13 | 1.5 | 0.8 | -0.1 | 0.3 | 251.2 | 13.0 | 36.6 | 30.5 | 4 |
| 5.8 | 13.88 | 12 | 1.4 | 0.7 | -0.1 | 0.3 | 251.4 | 12.5 | 39.0 | 30.2 | 4 |
| 6.8 | 12.88 | 11 | 1.4 | 0.7 | -0.2 | 0.3 | 251.2 | 12.6 | 42.7 | 30.4 | 4 |
| 7.8 | 11.88 | 10 | 1.3 | 0.7 | -0.2 | 0.3 | 251.7 | 12.5 | 46.4 | 30.9 | 4 |
| 8.8 | 10.88 | 9 | 1.2 | 0.6 | -0.2 | 0.2 | 252.0 | 12.8 | 51.8 | 32.1 | 4 |
| 9.8 | 9.88 | 8 | 1.1 | 0.6 | -0.2 | 0.2 | 252.5 | 13.5 | 56.8 | 34.4 | 3 |
| 10.8 | 8.88 | 7 | 1.0 | 0.6 | -0.1 | 0.2 | 252.6 | 14.0 | 60.9 | 36.7 | 3 |
| 11.8 | 7.88 | 6 | 0.9 | 0.6 | 0.0 | 0.2 | 251.0 | 16.8 | 65.1 | 40.8 | 2 |
| 12.8 | 6.88 | 5 | 0.7 | 0.6 | 0.1 | 0.3 | 248.0 | 24.1 | 70.4 | 47.1 | 2 |
| 13.8 | 5.88 | 4 | 0.6 | 0.5 | 0.2 | 0.3 | 239.7 | 41.6 | 80.1 | 56.9 | 2 |
| 14.8 | 4.88 | 3 | 0.6 | 0.4 | 0.3 | 0.4 | 227.8 | 64.7 | 93.1 | 67.5 | 2 |
| 15.8 | 3.88 | 2 | 0.6 | 0.4 | 0.3 | 0.5 | 210.8 | 85.6 | 111.8 | 74.2 | 3 |
| 16.8 | 2.88 | 1 | 0.6 | 0.3 | 0.3 | 0.5 | 191.7 | 79.4 | 130.1 | 62.4 | 4 |
| 17.9 | 0.8 | 1 | 0.3 | 0.2 | 0.1 | 0.2 | 195.0 | 45.1 | 149.5 | 38.1 | 4 |

*Depth beneath 19.7 m nominal surface height

AQD 8512

**Table B-2.** $S_2$ tidal characteristics from current meter records at Site B1. [cph, cycles per hour; SNR, signal-to-noise ratio]

| Site B1–$S_2$–0.08333 cph | | | | | | | | | | | |
|---|---|---|---|---|---|---|---|---|---|---|---|
| **Depth*** | **Elevation** | **Bin#** | **Major** | **error** | **Minor** | **error** | **Inclination** | **error** | **Phase** | **error** | **SNR** |
| 2.8 | 16.88 | 15 | 1.6 | 0.7 | -0.7 | 0.4 | 243.1 | 21.8 | 8.2 | 29.3 | 6 |
| 3.8 | 15.88 | 14 | 1.5 | 0.8 | -0.4 | 0.2 | 271.6 | 13.0 | 47.5 | 32.9 | 4 |
| 4.8 | 14.88 | 13 | 1.5 | 0.8 | -0.3 | 0.2 | 271.0 | 9.5 | 55.5 | 30.5 | 4 |
| 5.8 | 13.88 | 12 | 1.5 | 0.8 | -0.2 | 0.2 | 268.0 | 7.7 | 61.9 | 29.6 | 4 |
| 6.8 | 12.88 | 11 | 1.5 | 0.7 | -0.1 | 0.2 | 264.8 | 7.1 | 66.8 | 29.4 | 4 |
| 7.8 | 11.88 | 10 | 1.4 | 0.7 | -0.1 | 0.2 | 261.9 | 7.2 | 70.8 | 29.2 | 4 |
| 8.8 | 10.88 | 9 | 1.3 | 0.7 | 0.0 | 0.2 | 256.2 | 9.2 | 73.6 | 29.8 | 4 |
| 9.8 | 9.88 | 8 | 1.2 | 0.6 | 0.0 | 0.2 | 252.7 | 11.3 | 76.7 | 30.9 | 3 |
| 10.8 | 8.88 | 7 | 1.1 | 0.6 | 0.0 | 0.3 | 249.8 | 13.5 | 79.9 | 32.2 | 3 |
| 11.8 | 7.88 | 6 | 1.0 | 0.6 | 0.1 | 0.3 | 247.6 | 16.1 | 83.8 | 34.1 | 3 |
| 12.8 | 6.88 | 5 | 0.9 | 0.5 | 0.1 | 0.3 | 243.1 | 20.4 | 86.9 | 35.4 | 3 |
| 13.8 | 5.88 | 4 | 0.8 | 0.5 | 0.1 | 0.4 | 237.8 | 26.0 | 91.1 | 37.0 | 3 |
| 14.8 | 4.88 | 3 | 0.7 | 0.5 | 0.1 | 0.4 | 232.4 | 32.4 | 96.0 | 38.8 | 2 |
| 15.8 | 3.88 | 2 | 0.6 | 0.4 | 0.2 | 0.4 | 226.9 | 40.2 | 100.9 | 41.7 | 2 |
| 16.8 | 2.88 | 1 | 0.6 | 0.4 | 0.2 | 0.4 | 215.7 | 46.6 | 108.7 | 40.8 | 3 |
| 17.9 | 0.8 | 1 | 0.3 | 0.2 | 0.1 | 0.2 | 241.4 | 53.6 | 110.7 | 58.2 | 2 |

*Depth beneath 19.7 m nominal surface height

AQD 8512

**Table B-3.** $O_1$ tidal characteristics from current meter records at Site B1. [cph, cycles per hour; SNR, signal-to-noise ratio]

| Site B1–$O_1$–0.03873 cph | | | | | | | | | | | |
|---|---|---|---|---|---|---|---|---|---|---|---|
| **Depth*** | **Elevation** | **Bin#** | **Major** | **error** | **Minor** | **error** | **Inclination** | **error** | **Phase** | **error** | **SNR** |
| 2.8 | 16.88 | 15 | 2.3 | 0.9 | 0.4 | 0.5 | 250.1 | 10.8 | 324.6 | 20.4 | 6 |
| 3.8 | 15.88 | 14 | 2.1 | 1.1 | 0.2 | 0.2 | 272.7 | 6.4 | 321.6 | 26.1 | 4 |
| 4.8 | 14.88 | 13 | 2.2 | 1.1 | 0.2 | 0.2 | 273.6 | 5.6 | 324.8 | 24.3 | 4 |
| 5.8 | 13.88 | 12 | 2.2 | 1.0 | 0.2 | 0.2 | 273.3 | 4.9 | 326.4 | 22.9 | 5 |
| 6.8 | 12.88 | 11 | 2.3 | 1.0 | 0.2 | 0.2 | 273.2 | 4.2 | 327.0 | 21.5 | 5 |
| 7.8 | 11.88 | 10 | 2.3 | 0.9 | 0.2 | 0.2 | 273.3 | 3.7 | 327.2 | 20.3 | 6 |
| 8.8 | 10.88 | 9 | 2.3 | 0.9 | 0.1 | 0.1 | 273.3 | 3.2 | 326.6 | 19.2 | 7 |
| 9.8 | 9.88 | 8 | 2.3 | 0.9 | 0.1 | 0.1 | 273.0 | 3.2 | 325.3 | 18.8 | 7 |
| 10.8 | 8.88 | 7 | 2.2 | 0.8 | 0.1 | 0.1 | 272.7 | 3.1 | 324.1 | 18.6 | 7 |
| 11.8 | 7.88 | 6 | 2.1 | 0.8 | 0.1 | 0.1 | 272.6 | 3.2 | 322.6 | 18.4 | 7 |
| 12.8 | 6.88 | 5 | 2.0 | 0.8 | 0.0 | 0.1 | 272.3 | 3.5 | 320.7 | 18.2 | 7 |
| 13.8 | 5.88 | 4 | 1.9 | 0.7 | 0.0 | 0.2 | 271.4 | 4.2 | 318.5 | 18.1 | 7 |
| 14.8 | 4.88 | 3 | 1.8 | 0.7 | 0.0 | 0.2 | 271.3 | 5.1 | 316.1 | 18.4 | 7 |
| 15.8 | 3.88 | 2 | 1.6 | 0.6 | 0.0 | 0.2 | 270.8 | 6.2 | 312.6 | 18.6 | 7 |
| 16.8 | 2.88 | 1 | 1.4 | 0.5 | 0.0 | 0.2 | 270.0 | 7.5 | 307.4 | 18.7 | 7 |
| 17.9 | 0.8 | 1 | 0.4 | 0.2 | 0.0 | 0.2 | 298.9 | 20.4 | 294.1 | 26.1 | 4 |

*Depth beneath 19.7 m nominal surface height

AQD 8512

**Table B-4.** $K_1$ tidal characteristics from current meter records at Site B1. [cph, cycles per hour; SNR, signal-to-noise ratio]

| Site B1–$O_1$–.0.04178 cph | | | | | | | | | | | |
|---|---|---|---|---|---|---|---|---|---|---|---|
| **Depth*** | **Elevation** | **Bin#** | **Major** | **error** | **Minor** | **error** | **Inclination** | **error** | **Phase** | **error** | **SNR** |
| 2.8 | 16.88 | 15 | 3.5 | 0.9 | 0.2 | 0.6 | 238.7 | 8.8 | 355.6 | 12.7 | 17 |
| 3.8 | 15.88 | 14 | 3.2 | 1.1 | 0.1 | 0.3 | 261.9 | 4.7 | 344.5 | 18.3 | 8 |
| 4.8 | 14.88 | 13 | 3.3 | 1.1 | 0.0 | 0.2 | 267.1 | 3.4 | 338.0 | 17.1 | 9 |
| 5.8 | 13.88 | 12 | 3.3 | 1.0 | 0.0 | 0.2 | 270.3 | 2.8 | 152.4 | 16.1 | 11 |
| 6.8 | 12.88 | 11 | 3.4 | 1.0 | -0.1 | 0.2 | 272.8 | 2.6 | 148.8 | 15.2 | 12 |
| 7.8 | 11.88 | 10 | 3.4 | 0.9 | -0.1 | 0.2 | 274.8 | 2.5 | 145.9 | 14.4 | 13 |
| 8.8 | 10.88 | 9 | 3.4 | 0.9 | -0.1 | 0.2 | 276.4 | 2.6 | 142.7 | 13.7 | 15 |
| 9.8 | 9.88 | 8 | 3.4 | 0.9 | -0.1 | 0.2 | 278.4 | 2.8 | 140.7 | 13.3 | 15 |
| 10.8 | 8.88 | 7 | 3.3 | 0.8 | -0.1 | 0.2 | 280.0 | 3.1 | 138.9 | 13.0 | 16 |
| 11.8 | 7.88 | 6 | 3.2 | 0.8 | -0.1 | 0.2 | 281.3 | 3.4 | 137.3 | 12.7 | 17 |
| 12.8 | 6.88 | 5 | 3.1 | 0.7 | -0.2 | 0.2 | 282.6 | 3.7 | 135.4 | 12.4 | 18 |
| 13.8 | 5.88 | 4 | 3.0 | 0.7 | -0.2 | 0.2 | 284.1 | 4.2 | 133.5 | 12.2 | 18 |
| 14.8 | 4.88 | 3 | 2.8 | 0.6 | -0.3 | 0.3 | 285.6 | 4.9 | 131.5 | 12.2 | 19 |
| 15.8 | 3.88 | 2 | 2.6 | 0.6 | -0.4 | 0.3 | 287.0 | 5.7 | 128.9 | 12.2 | 19 |
| 16.8 | 2.88 | 1 | 2.2 | 0.5 | -0.4 | 0.3 | 289.1 | 6.9 | 127.2 | 12.5 | 19 |
| 17.9 | 0.8 | 1 | 0.8 | 0.2 | -0.2 | 0.2 | 320.3 | 14.2 | 128.5 | 13.1 | 18 |

*Depth beneath 19.7 m nominal surface height

AQD 8512

**Table B-5.** $M_2$ tidal characteristics from current meter records at Site B2. [cph, cycles per hour; SNR, signal-to-noise ratio]

| Site B2–$M_2$–0.08051 cph | | | | | | | | | | | |
|---|---|---|---|---|---|---|---|---|---|---|---|
| **Depth*** | **Elevation** | **Bin#** | **Major** | **error** | **Minor** | **error** | **Inclination** | **error** | **Phase** | **error** | **SNR** |
| 4.1 | 26.17 | 23 | 2.4 | 0.8 | -1.6 | 0.7 | 246.7 | 38.1 | 182.4 | 41.6 | 8 |
| 5.1 | 25.17 | 22 | 2.0 | 0.8 | -1.0 | 0.6 | 289.2 | 31.1 | 231.3 | 37.2 | 5 |
| 6.1 | 24.17 | 21 | 1.9 | 0.8 | -1.0 | 0.6 | 288.8 | 28.6 | 233.2 | 35.2 | 6 |
| 7.1 | 23.17 | 20 | 1.9 | 0.8 | -0.9 | 0.5 | 287.2 | 27.0 | 233.7 | 34.0 | 6 |
| 8.1 | 22.17 | 19 | 1.9 | 0.8 | -0.9 | 0.5 | 286.4 | 24.5 | 234.3 | 31.5 | 6 |
| 9.1 | 21.17 | 18 | 1.9 | 0.7 | -0.9 | 0.5 | 286.6 | 23.0 | 235.9 | 29.9 | 7 |
| 10.1 | 20.17 | 17 | 1.9 | 0.7 | -0.8 | 0.5 | 287.2 | 22.5 | 237.3 | 29.2 | 7 |
| 11.1 | 19.17 | 16 | 1.9 | 0.7 | -0.8 | 0.5 | 286.9 | 21.4 | 238.4 | 28.0 | 7 |
| 12.1 | 18.17 | 15 | 1.8 | 0.7 | -0.7 | 0.5 | 285.7 | 20.4 | 238.3 | 27.3 | 7 |
| 13.1 | 17.17 | 14 | 1.7 | 0.7 | -0.6 | 0.5 | 285.1 | 19.7 | 239.0 | 26.6 | 7 |
| 14.1 | 16.17 | 13 | 1.7 | 0.7 | -0.5 | 0.4 | 284.4 | 18.8 | 240.0 | 26.2 | 7 |
| 15.1 | 15.17 | 12 | 1.7 | 0.7 | -0.5 | 0.4 | 283.3 | 18.0 | 241.0 | 25.7 | 7 |
| 16.1 | 14.17 | 11 | 1.6 | 0.7 | -0.4 | 0.4 | 281.1 | 16.8 | 242.3 | 25.4 | 6 |
| 17.1 | 13.17 | 10 | 1.6 | 0.7 | -0.3 | 0.4 | 279.0 | 15.1 | 243.6 | 24.7 | 6 |
| 18.1 | 12.17 | 9 | 1.6 | 0.7 | -0.2 | 0.4 | 276.9 | 14.1 | 245.2 | 24.9 | 6 |
| 19.1 | 11.17 | 8 | 1.6 | 0.7 | -0.1 | 0.4 | 274.2 | 13.1 | 247.1 | 24.2 | 6 |
| 20.1 | 10.17 | 7 | 1.6 | 0.7 | 0.0 | 0.4 | 270.9 | 12.5 | 249.6 | 24.0 | 6 |
| 21.1 | 9.17 | 6 | 1.7 | 0.7 | 0.1 | 0.3 | 267.9 | 12.0 | 252.2 | 23.7 | 6 |
| 22.1 | 8.17 | 5 | 1.8 | 0.7 | 0.1 | 0.3 | 266.1 | 11.8 | 254.4 | 22.9 | 7 |
| 23.1 | 7.17 | 4 | 1.8 | 0.7 | 0.2 | 0.4 | 263.3 | 11.9 | 256.7 | 22.2 | 7 |
| 24.1 | 6.17 | 3 | 1.9 | 0.7 | 0.2 | 0.4 | 261.8 | 12.0 | 259.0 | 21.5 | 8 |
| 25.1 | 5.17 | 2 | 2.0 | 0.7 | 0.3 | 0.4 | 260.4 | 12.2 | 260.9 | 20.7 | 9 |
| 26.1 | 4.17 | 1 | 2.0 | 0.7 | 0.3 | 0.4 | 259.2 | 12.9 | 262.0 | 20.0 | 9 |
| 28.1 | 0.60 | 1 | 1.3 | 0.4 | 0.4 | 0.4 | 239.2 | 18.9 | 273.4 | 20.5 | 11 |

*Depth beneath 28.7 m nominal surface height

ADV 8523

**Table B-6.** $S_2$ tidal characteristics from current meter records at Site B2. [cph, cycles per hour; SNR, signal-to-noise ratio]

| Site B2–$S_2$–0.08333 cph | | | | | | | | | | | |
|---|---|---|---|---|---|---|---|---|---|---|---|
| **Depth*** | **Elevation** | **Bin#** | **Major** | **error** | **Minor** | **error** | **Inclination** | **error** | **Phase** | **error** | **SNR** |
| 4.1 | 26.17 | 23 | 1.9 | 0.7 | -1.5 | 0.7 | 313.6 | 71.3 | 248.3 | 71.6 | 7 |
| 5.1 | 25.17 | 22 | 1.8 | 0.8 | -0.9 | 0.7 | 306.2 | 34.0 | 249.3 | 36.6 | 5 |
| 6.1 | 24.17 | 21 | 1.5 | 0.8 | -0.7 | 0.6 | 303.3 | 35.9 | 250.9 | 39.9 | 4 |
| 7.1 | 23.17 | 20 | 1.4 | 0.7 | -0.7 | 0.6 | 299.3 | 35.8 | 252.8 | 41.7 | 4 |
| 8.1 | 22.17 | 19 | 1.3 | 0.7 | -0.6 | 0.5 | 294.5 | 35.3 | 254.2 | 43.0 | 3 |
| 9.1 | 21.17 | 18 | 1.3 | 0.7 | -0.6 | 0.5 | 290.2 | 33.7 | 255.2 | 43.0 | 3 |
| 10.1 | 20.17 | 17 | 1.2 | 0.7 | -0.5 | 0.5 | 287.6 | 31.6 | 256.5 | 41.7 | 3 |
| 11.1 | 19.17 | 16 | 1.2 | 0.7 | -0.4 | 0.5 | 283.8 | 28.7 | 256.8 | 39.5 | 3 |
| 12.1 | 18.17 | 15 | 1.2 | 0.7 | -0.4 | 0.4 | 281.3 | 26.7 | 256.2 | 37.8 | 3 |
| 13.1 | 17.17 | 14 | 1.2 | 0.7 | -0.3 | 0.4 | 279.3 | 23.8 | 256.3 | 34.7 | 3 |
| 14.1 | 16.17 | 13 | 1.2 | 0.7 | -0.3 | 0.4 | 277.1 | 21.9 | 255.8 | 33.1 | 3 |
| 15.1 | 15.17 | 12 | 1.3 | 0.7 | -0.2 | 0.4 | 275.8 | 20.0 | 256.1 | 31.2 | 4 |
| 16.1 | 14.17 | 11 | 1.3 | 0.7 | -0.2 | 0.4 | 274.0 | 18.1 | 256.2 | 29.8 | 4 |
| 17.1 | 13.17 | 10 | 1.3 | 0.7 | -0.1 | 0.4 | 271.7 | 16.5 | 256.8 | 28.9 | 4 |
| 18.1 | 12.17 | 9 | 1.3 | 0.7 | 0.0 | 0.4 | 268.9 | 15.9 | 257.3 | 29.3 | 4 |
| 19.1 | 11.17 | 8 | 1.3 | 0.7 | 0.1 | 0.4 | 265.5 | 15.8 | 259.3 | 29.3 | 4 |
| 20.1 | 10.17 | 7 | 1.3 | 0.7 | 0.1 | 0.4 | 261.3 | 15.8 | 260.9 | 29.2 | 4 |
| 21.1 | 9.17 | 6 | 1.3 | 0.7 | 0.1 | 0.4 | 256.9 | 16.4 | 262.9 | 29.2 | 4 |
| 22.1 | 8.17 | 5 | 1.3 | 0.7 | 0.2 | 0.4 | 251.8 | 17.5 | 264.8 | 28.9 | 4 |
| 23.1 | 7.17 | 4 | 1.3 | 0.6 | 0.2 | 0.4 | 246.6 | 19.2 | 266.9 | 28.8 | 4 |
| 24.1 | 6.17 | 3 | 1.3 | 0.6 | 0.2 | 0.5 | 241.9 | 20.2 | 269.1 | 27.6 | 5 |
| 25.1 | 5.17 | 2 | 1.4 | 0.6 | 0.2 | 0.5 | 238.6 | 20.6 | 271.1 | 26.0 | 5 |
| 26.1 | 4.17 | 1 | 1.4 | 0.6 | 0.2 | 0.5 | 235.9 | 21.1 | 273.2 | 24.9 | 6 |
| 28.1 | 0.60 | 1 | 1.1 | 0.4 | 0.2 | 0.4 | 224.5 | 22.1 | 282.9 | 22.1 | 8 |

*Depth beneath 28.7 m nominal surface height

ADV 8523

**Table B-7.** $O_1$ tidal characteristics from current meter records at Site B2. [cph, cycles per hour; SNR, signal-to-noise ratio]

| Site B2–$O_1$–0.03873 cph | | | | | | | | | | | |
|---|---|---|---|---|---|---|---|---|---|---|---|
| **Depth*** | **Elevation** | **Bin#** | **Major** | **error** | **Minor** | **error** | **Inclination** | **error** | **Phase** | **error** | **SNR** |
| 4.1 | 26.17 | 23 | 3.1 | 1.2 | 0.0 | 0.9 | 284.8 | 14.8 | 157.8 | 19.3 | 7 |
| 5.1 | 25.17 | 22 | 2.8 | 1.1 | 0.0 | 0.9 | 296.0 | 16.5 | 159.5 | 20.1 | 6 |
| 6.1 | 24.17 | 21 | 2.8 | 1.1 | 0.0 | 0.9 | 295.8 | 15.8 | 160.4 | 19.4 | 6 |
| 7.1 | 23.17 | 20 | 2.8 | 1.1 | -0.1 | 0.9 | 295.6 | 15.2 | 161.4 | 18.8 | 7 |
| 8.1 | 22.17 | 19 | 2.8 | 1.1 | -0.1 | 0.8 | 295.6 | 14.8 | 162.0 | 18.5 | 7 |
| 9.1 | 21.17 | 18 | 2.8 | 1.0 | -0.1 | 0.8 | 295.4 | 14.3 | 163.1 | 18.1 | 8 |
| 10.1 | 20.17 | 17 | 2.8 | 1.0 | -0.1 | 0.8 | 295.0 | 13.8 | 164.0 | 17.9 | 8 |
| 11.1 | 19.17 | 16 | 2.8 | 1.0 | -0.1 | 0.8 | 295.2 | 13.4 | 165.0 | 17.6 | 8 |
| 12.1 | 18.17 | 15 | 2.8 | 1.0 | -0.1 | 0.7 | 295.1 | 13.0 | 165.4 | 17.5 | 8 |
| 13.1 | 17.17 | 14 | 2.7 | 1.0 | 0.0 | 0.7 | 295.8 | 12.7 | 165.4 | 17.3 | 8 |
| 14.1 | 16.17 | 13 | 2.7 | 0.9 | 0.0 | 0.7 | 296.5 | 12.4 | 165.3 | 17.1 | 8 |
| 15.1 | 15.17 | 12 | 2.7 | 0.9 | 0.0 | 0.7 | 297.1 | 12.3 | 164.7 | 16.9 | 8 |
| 16.1 | 14.17 | 11 | 2.7 | 0.9 | 0.0 | 0.7 | 297.8 | 12.1 | 163.9 | 16.7 | 9 |
| 17.1 | 13.17 | 10 | 2.6 | 0.9 | 0.0 | 0.6 | 298.1 | 11.9 | 162.8 | 16.6 | 9 |
| 18.1 | 12.17 | 9 | 2.6 | 0.9 | 0.0 | 0.6 | 298.4 | 11.7 | 161.6 | 16.5 | 9 |
| 19.1 | 11.17 | 8 | 2.5 | 0.8 | 0.0 | 0.6 | 299.1 | 11.6 | 160.5 | 16.4 | 9 |
| 20.1 | 10.17 | 7 | 2.5 | 0.8 | 0.1 | 0.6 | 299.7 | 11.5 | 159.5 | 16.4 | 9 |
| 21.1 | 9.17 | 6 | 2.5 | 0.8 | 0.1 | 0.6 | 300.3 | 11.7 | 158.6 | 16.7 | 9 |
| 22.1 | 8.17 | 5 | 2.4 | 0.8 | 0.1 | 0.6 | 300.7 | 11.9 | 157.6 | 17.1 | 8 |
| 23.1 | 7.17 | 4 | 2.3 | 0.8 | 0.1 | 0.6 | 300.9 | 12.1 | 156.9 | 17.6 | 8 |
| 24.1 | 6.17 | 3 | 2.2 | 0.8 | 0.1 | 0.5 | 300.9 | 12.4 | 155.8 | 18.3 | 7 |
| 25.1 | 5.17 | 2 | 2.0 | 0.8 | 0.1 | 0.5 | 301.4 | 13.1 | 154.8 | 19.0 | 7 |
| 26.1 | 4.17 | 1 | 1.8 | 0.7 | 0.1 | 0.5 | 302.3 | 14.5 | 153.3 | 20.2 | 6 |
| 28.1 | 0.60 | 1 | 0.8 | 0.5 | 0.1 | 0.3 | 296.1 | 19.4 | 144.7 | 28.5 | 3 |

*Depth beneath 28.7 m nominal surface height

ADV 8523

**Table B-8.** $K_1$ tidal characteristics from current meter records at Site B2. [cph, cycles per hour; SNR, signal-to-noise ratio]

| Site B2–$O_1$–.0.04178 cph | | | | | | | | | | | |
|---|---|---|---|---|---|---|---|---|---|---|---|
| **Depth*** | **Elevation** | **Bin#** | **Major** | **error** | **Minor** | **error** | **Inclination** | **error** | **Phase** | **error** | **SNR** |
| 4.1 | 26.17 | 23 | 6.3 | 1.2 | -1.0 | 0.9 | 277.8 | 7.8 | 190.6 | 10.3 | 27 |
| 5.1 | 25.17 | 22 | 5.6 | 1.2 | -0.9 | 0.9 | 287.7 | 8.8 | 189.8 | 11.3 | 23 |
| 6.1 | 24.17 | 21 | 5.4 | 1.1 | -0.8 | 0.9 | 290.5 | 8.8 | 188.0 | 11.3 | 23 |
| 7.1 | 23.17 | 20 | 5.2 | 1.1 | -0.7 | 0.9 | 292.8 | 8.9 | 186.3 | 11.2 | 23 |
| 8.1 | 22.17 | 19 | 5.0 | 1.1 | -0.6 | 0.8 | 294.9 | 9.0 | 185.1 | 11.2 | 22 |
| 9.1 | 21.17 | 18 | 4.8 | 1.0 | -0.5 | 0.8 | 296.9 | 9.1 | 184.0 | 11.3 | 22 |
| 10.1 | 20.17 | 17 | 4.6 | 1.0 | -0.4 | 0.8 | 298.7 | 9.2 | 182.6 | 11.3 | 22 |
| 11.1 | 19.17 | 16 | 4.5 | 1.0 | -0.3 | 0.8 | 300.4 | 9.2 | 181.0 | 11.3 | 22 |
| 12.1 | 18.17 | 15 | 4.4 | 0.9 | -0.1 | 0.8 | 302.2 | 9.2 | 178.9 | 11.2 | 22 |
| 13.1 | 17.17 | 14 | 4.3 | 0.9 | 0.0 | 0.8 | 303.4 | 9.2 | 176.9 | 11.1 | 22 |
| 14.1 | 16.17 | 13 | 4.3 | 0.9 | 0.1 | 0.8 | 304.8 | 9.2 | 174.8 | 11.0 | 22 |
| 15.1 | 15.17 | 12 | 4.2 | 0.9 | 0.2 | 0.7 | 305.7 | 9.1 | 172.8 | 10.9 | 23 |
| 16.1 | 14.17 | 11 | 4.2 | 0.8 | 0.2 | 0.7 | 306.6 | 9.0 | 171.0 | 10.6 | 24 |
| 17.1 | 13.17 | 10 | 4.2 | 0.8 | 0.2 | 0.7 | 307.3 | 8.9 | 169.8 | 10.4 | 25 |
| 18.1 | 12.17 | 9 | 4.1 | 0.8 | 0.2 | 0.7 | 307.9 | 8.8 | 168.5 | 10.2 | 26 |
| 19.1 | 11.17 | 8 | 4.1 | 0.8 | 0.3 | 0.7 | 308.2 | 8.7 | 167.3 | 10.1 | 27 |
| 20.1 | 10.17 | 7 | 4.0 | 0.8 | 0.3 | 0.7 | 308.7 | 8.7 | 166.0 | 10.0 | 27 |
| 21.1 | 9.17 | 6 | 4.0 | 0.8 | 0.3 | 0.7 | 309.1 | 8.7 | 164.7 | 10.1 | 27 |
| 22.1 | 8.17 | 5 | 3.9 | 0.8 | 0.3 | 0.7 | 309.6 | 8.8 | 163.5 | 10.1 | 27 |
| 23.1 | 7.17 | 4 | 3.8 | 0.7 | 0.2 | 0.7 | 310.4 | 9.0 | 162.2 | 10.2 | 27 |
| 24.1 | 6.17 | 3 | 3.7 | 0.7 | 0.2 | 0.7 | 311.2 | 9.1 | 161.0 | 10.1 | 27 |
| 25.1 | 5.17 | 2 | 3.6 | 0.7 | 0.1 | 0.6 | 312.2 | 9.4 | 159.3 | 10.1 | 27 |
| 26.1 | 4.17 | 1 | 3.4 | 0.7 | 0.1 | 0.6 | 313.3 | 9.8 | 156.8 | 10.2 | 26 |
| 28.1 | 0.60 | 1 | 1.8 | 0.4 | -0.2 | 0.4 | 306.6 | 11.3 | 149.3 | 13.5 | 16 |

*Depth beneath 28.7 m nominal surface height

ADV 8523

**Table B-9.** $M_2$ tidal characteristics from current meter records at Site B3. [cph, cycles per hour; SNR, signal-to-noise ratio]

| Site B3–$M_2$–0.08051 cph | | | | | | | | | | | |
|---|---|---|---|---|---|---|---|---|---|---|---|
| **Depth*** | **Elevation** | **Bin#** | **Major** | **error** | **Minor** | **error** | **Inclination** | **error** | **Phase** | **error** | **SNR** |
| 6.6 | 47.29 | 21 | 2.1 | 1.0 | -1.1 | 0.6 | 271.7 | 29.2 | 182.4 | 39.1 | 5 |
| 8.6 | 45.29 | 20 | 2.1 | 0.9 | -1.1 | 0.5 | 268.0 | 26.5 | 357.9 | 36.3 | 5 |
| 10.6 | 43.29 | 19 | 2.2 | 0.9 | -1.1 | 0.5 | 267.6 | 22.5 | 353.9 | 31.8 | 6 |
| 12.6 | 41.29 | 18 | 2.3 | 0.9 | -1.0 | 0.5 | 268.0 | 20.0 | 351.2 | 28.5 | 7 |
| 14.6 | 39.29 | 17 | 2.3 | 0.8 | -0.9 | 0.5 | 269.1 | 17.2 | 350.8 | 24.7 | 9 |
| 16.6 | 37.29 | 16 | 2.4 | 0.8 | -0.9 | 0.5 | 270.5 | 15.2 | 171.8 | 22.5 | 10 |
| 18.6 | 35.29 | 15 | 2.4 | 0.8 | -0.8 | 0.4 | 272.5 | 14.2 | 174.0 | 21.3 | 10 |
| 20.6 | 33.29 | 14 | 2.4 | 0.7 | -0.8 | 0.4 | 274.3 | 13.9 | 177.6 | 20.7 | 11 |
| 22.6 | 31.29 | 13 | 2.4 | 0.7 | -0.8 | 0.4 | 276.1 | 13.4 | 181.6 | 19.9 | 11 |
| 24.6 | 29.29 | 12 | 2.4 | 0.7 | -0.6 | 0.5 | 278.2 | 12.7 | 186.5 | 18.7 | 12 |
| 26.6 | 27.29 | 11 | 2.5 | 0.7 | -0.5 | 0.4 | 280.1 | 11.3 | 192.6 | 17.3 | 13 |
| 28.6 | 25.29 | 10 | 2.5 | 0.7 | -0.2 | 0.4 | 279.6 | 10.5 | 197.5 | 16.3 | 14 |
| 30.6 | 23.29 | 9 | 2.6 | 0.7 | 0.0 | 0.5 | 276.7 | 10.3 | 201.7 | 16.1 | 13 |
| 32.6 | 21.29 | 8 | 2.7 | 0.7 | 0.1 | 0.5 | 271.9 | 10.2 | 205.9 | 15.6 | 14 |
| 34.6 | 19.29 | 7 | 2.9 | 0.7 | 0.0 | 0.5 | 266.6 | 10.0 | 209.4 | 14.8 | 16 |
| 36.6 | 17.29 | 6 | 3.1 | 0.7 | 0.0 | 0.5 | 262.2 | 9.7 | 212.1 | 14.2 | 17 |
| 38.6 | 15.29 | 5 | 3.4 | 0.8 | -0.1 | 0.6 | 258.6 | 9.5 | 213.6 | 13.3 | 20 |
| 40.6 | 13.29 | 4 | 3.7 | 0.8 | -0.1 | 0.6 | 255.3 | 9.5 | 214.0 | 12.5 | 23 |
| 42.6 | 11.29 | 3 | 4.0 | 0.8 | -0.2 | 0.6 | 251.8 | 9.4 | 212.8 | 11.6 | 26 |
| 44.6 | 9.29 | 2 | 4.3 | 0.8 | -0.3 | 0.7 | 249.0 | 9.3 | 211.2 | 10.5 | 32 |
| 46.6 | 7.29 | 1 | 4.7 | 0.7 | -0.3 | 0.7 | 245.8 | 9.0 | 208.7 | 9.4 | 40 |
| 53.44 | 0.45 | 1 | 3.9 | 0.6 | 0.5 | 0.6 | 248.8 | 8.7 | 199.9 | 8.9 | 46 |
| 53.57 | 0.32 | 2 | 3.7 | 0.5 | 0.5 | 0.5 | 248.4 | 8.7 | 199.9 | 9.0 | 46 |
| 53.61 | 0.28 | 1 | 3.4 | 0.5 | 0.4 | 0.5 | 251.6 | 8.7 | 229.7 | 9.3 | |
| 53.69 | 0.20 | 3 | 3.3 | 0.5 | 0.5 | 0.5 | 248.0 | 8.8 | 200.1 | 9.1 | 45 |
| 53.8 | 0.07 | 4 | 2.8 | 0.4 | 0.4 | 0.4 | 248.0 | 9.1 | 200.3 | 9.3 | 43 |

*Depth beneath 53.9 m nominal surface height

ADCP 8421 (white)

PCADP 8424 (orange)

ADV 8425 (blue)

**Table B-10.** $S_2$ tidal characteristics from current meter records at Site B3. [cph, cycles per hour; SNR, signal-to-noise ratio]

| Site B3–$S_2$–0.08333 cph | | | | | | | | | | | |
|---|---|---|---|---|---|---|---|---|---|---|---|
| **Depth*** | **Elevation** | **Bin#** | **Major** | **error** | **Minor** | **error** | **Inclination** | **error** | **Phase** | **error** | **SNR** |
| 6.6 | 47.29 | 21 | 2.5 | 1.0 | -1.5 | 0.6 | 276.2 | 27.7 | 225.8 | 35.2 | 7 |
| 8.6 | 45.29 | 20 | 2.4 | 0.9 | -1.3 | 0.5 | 276.6 | 25.3 | 224.4 | 33.4 | 7 |
| 10.6 | 43.29 | 19 | 2.3 | 0.9 | -1.2 | 0.5 | 278.5 | 22.8 | 222.3 | 30.9 | 7 |
| 12.6 | 41.29 | 18 | 2.2 | 0.8 | -1.1 | 0.5 | 280.7 | 22.4 | 221.5 | 30.1 | 7 |
| 14.6 | 39.29 | 17 | 2.1 | 0.8 | -1.0 | 0.5 | 283.7 | 21.7 | 221.5 | 28.9 | 7 |
| 16.6 | 37.29 | 16 | 1.9 | 0.8 | -0.8 | 0.5 | 285.0 | 19.9 | 220.3 | 27.4 | 7 |
| 18.6 | 35.29 | 15 | 1.8 | 0.7 | -0.6 | 0.5 | 285.0 | 18.7 | 217.4 | 26.7 | 6 |
| 20.6 | 33.29 | 14 | 1.7 | 0.7 | -0.4 | 0.5 | 286.0 | 18.1 | 215.1 | 26.4 | 6 |
| 22.6 | 31.29 | 13 | 1.6 | 0.7 | -0.2 | 0.5 | 287.2 | 17.8 | 213.1 | 26.3 | 5 |
| 24.6 | 29.29 | 12 | 1.5 | 0.7 | 0.0 | 0.5 | 287.5 | 18.1 | 213.4 | 26.5 | 5 |
| 26.6 | 27.29 | 11 | 1.4 | 0.7 | 0.2 | 0.4 | 282.7 | 19.5 | 215.4 | 29.5 | 4 |
| 28.6 | 25.29 | 10 | 1.3 | 0.7 | 0.3 | 0.4 | 271.2 | 21.6 | 222.4 | 32.7 | 4 |
| 30.6 | 23.29 | 9 | 1.4 | 0.7 | 0.3 | 0.5 | 260.0 | 20.6 | 231.0 | 30.3 | 4 |
| 32.6 | 21.29 | 8 | 1.6 | 0.7 | 0.2 | 0.5 | 253.1 | 19.2 | 235.1 | 26.7 | 5 |
| 34.6 | 19.29 | 7 | 1.7 | 0.7 | 0.2 | 0.5 | 248.9 | 18.3 | 236.5 | 24.2 | 6 |
| 36.6 | 17.29 | 6 | 1.9 | 0.7 | 0.2 | 0.6 | 246.5 | 17.4 | 236.7 | 22.5 | 7 |
| 38.6 | 15.29 | 5 | 2.0 | 0.7 | 0.3 | 0.6 | 243.3 | 18.0 | 236.3 | 22.0 | 7 |
| 40.6 | 13.29 | 4 | 2.1 | 0.7 | 0.3 | 0.6 | 240.4 | 18.0 | 235.4 | 20.8 | 8 |
| 42.6 | 11.29 | 3 | 2.3 | 0.8 | 0.3 | 0.7 | 239.1 | 17.4 | 233.4 | 19.5 | 9 |
| 44.6 | 9.29 | 2 | 2.4 | 0.7 | 0.4 | 0.7 | 237.4 | 17.2 | 232.3 | 18.3 | 11 |
| 46.6 | 7.29 | 1 | 2.6 | 0.7 | 0.5 | 0.7 | 233.9 | 17.1 | 232.3 | 17.4 | 12 |
| 53.44 | 0.45 | 1 | 1.9 | 0.6 | 0.6 | 0.6 | 232.5 | 20.0 | 235.4 | 20.1 | 11 |
| 53.57 | 0.32 | 2 | 1.8 | 0.5 | 0.6 | 0.5 | 231.9 | 19.9 | 235.9 | 20.1 | 11 |
| 53.61 | 0.28 | 1 | 1.7 | 0.5 | 0.5 | 0.5 | 235.1 | 19.9 | 267.0 | 20.4 | 11 |
| 53.69 | 0.20 | 3 | 1.6 | 0.5 | 0.5 | 0.5 | 231.3 | 19.9 | 236.4 | 20.0 | 11 |
| 53.8 | 0.07 | 4 | 1.4 | 0.4 | 0.5 | 0.4 | 230.4 | 20.6 | 237.5 | 20.7 | 11 |

*Depth beneath 53.9 m nominal surface height

ADCP 8421

PCADP 8424

ADV 8425

**Table B-11.** $O_1$ tidal characteristics from current meter records at Site B3. [cph, cycles per hour; SNR, signal-to-noise ratio]

| Site B3–$O_1$–.0.03873 cph | | | | | | | | | | | |
|---|---|---|---|---|---|---|---|---|---|---|---|
| **Depth*** | **Elevation** | **Bin#** | **Major** | **error** | **Minor** | **error** | **Inclination** | **error** | **Phase** | **error** | **SNR** |
| 6.6 | 47.29 | 21 | 2.0 | 1.3 | -0.2 | 0.8 | 163.8 | 20.7 | 141.6 | 31.1 | 3 |
| 8.6 | 45.29 | 20 | 2.0 | 1.2 | -0.2 | 0.8 | 165.2 | 19.0 | 139.1 | 29.8 | 3 |
| 10.6 | 43.29 | 19 | 2.0 | 1.2 | -0.2 | 0.7 | 167.5 | 16.4 | 139.0 | 28.3 | 3 |
| 12.6 | 41.29 | 18 | 2.0 | 1.1 | -0.1 | 0.6 | 168.7 | 14.7 | 138.2 | 26.8 | 3 |
| 14.6 | 39.29 | 17 | 2.0 | 1.1 | -0.1 | 0.6 | 169.7 | 13.4 | 137.3 | 25.9 | 4 |
| 16.6 | 37.29 | 16 | 2.0 | 1.0 | 0.0 | 0.5 | 170.9 | 12.5 | 135.6 | 25.1 | 4 |
| 18.6 | 35.29 | 15 | 2.0 | 1.0 | 0.1 | 0.5 | 170.8 | 12.0 | 134.2 | 23.4 | 4 |
| 20.6 | 33.29 | 14 | 2.1 | 0.9 | 0.1 | 0.5 | 170.9 | 11.6 | 132.8 | 22.3 | 5 |
| 22.6 | 31.29 | 13 | 2.1 | 0.9 | 0.2 | 0.5 | 168.6 | 12.1 | 132.3 | 21.9 | 5 |
| 24.6 | 29.29 | 12 | 2.0 | 0.9 | 0.2 | 0.5 | 166.6 | 12.5 | 132.3 | 22.4 | 5 |
| 26.6 | 27.29 | 11 | 2.0 | 0.9 | 0.2 | 0.5 | 165.9 | 12.3 | 133.0 | 23.1 | 5 |
| 28.6 | 25.29 | 10 | 2.0 | 1.0 | 0.2 | 0.5 | 165.2 | 12.1 | 134.0 | 23.7 | 4 |
| 30.6 | 23.29 | 9 | 2.0 | 1.0 | 0.1 | 0.5 | 164.7 | 12.1 | 135.9 | 24.0 | 4 |
| 32.6 | 21.29 | 8 | 2.0 | 1.0 | 0.1 | 0.5 | 163.3 | 12.1 | 137.7 | 24.1 | 4 |
| 34.6 | 19.29 | 7 | 1.9 | 1.0 | -0.1 | 0.5 | 161.5 | 12.5 | 137.8 | 24.7 | 4 |
| 36.6 | 17.29 | 6 | 1.9 | 1.0 | -0.1 | 0.5 | 158.7 | 14.1 | 136.4 | 25.8 | 4 |
| 38.6 | 15.29 | 5 | 1.8 | 1.0 | -0.1 | 0.6 | 154.7 | 16.0 | 135.6 | 26.0 | 4 |
| 40.6 | 13.29 | 4 | 1.8 | 0.9 | -0.1 | 0.6 | 151.7 | 17.4 | 135.2 | 26.1 | 4 |
| 42.6 | 11.29 | 3 | 1.7 | 0.9 | -0.1 | 0.6 | 150.5 | 18.5 | 135.6 | 27.0 | 3 |
| 44.6 | 9.29 | 2 | 1.7 | 0.9 | 0.0 | 0.6 | 150.8 | 18.0 | 136.0 | 26.4 | 4 |
| 46.6 | 7.29 | 1 | 1.7 | 0.9 | 0.0 | 0.6 | 151.9 | 16.5 | 137.3 | 24.4 | 4 |
| 53.44 | 0.45 | 1 | 1.3 | 0.5 | 0.0 | 0.5 | 136.5 | 18.1 | 133.7 | 18.4 | 7 |
| 53.57 | 0.32 | 2 | 1.2 | 0.5 | 0.0 | 0.5 | 136.2 | 18.2 | 133.8 | 18.4 | 7 |
| 53.61 | 0.28 | 1 | 1.1 | 0.4 | 0.0 | 0.4 | 131.4 | 18.7 | 145.1 | 18.2 | 7 |
| 53.69 | 0.20 | 3 | 1.1 | 0.4 | 0.0 | 0.4 | 135.2 | 18.5 | 133.3 | 18.6 | 7 |
| 53.82 | 0.07 | 4 | 1.0 | 0.4 | 0.0 | 0.4 | 132.9 | 18.5 | 131.3 | 18.2 | 7 |

*Depth beneath 53.9 m nominal surface height

ADCP 8421

PCADP 8424

ADV 8425

**Table B-12.** $K_1$ tidal characteristics from current meter records at Site B3. [cph, cycles per hour; SNR, signal-to-noise ratio]

| Site B3–$O_1$–.0.04178 cph | | | | | | | | | | | |
|---|---|---|---|---|---|---|---|---|---|---|---|
| **Depth*** | **Elevation** | **Bin#** | **Major** | **error** | **Minor** | **error** | **Inclination** | **error** | **Phase** | **error** | **SNR** |
| 6.6 | 47.29 | 21 | 5.8 | 1.3 | -1.1 | 0.8 | 175.4 | 7.7 | 185.3 | 12.2 | 20 |
| 8.6 | 45.29 | 20 | 5.3 | 1.2 | -0.9 | 0.7 | 171.3 | 7.7 | 182.2 | 12.3 | 19 |
| 10.6 | 43.29 | 19 | 5.0 | 1.2 | -0.7 | 0.7 | 169.0 | 7.2 | 178.3 | 12.5 | 18 |
| 12.6 | 41.29 | 18 | 4.7 | 1.1 | -0.6 | 0.6 | 165.8 | 7.2 | 174.3 | 12.4 | 18 |
| 14.6 | 39.29 | 17 | 4.5 | 1.0 | -0.5 | 0.6 | 162.8 | 7.1 | 170.5 | 12.3 | 18 |
| 16.6 | 37.29 | 16 | 4.4 | 1.0 | -0.4 | 0.6 | 159.6 | 7.1 | 166.4 | 11.8 | 20 |
| 18.6 | 35.29 | 15 | 4.3 | 0.9 | -0.2 | 0.6 | 156.2 | 7.2 | 161.8 | 11.1 | 22 |
| 20.6 | 33.29 | 14 | 4.3 | 0.9 | -0.2 | 0.6 | 152.6 | 7.3 | 157.9 | 10.5 | 25 |
| 22.6 | 31.29 | 13 | 4.2 | 0.8 | -0.1 | 0.6 | 149.9 | 7.6 | 154.6 | 10.3 | 26 |
| 24.6 | 29.29 | 12 | 4.2 | 0.8 | 0.0 | 0.6 | 148.1 | 7.9 | 151.8 | 10.3 | 25 |
| 26.6 | 27.29 | 11 | 4.1 | 0.8 | 0.1 | 0.6 | 146.9 | 8.2 | 149.8 | 10.7 | 24 |
| 28.6 | 25.29 | 10 | 3.9 | 0.9 | 0.0 | 0.6 | 147.2 | 8.5 | 148.8 | 11.3 | 21 |
| 30.6 | 23.29 | 9 | 3.9 | 0.9 | 0.0 | 0.6 | 148.6 | 8.4 | 148.9 | 11.8 | 20 |
| 32.6 | 21.29 | 8 | 3.9 | 0.9 | -0.1 | 0.6 | 149.9 | 8.2 | 149.3 | 11.9 | 19 |
| 34.6 | 19.29 | 7 | 3.9 | 0.9 | -0.2 | 0.6 | 151.3 | 7.9 | 149.3 | 12.0 | 19 |
| 36.6 | 17.29 | 6 | 3.9 | 0.9 | -0.2 | 0.6 | 152.4 | 7.9 | 148.9 | 12.4 | 18 |
| 38.6 | 15.29 | 5 | 3.9 | 1.0 | -0.2 | 0.6 | 154.0 | 7.9 | 148.6 | 12.7 | 17 |
| 40.6 | 13.29 | 4 | 3.9 | 1.0 | -0.2 | 0.6 | 154.7 | 8.1 | 149.0 | 13.0 | 16 |
| 42.6 | 11.29 | 3 | 3.8 | 1.0 | -0.3 | 0.6 | 155.1 | 8.2 | 150.2 | 13.3 | 16 |
| 44.6 | 9.29 | 2 | 3.7 | 0.9 | -0.4 | 0.6 | 154.3 | 8.4 | 151.2 | 13.2 | 16 |
| 46.6 | 7.29 | 1 | 3.6 | 0.9 | -0.4 | 0.6 | 152.4 | 8.6 | 151.4 | 12.6 | 18 |
| 53.44 | 0.45 | 1 | 2.2 | 0.5 | -0.5 | 0.5 | 135.2 | 12.3 | 148.0 | 12.3 | 21 |
| 53.57 | 0.32 | 2 | 2.1 | 0.5 | -0.5 | 0.5 | 134.6 | 12.4 | 148.2 | 12.4 | 21 |
| 53.61 | 0.28 | 1 | 1.9 | 0.4 | -0.4 | 0.4 | 131.0 | 12.6 | 163.8 | 12.3 | 21 |
| 53.69 | 0.20 | 3 | 1.9 | 0.4 | -0.4 | 0.4 | 134.0 | 12.6 | 148.2 | 12.5 | 20 |
| 53.82 | 0.07 | 4 | 1.7 | 0.4 | -0.4 | 0.4 | 132.8 | 12.4 | 148.8 | 12.3 | 21 |

*Depth beneath 53.9 m nominal surface height

ADCP 8421

PCADP 8424

ADV 8425

**Table B-13.** $M_2$ tidal characteristics from near-bottom 1,200-kHz ADCP current meter records at Site B3. [cph, cycles per hour; SNR, signal-to-noise ratio]

| Site B3 –$M_2$–0.08051 cph | | | | | | | | | | | |
|---|---|---|---|---|---|---|---|---|---|---|---|
| **Depth*** | **Elevation** | **Bin#** | **Major** | **error** | **Minor** | **error** | **Inclination** | **error** | **Phase** | **error** | **SNR** |
| 41.9 | 14.11 | 52 | 4.9 | 1.4 | 0.1 | 0.9 | 272.4 | 10.7 | 190.0 | 17.2 | 12 |
| 42.9 | 13.11 | 48 | 4.9 | 1.4 | 0.0 | 0.9 | 271.5 | 10.5 | 190.8 | 16.9 | 12 |
| 43.9 | 12.11 | 44 | 5.0 | 1.4 | 0.0 | 0.9 | 271.0 | 10.3 | 194.4 | 17.2 | 12 |
| 44.9 | 11.11 | 40 | 5.1 | 1.6 | -0.1 | 0.9 | 268.6 | 10.5 | 195.8 | 18.2 | 11 |
| 45.9 | 10.11 | 36 | 5.2 | 1.6 | -0.2 | 1.0 | 267.7 | 11.0 | 196.4 | 18.5 | 10 |
| 46.9 | 9.11 | 32 | 5.4 | 1.6 | -0.2 | 1.0 | 266.8 | 11.0 | 195.5 | 17.6 | 11 |
| 47.9 | 8.11 | 28 | 5.6 | 1.7 | -0.1 | 1.0 | 266.4 | 10.8 | 194.5 | 17.4 | 12 |
| 48.1 | 7.86 | 27 | 5.6 | 1.6 | -0.1 | 1.0 | 266.1 | 10.8 | 194.1 | 17.3 | 12 |
| 48.4 | 7.61 | 26 | 5.7 | 1.7 | -0.1 | 1.0 | 265.1 | 10.6 | 193.5 | 17.1 | 12 |
| 48.6 | 7.36 | 25 | 5.8 | 1.7 | -0.1 | 1.1 | 264.5 | 10.8 | 193.6 | 17.1 | 12 |
| 48.9 | 7.11 | 24 | 5.8 | 1.7 | -0.1 | 1.0 | 264.1 | 10.5 | 193.0 | 17.1 | 12 |
| 49.1 | 6.86 | 23 | 5.8 | 1.7 | -0.1 | 1.0 | 263.8 | 10.4 | 192.1 | 17.4 | 12 |
| 49.4 | 6.61 | 22 | 5.9 | 1.7 | -0.2 | 1.0 | 263.9 | 10.0 | 191.7 | 17.4 | 12 |
| 49.6 | 6.36 | 21 | 5.9 | 1.7 | -0.1 | 1.0 | 263.2 | 10.1 | 191.2 | 17.2 | 12 |
| 49.9 | 6.11 | 20 | 5.9 | 1.7 | -0.1 | 1.0 | 262.8 | 9.9 | 191.2 | 17.0 | 12 |
| 50.1 | 5.86 | 19 | 6.0 | 1.7 | -0.1 | 1.0 | 262.4 | 9.7 | 190.6 | 16.9 | 12 |
| 50.4 | 5.61 | 18 | 6.0 | 1.7 | -0.1 | 1.0 | 261.0 | 9.7 | 189.0 | 16.6 | 13 |
| 50.6 | 5.36 | 17 | 6.1 | 1.7 | -0.1 | 1.0 | 260.5 | 9.6 | 189.0 | 16.5 | 13 |
| 50.9 | 5.11 | 16 | 6.0 | 1.7 | 0.0 | 1.0 | 260.4 | 9.5 | 188.1 | 16.4 | 13 |
| 51.1 | 4.86 | 15 | 6.0 | 1.7 | -0.1 | 1.0 | 258.9 | 9.5 | 187.5 | 16.3 | 13 |
| 51.4 | 4.61 | 14 | 6.0 | 1.6 | -0.1 | 1.0 | 258.7 | 9.3 | 187.1 | 16.0 | 14 |
| 51.6 | 4.36 | 13 | 6.0 | 1.6 | 0.0 | 1.0 | 257.8 | 9.5 | 186.9 | 15.9 | 14 |
| 51.9 | 4.11 | 12 | 6.0 | 1.6 | 0.0 | 0.9 | 257.0 | 9.2 | 186.4 | 15.7 | 14 |
| 52.1 | 3.86 | 11 | 6.0 | 1.6 | 0.0 | 0.9 | 256.4 | 9.2 | 186.0 | 15.7 | 14 |
| 52.4 | 3.61 | 10 | 6.0 | 1.5 | 0.1 | 0.9 | 255.0 | 9.2 | 185.1 | 15.2 | 15 |
| 52.6 | 3.36 | 9 | 5.9 | 1.5 | 0.2 | 0.9 | 254.4 | 9.3 | 184.2 | 15.0 | 16 |
| 52.9 | 3.11 | 8 | 5.9 | 1.5 | 0.2 | 0.9 | 253.4 | 9.2 | 183.6 | 14.9 | 16 |
| 53.1 | 2.86 | 7 | 5.8 | 1.5 | 0.3 | 0.9 | 253.3 | 9.4 | 182.7 | 14.8 | 16 |
| 53.4 | 2.61 | 6 | 5.8 | 1.4 | 0.3 | 0.9 | 252.2 | 9.3 | 182.0 | 14.6 | 17 |
| 53.6 | 2.36 | 5 | 5.7 | 1.4 | 0.4 | 0.8 | 251.7 | 8.9 | 182.0 | 14.3 | 17 |
| 53.9 | 2.11 | 4 | 5.5 | 1.3 | 0.4 | 0.8 | 251.1 | 9.1 | 181.2 | 13.8 | 19 |
| 54.1 | 1.86 | 3 | 5.3 | 1.2 | 0.4 | 0.8 | 250.0 | 9.2 | 180.6 | 13.6 | 19 |
| 54.4 | 1.61 | 2 | 5.0 | 1.1 | 0.4 | 0.8 | 249.5 | 9.4 | 178.7 | 13.4 | 20 |
| 54.6 | 1.36 | 1 | 4.7 | 1.1 | 0.5 | 0.8 | 248.6 | 9.9 | 178.2 | 13.4 | 20 |

*Depth beneath 53.9 m nominal surface height

**Table B-14.** $S_2$ tidal characteristics from near-bottom 1,200-kHz ADCP current meter records at Site B3. [cph, cycles per hour; SNR, signal-to-noise ratio]

| Site B3–$S_2$–0.08333 cph | | | | | | | | | | | |
|---|---|---|---|---|---|---|---|---|---|---|---|
| Depth* | Elevation | Bin# | Major | error | Minor | error | Inclination | error | Phase | error | SNR |
| 41.9 | 14.11 | 52 | 2.4 | 1.4 | 0.9 | 0.9 | 270.9 | 28.8 | 225.3 | 40.5 | 3 |
| 42.9 | 13.11 | 48 | 2.3 | 1.4 | 0.9 | 0.9 | 270.0 | 29.7 | 226.4 | 42.0 | 3 |
| 43.9 | 12.11 | 44 | 2.2 | 1.4 | 0.8 | 0.9 | 270.5 | 31.7 | 227.9 | 45.6 | 2 |
| 44.9 | 11.11 | 40 | 2.1 | 1.6 | 0.9 | 0.9 | 263.5 | 38.2 | 234.3 | 53.8 | 2 |
| 45.9 | 10.11 | 36 | 2.2 | 1.6 | 0.8 | 1.0 | 260.5 | 36.2 | 238.7 | 51.4 | 2 |
| 46.9 | 9.11 | 32 | 2.3 | 1.6 | 0.8 | 1.0 | 257.7 | 33.2 | 241.4 | 46.3 | 2 |
| 47.9 | 8.11 | 28 | 2.3 | 1.6 | 0.7 | 1.1 | 254.1 | 32.0 | 241.9 | 44.4 | 2 |
| 48.1 | 7.86 | 27 | 2.4 | 1.6 | 0.7 | 1.1 | 252.8 | 30.5 | 242.4 | 42.2 | 2 |
| 48.4 | 7.61 | 26 | 2.5 | 1.6 | 0.6 | 1.1 | 252.5 | 29.0 | 241.8 | 40.5 | 2 |
| 48.6 | 7.36 | 25 | 2.5 | 1.6 | 0.6 | 1.1 | 250.9 | 29.7 | 241.6 | 40.5 | 2 |
| 48.9 | 7.11 | 24 | 2.5 | 1.6 | 0.6 | 1.1 | 249.8 | 29.5 | 242.8 | 40.6 | 2 |
| 49.1 | 6.86 | 23 | 2.6 | 1.7 | 0.6 | 1.1 | 249.8 | 27.9 | 242.3 | 39.4 | 2 |
| 49.4 | 6.61 | 22 | 2.6 | 1.7 | 0.6 | 1.1 | 249.6 | 27.0 | 240.9 | 38.9 | 3 |
| 49.6 | 6.36 | 21 | 2.7 | 1.6 | 0.7 | 1.1 | 248.8 | 27.1 | 240.8 | 38.0 | 3 |
| 49.9 | 6.11 | 20 | 2.7 | 1.6 | 0.6 | 1.1 | 247.6 | 26.1 | 240.9 | 36.5 | 3 |
| 50.1 | 5.86 | 19 | 2.7 | 1.6 | 0.6 | 1.1 | 248.6 | 25.9 | 241.1 | 37.0 | 3 |
| 50.4 | 5.61 | 18 | 2.8 | 1.6 | 0.6 | 1.1 | 246.4 | 24.5 | 240.8 | 34.2 | 3 |
| 50.6 | 5.36 | 17 | 2.9 | 1.6 | 0.7 | 1.1 | 246.4 | 24.3 | 240.3 | 33.9 | 3 |
| 50.9 | 5.11 | 16 | 2.9 | 1.6 | 0.6 | 1.1 | 245.4 | 23.9 | 239.7 | 33.1 | 3 |
| 51.1 | 4.86 | 15 | 3.0 | 1.6 | 0.6 | 1.1 | 244.2 | 23.6 | 240.3 | 32.3 | 4 |
| 51.4 | 4.61 | 14 | 3.0 | 1.5 | 0.7 | 1.1 | 244.6 | 22.7 | 241.2 | 31.1 | 4 |
| 51.6 | 4.36 | 13 | 3.0 | 1.5 | 0.7 | 1.1 | 244.2 | 23.0 | 240.2 | 31.0 | 4 |
| 51.9 | 4.11 | 12 | 3.2 | 1.5 | 0.7 | 1.1 | 244.4 | 21.4 | 239.6 | 29.3 | 4 |
| 52.1 | 3.86 | 11 | 3.2 | 1.5 | 0.8 | 1.1 | 243.5 | 21.8 | 239.6 | 29.3 | 4 |
| 52.4 | 3.61 | 10 | 3.2 | 1.5 | 0.8 | 1.1 | 242.6 | 21.3 | 238.9 | 28.2 | 5 |
| 52.6 | 3.36 | 9 | 3.3 | 1.4 | 0.8 | 1.1 | 242.3 | 20.6 | 239.3 | 27.0 | 5 |
| 52.9 | 3.11 | 8 | 3.3 | 1.4 | 0.8 | 1.0 | 241.2 | 20.4 | 239.6 | 26.4 | 6 |
| 53.1 | 2.86 | 7 | 3.3 | 1.4 | 0.8 | 1.0 | 241.8 | 20.4 | 239.5 | 26.4 | 6 |
| 53.4 | 2.61 | 6 | 3.2 | 1.3 | 0.9 | 1.0 | 240.9 | 20.9 | 239.7 | 26.5 | 6 |
| 53.6 | 2.36 | 5 | 3.1 | 1.3 | 1.0 | 1.0 | 241.3 | 20.8 | 238.8 | 26.8 | 6 |
| 53.9 | 2.11 | 4 | 3.1 | 1.2 | 1.0 | 0.9 | 241.0 | 20.4 | 238.4 | 25.5 | 7 |
| 54.1 | 1.86 | 3 | 3.0 | 1.1 | 0.9 | 0.9 | 239.9 | 20.4 | 237.6 | 25.0 | 7 |
| 54.4 | 1.61 | 2 | 2.9 | 1.1 | 0.9 | 0.9 | 239.4 | 20.3 | 235.9 | 24.4 | 7 |
| 54.6 | 1.36 | 1 | 2.8 | 1.0 | 0.9 | 0.8 | 237.2 | 20.7 | 236.2 | 23.8 | 8 |

*Depth beneath 53.9 m nominal surface height

**Table B-15.** $O_1$ tidal characteristics from near-bottom 1,200-kHz ADCP current meter records at Site B3. [cph, cycles per hour; SNR, signal-to-noise ratio ]

| Site B3–$O_1$–.0.03873 cph | | | | | | | | | | | |
|---|---|---|---|---|---|---|---|---|---|---|---|
| **Depth*** | **Elevation** | **Bin#** | **Major** | **error** | **Minor** | **error** | **Inclination** | **error** | **Phase** | **error** | **SNR** |
| 41.9 | 14.11 | 52 | 1.4 | 2.3 | 0.6 | 1.4 | 288.9 | 68.4 | 177.1 | 95.5 | 0 |
| 42.9 | 13.11 | 48 | 1.4 | 2.2 | 0.6 | 1.5 | 291.6 | 73.0 | 175.9 | 96.6 | 0 |
| 43.9 | 12.11 | 44 | 1.3 | 2.1 | 0.6 | 1.5 | 296.5 | 90.8 | 171.0 | 112.7 | 0 |
| 44.9 | 11.11 | 40 | 1.2 | 2.0 | 0.6 | 1.6 | 303.6 | 98.3 | 167.7 | 113.0 | 0 |
| 45.9 | 10.11 | 36 | 1.3 | 2.0 | 0.7 | 1.5 | 303.3 | 95.4 | 165.8 | 109.7 | 0 |
| 46.9 | 9.11 | 32 | 1.3 | 1.9 | 0.7 | 1.6 | 307.4 | 104.2 | 162.4 | 113.6 | 0 |
| 47.9 | 8.11 | 28 | 1.4 | 1.7 | 0.8 | 1.6 | 311.5 | 96.7 | 157.7 | 101.1 | 1 |
| 48.1 | 7.86 | 27 | 1.4 | 1.7 | 0.8 | 1.5 | 308.8 | 90.8 | 161.7 | 98.1 | 1 |
| 48.4 | 7.61 | 26 | 1.4 | 1.7 | 0.8 | 1.4 | 306.6 | 84.3 | 161.8 | 94.8 | 1 |
| 48.6 | 7.36 | 25 | 1.5 | 1.7 | 0.8 | 1.4 | 308.4 | 78.7 | 159.0 | 86.7 | 1 |
| 48.9 | 7.11 | 24 | 1.5 | 1.7 | 0.8 | 1.4 | 308.8 | 74.8 | 158.4 | 82.2 | 1 |
| 49.1 | 6.86 | 23 | 1.5 | 1.7 | 0.8 | 1.4 | 307.5 | 80.0 | 159.1 | 88.9 | 1 |
| 49.4 | 6.61 | 22 | 1.5 | 1.7 | 0.8 | 1.4 | 309.1 | 71.0 | 157.6 | 78.1 | 1 |
| 49.6 | 6.36 | 21 | 1.6 | 1.7 | 0.8 | 1.4 | 308.0 | 73.7 | 157.3 | 81.9 | 1 |
| 49.9 | 6.11 | 20 | 1.6 | 1.7 | 0.8 | 1.3 | 307.4 | 67.0 | 156.4 | 75.9 | 1 |
| 50.1 | 5.86 | 19 | 1.6 | 1.6 | 0.8 | 1.4 | 308.9 | 70.5 | 154.4 | 77.7 | 1 |
| 50.4 | 5.61 | 18 | 1.6 | 1.6 | 0.9 | 1.3 | 308.7 | 71.0 | 154.9 | 78.3 | 1 |
| 50.6 | 5.36 | 17 | 1.6 | 1.5 | 0.9 | 1.3 | 310.1 | 68.0 | 152.8 | 73.6 | 1 |
| 50.9 | 5.11 | 16 | 1.6 | 1.5 | 0.9 | 1.4 | 312.2 | 66.8 | 151.5 | 69.9 | 1 |
| 51.1 | 4.86 | 15 | 1.6 | 1.5 | 0.9 | 1.4 | 312.9 | 69.6 | 151.2 | 71.9 | 1 |
| 51.4 | 4.61 | 14 | 1.7 | 1.4 | 0.9 | 1.4 | 313.4 | 68.0 | 149.6 | 69.7 | 1 |
| 51.6 | 4.36 | 13 | 1.6 | 1.3 | 0.9 | 1.4 | 315.6 | 69.2 | 147.9 | 68.6 | 2 |
| 51.9 | 4.11 | 12 | 1.6 | 1.3 | 0.9 | 1.4 | 316.5 | 67.5 | 145.6 | 65.9 | 2 |
| 52.1 | 3.86 | 11 | 1.7 | 1.2 | 0.9 | 1.4 | 318.7 | 64.0 | 145.0 | 60.3 | 2 |
| 52.4 | 3.61 | 10 | 1.6 | 1.2 | 0.9 | 1.3 | 318.0 | 62.6 | 144.2 | 59.7 | 2 |
| 52.6 | 3.36 | 9 | 1.6 | 1.2 | 0.9 | 1.3 | 318.0 | 61.9 | 142.7 | 59.0 | 2 |
| 52.9 | 3.11 | 8 | 1.7 | 1.2 | 0.8 | 1.3 | 318.4 | 55.8 | 143.0 | 52.6 | 2 |
| 53.1 | 2.86 | 7 | 1.6 | 1.1 | 0.8 | 1.2 | 319.2 | 56.8 | 140.7 | 53.0 | 2 |
| 53.4 | 2.61 | 6 | 1.5 | 1.1 | 0.8 | 1.2 | 319.6 | 61.1 | 141.4 | 57.1 | 2 |
| 53.6 | 2.36 | 5 | 1.5 | 1.0 | 0.8 | 1.2 | 319.3 | 56.5 | 139.2 | 52.9 | 2 |
| 53.9 | 2.11 | 4 | 1.4 | 1.0 | 0.7 | 1.1 | 319.2 | 54.4 | 138.8 | 50.9 | 2 |
| 54.1 | 1.86 | 3 | 1.3 | 1.0 | 0.7 | 1.1 | 319.1 | 60.6 | 138.3 | 57.1 | 2 |
| 54.4 | 1.61 | 2 | 1.2 | 0.9 | 0.6 | 1.0 | 320.1 | 58.0 | 137.8 | 53.7 | 2 |
| 54.6 | 1.36 | 1 | 1.1 | 0.9 | 0.6 | 1.0 | 320.1 | 63.0 | 136.0 | 58.7 | 2 |

*Depth beneath 53.9 m nominal surface height

**Table B-16.** $K_1$ tidal characteristics from near-bottom 1,200-kHz ADCP current meter records at Site B3. [cph, cycles per hour; SNR, signal-to-noise ratio]

| Site B3–$K_1$–.0.04178 cph | | | | | | | | | | | |
|---|---|---|---|---|---|---|---|---|---|---|---|
| **Depth*** | **Elevation** | **Bin#** | **Major** | **error** | **Minor** | **error** | **Inclination** | **error** | **Phase** | **error** | **SNR** |
| 41.9 | 14.11 | 52 | 4.6 | 1.9 | -0.7 | 1.8 | 312.2 | 21.5 | 120.3 | 22.7 | 6 |
| 42.9 | 13.11 | 48 | 4.7 | 1.9 | -0.7 | 1.8 | 312.0 | 20.7 | 120.6 | 21.9 | 6 |
| 43.9 | 12.11 | 44 | 4.8 | 1.9 | -0.9 | 1.8 | 310.2 | 20.3 | 120.6 | 22.2 | 6 |
| 44.9 | 11.11 | 40 | 4.8 | 1.9 | -0.9 | 1.7 | 309.1 | 20.0 | 122.0 | 22.3 | 6 |
| 45.9 | 10.11 | 36 | 4.5 | 1.8 | -1.0 | 1.7 | 311.2 | 21.0 | 124.3 | 22.6 | 6 |
| 46.9 | 9.11 | 32 | 4.4 | 1.8 | -1.1 | 1.7 | 313.2 | 21.8 | 125.9 | 22.6 | 6 |
| 47.9 | 8.11 | 28 | 4.4 | 1.6 | -1.1 | 1.7 | 315.6 | 21.9 | 127.6 | 21.6 | 7 |
| 48.1 | 7.86 | 27 | 4.3 | 1.6 | -1.1 | 1.6 | 316.0 | 21.7 | 127.5 | 21.3 | 7 |
| 48.4 | 7.61 | 26 | 4.3 | 1.5 | -1.2 | 1.6 | 316.9 | 21.7 | 128.2 | 20.8 | 8 |
| 48.6 | 7.36 | 25 | 4.2 | 1.5 | -1.1 | 1.6 | 317.2 | 21.8 | 128.3 | 20.8 | 8 |
| 48.9 | 7.11 | 24 | 4.2 | 1.5 | -1.2 | 1.6 | 317.9 | 22.6 | 128.3 | 21.2 | 8 |
| 49.1 | 6.86 | 23 | 4.2 | 1.5 | -1.2 | 1.6 | 318.5 | 22.8 | 128.7 | 21.0 | 8 |
| 49.4 | 6.61 | 22 | 4.2 | 1.5 | -1.1 | 1.6 | 318.4 | 22.3 | 129.1 | 20.6 | 8 |
| 49.6 | 6.36 | 21 | 4.1 | 1.5 | -1.1 | 1.6 | 319.4 | 23.0 | 129.4 | 20.7 | 8 |
| 49.9 | 6.11 | 20 | 4.1 | 1.4 | -1.2 | 1.6 | 320.0 | 22.7 | 129.0 | 20.2 | 9 |
| 50.1 | 5.86 | 19 | 4.1 | 1.4 | -1.2 | 1.6 | 319.9 | 22.8 | 129.4 | 20.2 | 9 |
| 50.4 | 5.61 | 18 | 4.0 | 1.4 | -1.2 | 1.6 | 320.8 | 23.4 | 130.1 | 20.3 | 9 |
| 50.6 | 5.36 | 17 | 4.0 | 1.3 | -1.2 | 1.6 | 320.5 | 22.6 | 130.1 | 19.7 | 9 |
| 50.9 | 5.11 | 16 | 4.0 | 1.3 | -1.2 | 1.6 | 321.0 | 22.9 | 130.6 | 19.7 | 9 |
| 51.1 | 4.86 | 15 | 4.0 | 1.3 | -1.1 | 1.6 | 321.5 | 22.8 | 130.6 | 19.4 | 10 |
| 51.4 | 4.61 | 14 | 3.9 | 1.2 | -1.2 | 1.5 | 322.7 | 23.0 | 130.9 | 19.1 | 10 |
| 51.6 | 4.36 | 13 | 3.9 | 1.2 | -1.2 | 1.5 | 323.0 | 23.2 | 131.9 | 19.1 | 10 |
| 51.9 | 4.11 | 12 | 3.8 | 1.2 | -1.2 | 1.5 | 323.6 | 23.5 | 132.6 | 19.1 | 11 |
| 52.1 | 3.86 | 11 | 3.7 | 1.1 | -1.2 | 1.5 | 323.6 | 23.2 | 132.2 | 18.9 | 11 |
| 52.4 | 3.61 | 10 | 3.6 | 1.1 | -1.2 | 1.4 | 324.2 | 23.2 | 132.2 | 18.7 | 12 |
| 52.6 | 3.36 | 9 | 3.6 | 1.0 | -1.2 | 1.4 | 325.1 | 23.2 | 132.3 | 18.3 | 12 |
| 52.9 | 3.11 | 8 | 3.5 | 1.0 | -1.2 | 1.4 | 325.8 | 24.4 | 132.9 | 18.9 | 12 |
| 53.1 | 2.86 | 7 | 3.4 | 1.0 | -1.2 | 1.3 | 326.3 | 23.9 | 133.3 | 18.6 | 12 |
| 53.4 | 2.61 | 6 | 3.2 | 0.9 | -1.2 | 1.3 | 325.8 | 24.6 | 132.1 | 19.6 | 12 |
| 53.6 | 2.36 | 5 | 3.1 | 0.9 | -1.2 | 1.3 | 327.2 | 24.7 | 133.3 | 19.2 | 12 |
| 53.9 | 2.11 | 4 | 3.0 | 0.8 | -1.2 | 1.2 | 327.2 | 25.0 | 133.1 | 19.7 | 13 |
| 54.1 | 1.86 | 3 | 2.7 | 0.9 | -1.1 | 1.1 | 326.3 | 27.5 | 132.6 | 22.5 | 10 |
| 54.4 | 1.61 | 2 | 2.6 | 0.8 | -1.1 | 1.1 | 327.2 | 27.4 | 132.7 | 22.3 | 11 |
| 54.6 | 1.36 | 1 | 2.4 | 0.8 | -1.1 | 1.0 | 327.5 | 29.4 | 133.4 | 24.1 | 10 |

*Depth beneath 53.9 m nominal surface height

Table **B-17.** $M_2$ tidal characteristics from current meter records at Site B5. [cph, cycles per hour; SNR, signal-to-noise ratio]

| Site B5–$M_2$–0.08051 cph | | | | | | | | | | | |
|---|---|---|---|---|---|---|---|---|---|---|---|
| **Depth*** | **Elevation** | **Bin#** | **Major** | **error** | **Minor** | **error** | **Inclination** | **error** | **Phase** | **error** | **SNR** |
| 8.2 | 57.47 | 26 | 4.6 | 0.9 | -1.3 | 0.6 | 278.5 | 9.8 | 201.8 | 13.6 | 23 |
| 10.2 | 55.47 | 25 | 4.4 | 0.9 | -1.3 | 0.6 | 277.2 | 9.9 | 200.1 | 13.5 | 24 |
| 12.2 | 53.47 | 24 | 4.3 | 0.9 | -1.2 | 0.6 | 276.3 | 9.8 | 197.9 | 13.1 | 25 |
| 14.2 | 51.47 | 23 | 4.3 | 0.8 | -1.1 | 0.6 | 275.7 | 9.4 | 196.0 | 12.6 | 26 |
| 16.2 | 49.47 | 22 | 4.2 | 0.8 | -1.0 | 0.6 | 275.1 | 8.9 | 194.3 | 12.1 | 28 |
| 18.2 | 47.47 | 21 | 4.1 | 0.7 | -0.9 | 0.5 | 274.6 | 8.4 | 192.8 | 11.5 | 30 |
| 20.2 | 45.47 | 20 | 4.1 | 0.7 | -0.8 | 0.5 | 274.3 | 8.0 | 191.2 | 10.8 | 33 |
| 22.2 | 43.47 | 19 | 4.1 | 0.7 | -0.8 | 0.5 | 274.8 | 7.8 | 190.4 | 10.1 | 37 |
| 24.2 | 41.47 | 18 | 4.1 | 0.6 | -0.7 | 0.5 | 276.2 | 7.6 | 190.7 | 9.6 | 41 |
| 26.2 | 39.47 | 17 | 4.1 | 0.6 | -0.6 | 0.5 | 276.9 | 7.2 | 191.7 | 9.4 | 42 |
| 28.2 | 37.47 | 16 | 4.2 | 0.7 | -0.4 | 0.5 | 277.1 | 6.7 | 193.1 | 9.3 | 41 |
| 30.2 | 35.47 | 15 | 4.4 | 0.7 | -0.2 | 0.5 | 276.4 | 6.1 | 194.9 | 9.3 | 40 |
| 32.2 | 33.47 | 14 | 4.6 | 0.7 | 0.0 | 0.5 | 274.6 | 5.8 | 196.9 | 9.4 | 40 |
| 34.2 | 31.47 | 13 | 4.8 | 0.8 | 0.1 | 0.5 | 271.8 | 5.7 | 199.6 | 9.4 | 40 |
| 36.2 | 29.47 | 12 | 5.1 | 0.8 | 0.3 | 0.5 | 269.0 | 5.8 | 202.5 | 9.1 | 42 |
| 38.2 | 27.47 | 11 | 5.4 | 0.8 | 0.4 | 0.5 | 266.2 | 5.9 | 204.9 | 8.7 | 47 |
| 40.2 | 25.47 | 10 | 5.8 | 0.8 | 0.5 | 0.6 | 263.4 | 5.9 | 206.8 | 8.1 | 54 |
| 42.2 | 23.47 | 9 | 6.1 | 0.8 | 0.5 | 0.6 | 261.1 | 5.9 | 208.1 | 7.6 | 62 |
| 44.2 | 21.47 | 8 | 6.3 | 0.8 | 0.4 | 0.6 | 259.6 | 5.9 | 208.5 | 7.3 | 67 |
| 46.2 | 19.47 | 7 | 6.4 | 0.8 | 0.4 | 0.6 | 258.9 | 5.8 | 208.3 | 7.1 | 71 |
| 48.2 | 17.47 | 6 | 6.4 | 0.8 | 0.4 | 0.6 | 259.0 | 5.8 | 207.4 | 7.0 | 73 |
| 50.2 | 15.47 | 5 | 6.4 | 0.7 | 0.3 | 0.6 | 259.4 | 5.9 | 205.7 | 6.8 | 77 |
| 52.2 | 13.47 | 4 | 6.2 | 0.7 | 0.3 | 0.7 | 259.5 | 6.2 | 203.1 | 6.6 | 82 |
| 54.2 | 11.47 | 3 | 6.0 | 0.6 | 0.3 | 0.7 | 259.1 | 6.4 | 199.8 | 6.3 | 90 |
| 56.2 | 9.47 | 2 | 5.8 | 0.6 | 0.3 | 0.6 | 258.8 | 6.4 | 195.9 | 6.0 | 100 |
| 58.2 | 7.47 | 1 | 5.7 | 0.5 | 0.4 | 0.6 | 257.9 | 6.2 | 191.9 | 5.7 | 110 |
| 65.3 | 0.40 | 1 | 4.0 | 0.3 | 1.3 | 0.4 | 253.7 | 7.0 | 165.8 | 6.1 | 140 |
| 65.4 | 0.28 | 2 | 3.9 | 0.3 | 1.3 | 0.4 | 253.9 | 7.1 | 165.5 | 6.2 | 140 |
| 65.4 | 0.23 | 1 | 3.4 | 0.3 | 1.1 | 0.4 | 251.0 | 7.2 | 166.9 | 6.1 | 140 |
| 65.5 | 0.15 | 3 | 3.5 | 0.3 | 1.2 | 0.4 | 254.1 | 7.2 | 165.4 | 6.3 | 140 |
| 65.6 | 0.03 | 4 | 2.9 | 0.3 | 1.0 | 0.3 | 256.3 | 7.5 | 163.8 | 6.6 | 130 |

*Depth beneath 65.65 m nominal surface height

ADCP 8441

PCADP 844

ADV 8446

**Table B-18.** $S_2$ tidal characteristics from current meter records at Site B5. [cph, cycles per hour; SNR, signal-to-noise ratio]

| Site B5–$S_2$–0.08333 cph | | | | | | | | | | | |
|---|---|---|---|---|---|---|---|---|---|---|---|
| **Depth*** | **Elevation** | **Bin#** | **Major** | **error** | **Minor** | **error** | **Inclination** | **error** | **Phase** | **error** | **SNR** |
| 8.2 | 57.47 | 26 | 3.0 | 0.9 | -1.3 | 0.6 | 277.4 | 17.6 | 231.6 | 23.0 | 10 |
| 10.2 | 55.47 | 25 | 2.9 | 0.9 | -1.2 | 0.6 | 277.9 | 17.7 | 231.4 | 22.7 | 10 |
| 12.2 | 53.47 | 24 | 2.9 | 0.9 | -1.2 | 0.6 | 278.5 | 16.4 | 230.9 | 20.9 | 11 |
| 14.2 | 51.47 | 23 | 2.9 | 0.8 | -1.0 | 0.6 | 279.2 | 15.1 | 229.6 | 19.4 | 12 |
| 16.2 | 49.47 | 22 | 2.8 | 0.8 | -0.9 | 0.6 | 279.7 | 13.7 | 228.1 | 17.9 | 13 |
| 18.2 | 47.47 | 21 | 2.8 | 0.7 | -0.8 | 0.5 | 280.5 | 12.7 | 226.0 | 16.7 | 14 |
| 20.2 | 45.47 | 20 | 2.7 | 0.7 | -0.6 | 0.5 | 281.9 | 12.0 | 223.9 | 15.8 | 15 |
| 22.2 | 43.47 | 19 | 2.6 | 0.7 | -0.4 | 0.5 | 283.6 | 11.9 | 222.0 | 15.1 | 16 |
| 24.2 | 41.47 | 18 | 2.5 | 0.6 | -0.3 | 0.5 | 283.8 | 11.7 | 220.6 | 14.5 | 16 |
| 26.2 | 39.47 | 17 | 2.5 | 0.6 | -0.2 | 0.5 | 283.2 | 11.4 | 220.7 | 14.7 | 15 |
| 28.2 | 37.47 | 16 | 2.5 | 0.7 | -0.1 | 0.5 | 281.5 | 10.9 | 222.3 | 15.0 | 15 |
| 30.2 | 35.47 | 15 | 2.6 | 0.7 | 0.0 | 0.5 | 279.9 | 10.2 | 225.4 | 15.3 | 14 |
| 32.2 | 33.47 | 14 | 2.7 | 0.7 | 0.0 | 0.5 | 278.4 | 9.8 | 229.2 | 15.5 | 14 |
| 34.2 | 31.47 | 13 | 2.7 | 0.8 | 0.1 | 0.5 | 275.4 | 9.9 | 231.6 | 16.1 | 13 |
| 36.2 | 29.47 | 12 | 2.7 | 0.8 | 0.1 | 0.5 | 271.8 | 10.4 | 233.6 | 16.4 | 12 |
| 38.2 | 27.47 | 11 | 2.8 | 0.8 | 0.1 | 0.5 | 268.0 | 10.8 | 234.8 | 16.1 | 13 |
| 40.2 | 25.47 | 10 | 2.9 | 0.8 | 0.0 | 0.6 | 264.8 | 11.1 | 235.6 | 15.3 | 14 |
| 42.2 | 23.47 | 9 | 3.1 | 0.8 | -0.1 | 0.6 | 261.6 | 11.1 | 236.6 | 14.3 | 16 |
| 44.2 | 21.47 | 8 | 3.3 | 0.8 | -0.1 | 0.6 | 259.1 | 11.0 | 236.2 | 13.6 | 18 |
| 46.2 | 19.47 | 7 | 3.3 | 0.8 | -0.1 | 0.6 | 257.1 | 10.9 | 235.2 | 13.1 | 19 |
| 48.2 | 17.47 | 6 | 3.3 | 0.8 | 0.0 | 0.6 | 255.1 | 11.1 | 234.0 | 13.1 | 19 |
| 50.2 | 15.47 | 5 | 3.2 | 0.7 | 0.0 | 0.6 | 254.4 | 11.4 | 233.1 | 12.9 | 20 |
| 52.2 | 13.47 | 4 | 3.1 | 0.7 | 0.1 | 0.7 | 253.7 | 12.2 | 231.0 | 12.8 | 20 |
| 54.2 | 11.47 | 3 | 2.9 | 0.6 | 0.2 | 0.7 | 254.4 | 12.9 | 227.9 | 12.7 | 21 |
| 56.2 | 9.47 | 2 | 2.7 | 0.6 | 0.2 | 0.6 | 255.9 | 13.5 | 224.0 | 12.6 | 21 |
| 58.2 | 7.47 | 1 | 2.5 | 0.5 | 0.4 | 0.6 | 256.6 | 14.0 | 220.5 | 13.1 | 21 |
| 65.3 | 0.40 | 1 | 1.4 | 0.4 | 0.7 | 0.4 | 249.0 | 24.6 | 199.5 | 22.5 | 17 |
| 65.4 | 0.28 | 2 | 1.3 | 0.3 | 0.7 | 0.4 | 248.7 | 25.6 | 199.6 | 23.6 | 16 |
| 65.4 | 0.23 | 1 | 1.2 | 0.3 | 0.6 | 0.4 | 246.3 | 24.8 | 201.6 | 22.3 | 17 |
| 65.5 | 0.15 | 3 | 1.2 | 0.3 | 0.7 | 0.4 | 248.6 | 25.3 | 199.6 | 23.3 | 16 |
| 65.6 | 0.03 | 4 | 1.0 | 0.3 | 0.6 | 0.3 | 252.0 | 27.9 | 197.5 | 25.8 | 15 |

*Depth beneath 65.65 m nominal surface height

ADCP 8441

PCADP 844

ADV 8446

**Table B-19.** $O_1$ tidal characteristics from current meter records at Site B5. [cph, cycles per hour; SNR, signal-to-noise ratio]

| Site B5–$O_1$–.0.03873 cph | | | | | | | | | | | |
|---|---|---|---|---|---|---|---|---|---|---|---|
| **Depth*** | **Elevation** | **Bin#** | **Major** | **error** | **Minor** | **error** | **Inclination** | **error** | **Phase** | **error** | **SNR** |
| 8.2 | 57.47 | 26 | 1.5 | 0.9 | -0.7 | 0.7 | 276.1 | 33.9 | 149.7 | 39.9 | 3 |
| 10.2 | 55.47 | 25 | 1.6 | 0.9 | -0.7 | 0.7 | 273.3 | 29.3 | 147.8 | 35.2 | 4 |
| 12.2 | 53.47 | 24 | 1.6 | 0.8 | -0.7 | 0.6 | 273.8 | 25.7 | 148.4 | 31.7 | 4 |
| 14.2 | 51.47 | 23 | 1.7 | 0.8 | -0.6 | 0.6 | 274.2 | 21.1 | 148.0 | 27.2 | 5 |
| 16.2 | 49.47 | 22 | 1.8 | 0.8 | -0.5 | 0.5 | 274.6 | 17.5 | 147.7 | 24.0 | 5 |
| 18.2 | 47.47 | 21 | 1.8 | 0.7 | -0.5 | 0.5 | 276.0 | 14.5 | 146.8 | 20.9 | 6 |
| 20.2 | 45.47 | 20 | 1.9 | 0.7 | -0.4 | 0.5 | 277.3 | 12.8 | 145.3 | 19.0 | 7 |
| 22.2 | 43.47 | 19 | 1.9 | 0.7 | -0.3 | 0.4 | 278.2 | 12.0 | 143.4 | 18.3 | 8 |
| 24.2 | 41.47 | 18 | 1.9 | 0.7 | -0.3 | 0.4 | 280.5 | 11.8 | 142.1 | 18.3 | 8 |
| 26.2 | 39.47 | 17 | 1.9 | 0.7 | -0.3 | 0.4 | 284.6 | 11.8 | 140.3 | 18.4 | 8 |
| 28.2 | 37.47 | 16 | 1.9 | 0.7 | -0.2 | 0.5 | 288.4 | 12.3 | 138.2 | 19.3 | 7 |
| 30.2 | 35.47 | 15 | 1.8 | 0.8 | -0.2 | 0.5 | 290.7 | 13.3 | 136.0 | 20.6 | 6 |
| 32.2 | 33.47 | 14 | 1.8 | 0.8 | -0.1 | 0.5 | 292.9 | 14.6 | 134.3 | 21.6 | 5 |
| 34.2 | 31.47 | 13 | 1.7 | 0.8 | -0.2 | 0.5 | 294.1 | 15.2 | 133.3 | 21.9 | 5 |
| 36.2 | 29.47 | 12 | 1.8 | 0.8 | -0.2 | 0.5 | 294.3 | 15.3 | 133.3 | 21.9 | 5 |
| 38.2 | 27.47 | 11 | 1.8 | 0.8 | -0.3 | 0.5 | 294.5 | 15.7 | 133.3 | 22.1 | 5 |
| 40.2 | 25.47 | 10 | 1.7 | 0.7 | -0.4 | 0.5 | 295.3 | 16.6 | 133.8 | 22.8 | 5 |
| 42.2 | 23.47 | 9 | 1.7 | 0.7 | -0.5 | 0.5 | 296.8 | 17.4 | 135.0 | 23.1 | 5 |
| 44.2 | 21.47 | 8 | 1.8 | 0.7 | -0.5 | 0.5 | 296.4 | 16.9 | 136.2 | 22.3 | 6 |
| 46.2 | 19.47 | 7 | 1.8 | 0.7 | -0.4 | 0.5 | 296.1 | 15.7 | 137.6 | 20.6 | 7 |
| 48.2 | 17.47 | 6 | 1.9 | 0.7 | -0.4 | 0.5 | 295.8 | 14.7 | 138.7 | 18.9 | 8 |
| 50.2 | 15.47 | 5 | 2.0 | 0.7 | -0.3 | 0.5 | 296.6 | 14.3 | 139.6 | 17.6 | 9 |
| 52.2 | 13.47 | 4 | 2.0 | 0.7 | -0.3 | 0.6 | 297.9 | 14.0 | 140.2 | 16.6 | 9 |
| 54.2 | 11.47 | 3 | 2.0 | 0.6 | -0.2 | 0.5 | 298.0 | 13.6 | 139.4 | 16.0 | 10 |
| 56.2 | 9.47 | 2 | 1.9 | 0.6 | -0.2 | 0.5 | 298.9 | 13.6 | 138.7 | 15.8 | 10 |
| 58.2 | 7.47 | 1 | 1.7 | 0.6 | -0.1 | 0.5 | 299.3 | 13.6 | 137.9 | 15.9 | 10 |
| 65.3 | 0.40 | 1 | 0.8 | 0.3 | -0.1 | 0.3 | 301.1 | 18.7 | 125.1 | 20.4 | 6 |
| 65.4 | 0.28 | 2 | 0.8 | 0.3 | -0.1 | 0.3 | 301.9 | 18.9 | 126.2 | 20.6 | 6 |
| 65.4 | 0.23 | 1 | 0.7 | 0.3 | -0.1 | 0.3 | 300.5 | 18.4 | 127.7 | 20.2 | 6 |
| 65.5 | 0.15 | 3 | 0.7 | 0.3 | -0.1 | 0.3 | 303.2 | 18.8 | 126.4 | 20.2 | 6 |
| 65.6 | 0.03 | 4 | 0.6 | 0.2 | 0.0 | 0.2 | 303.4 | 18.1 | 127.2 | 19.2 | 7 |

*Depth beneath 65.65 m nominal surface height

- ADCP 8441 (white)
- PCADP 844 (yellow)
- ADV 8446 (blue)

**Table B-20.** $K_1$ tidal characteristics from current meter records at Site B5. [cph, cycles per hour; SNR, signal-to-noise ratio]

| Site B5 –$K_1$–.0.04178 cph | | | | | | | | | | | |
|---|---|---|---|---|---|---|---|---|---|---|---|
| Depth* | Elevation | Bin# | Major | error | Minor | error | Inclination | error | Phase | error | SNR |
| 8.2 | 57.47 | 26 | 4.3 | 0.9 | -1.6 | 0.7 | 278.9 | 10.7 | 186.3 | 13.0 | 23 |
| 10.2 | 55.47 | 25 | 4.0 | 0.9 | -1.3 | 0.7 | 283.3 | 10.7 | 179.2 | 13.1 | 22 |
| 12.2 | 53.47 | 24 | 3.7 | 0.8 | -1.1 | 0.6 | 287.7 | 10.5 | 173.1 | 12.8 | 21 |
| 14.2 | 51.47 | 23 | 3.6 | 0.8 | -0.9 | 0.6 | 291.4 | 9.9 | 168.5 | 12.2 | 22 |
| 16.2 | 49.47 | 22 | 3.5 | 0.7 | -0.8 | 0.6 | 294.8 | 9.1 | 164.7 | 11.4 | 24 |
| 18.2 | 47.47 | 21 | 3.5 | 0.7 | -0.6 | 0.5 | 296.8 | 8.5 | 161.3 | 10.6 | 26 |
| 20.2 | 45.47 | 20 | 3.5 | 0.7 | -0.5 | 0.5 | 298.1 | 8.0 | 158.4 | 10.0 | 29 |
| 22.2 | 43.47 | 19 | 3.6 | 0.6 | -0.4 | 0.5 | 299.2 | 7.6 | 155.9 | 9.6 | 30 |
| 24.2 | 41.47 | 18 | 3.5 | 0.6 | -0.3 | 0.5 | 300.7 | 7.6 | 153.7 | 9.5 | 30 |
| 26.2 | 39.47 | 17 | 3.5 | 0.7 | -0.2 | 0.5 | 302.3 | 7.8 | 151.9 | 9.7 | 29 |
| 28.2 | 37.47 | 16 | 3.5 | 0.7 | -0.2 | 0.5 | 303.7 | 8.2 | 151.0 | 10.1 | 27 |
| 30.2 | 35.47 | 15 | 3.4 | 0.7 | -0.3 | 0.6 | 304.6 | 8.8 | 150.3 | 10.7 | 24 |
| 32.2 | 33.47 | 14 | 3.4 | 0.7 | -0.3 | 0.6 | 305.0 | 9.3 | 149.4 | 11.2 | 22 |
| 34.2 | 31.47 | 13 | 3.3 | 0.7 | -0.4 | 0.6 | 304.8 | 9.4 | 148.4 | 11.4 | 22 |
| 36.2 | 29.47 | 12 | 3.4 | 0.7 | -0.4 | 0.6 | 305.1 | 9.4 | 148.2 | 11.3 | 22 |
| 38.2 | 27.47 | 11 | 3.4 | 0.7 | -0.5 | 0.6 | 305.8 | 9.4 | 148.6 | 11.1 | 23 |
| 40.2 | 25.47 | 10 | 3.3 | 0.7 | -0.4 | 0.6 | 306.6 | 9.5 | 149.4 | 11.1 | 23 |
| 42.2 | 23.47 | 9 | 3.3 | 0.7 | -0.4 | 0.6 | 308.0 | 9.8 | 150.8 | 11.1 | 23 |
| 44.2 | 21.47 | 8 | 3.2 | 0.7 | -0.3 | 0.6 | 309.4 | 9.9 | 153.4 | 10.9 | 23 |
| 46.2 | 19.47 | 7 | 3.1 | 0.7 | -0.2 | 0.6 | 309.7 | 10.0 | 156.4 | 10.9 | 23 |
| 48.2 | 17.47 | 6 | 3.1 | 0.6 | -0.1 | 0.6 | 309.2 | 10.1 | 158.5 | 11.0 | 23 |
| 50.2 | 15.47 | 5 | 3.0 | 0.6 | -0.1 | 0.6 | 307.6 | 10.2 | 160.7 | 11.2 | 22 |
| 52.2 | 13.47 | 4 | 2.9 | 0.6 | -0.1 | 0.6 | 306.9 | 10.4 | 161.9 | 11.3 | 21 |
| 54.2 | 11.47 | 3 | 2.8 | 0.6 | -0.1 | 0.6 | 306.7 | 10.3 | 163.3 | 11.2 | 22 |
| 56.2 | 9.47 | 2 | 2.7 | 0.6 | -0.1 | 0.5 | 307.0 | 10.2 | 166.3 | 11.0 | 23 |
| 58.2 | 7.47 | 1 | 2.5 | 0.5 | -0.2 | 0.5 | 307.7 | 10.3 | 169.5 | 11.1 | 22 |
| 65.3 | 0.40 | 1 | 1.1 | 0.3 | -0.4 | 0.3 | 317.7 | 17.8 | 164.3 | 17.6 | 13 |
| 65.4 | 0.28 | 2 | 1.1 | 0.3 | -0.4 | 0.3 | 317.1 | 17.8 | 164.5 | 17.6 | 13 |
| 65.4 | 0.23 | 1 | 1.0 | 0.3 | -0.3 | 0.3 | 318.3 | 17.7 | 166.1 | 17.4 | 13 |
| 65.5 | 0.15 | 3 | 1.0 | 0.3 | -0.4 | 0.3 | 317.1 | 17.6 | 164.6 | 17.5 | 13 |
| 65.6 | 0.03 | 4 | 0.9 | 0.2 | -0.2 | 0.2 | 317.9 | 15.7 | 165.5 | 15.5 | 14 |

*Depth beneath 65.65m nominal surface height

ADCP 8441 (white)
PCADP 844 (yellow)
ADV 8446 (blue)

**Table B-21.** $M_2$ tidal characteristics from current meter records at Site B6. [cph, cycles per hour; SNR, signal-to-noise ratio]

| Site B6–$M_2$–0.08051 cph | | | | | | | | | | | |
|---|---|---|---|---|---|---|---|---|---|---|---|
| **Depth*** | **Elevation** | **Bin#** | **Major** | **error** | **Minor** | **error** | **Inclination** | **error** | **Phase** | **error** | **SNR** |
| 6.3 | 51.31 | 23 | 8.0 | 0.9 | -2.4 | 0.7 | 279.3 | 6.4 | 195.7 | 7.8 | 74 |
| 8.3 | 49.31 | 22 | 7.7 | 0.9 | -2.5 | 0.8 | 281.5 | 6.9 | 199.6 | 8.0 | 72 |
| 10.3 | 47.31 | 21 | 7.6 | 0.9 | -2.4 | 0.8 | 281.6 | 7.0 | 199.0 | 8.0 | 72 |
| 12.3 | 45.31 | 20 | 7.4 | 0.9 | -2.3 | 0.8 | 282.3 | 7.0 | 198.4 | 8.0 | 72 |
| 14.3 | 43.31 | 19 | 7.3 | 0.9 | -2.2 | 0.8 | 282.6 | 7.1 | 197.6 | 7.9 | 73 |
| 16.3 | 41.31 | 18 | 7.2 | 0.8 | -2.0 | 0.8 | 282.6 | 7.0 | 196.3 | 7.6 | 75 |
| 18.3 | 39.31 | 17 | 7.1 | 0.8 | -1.9 | 0.7 | 282.5 | 6.8 | 195.0 | 7.3 | 80 |
| 20.3 | 37.31 | 16 | 7.1 | 0.7 | -1.8 | 0.7 | 282.5 | 6.4 | 194.1 | 6.8 | 91 |
| 22.3 | 35.31 | 15 | 7.1 | 0.7 | -1.7 | 0.6 | 282.7 | 5.9 | 193.6 | 6.2 | 110 |
| 24.3 | 33.31 | 14 | 7.1 | 0.6 | -1.6 | 0.6 | 283.2 | 5.3 | 193.7 | 5.6 | 130 |
| 26.3 | 31.31 | 13 | 7.0 | 0.6 | -1.4 | 0.5 | 283.3 | 4.7 | 193.8 | 5.2 | 150 |
| 28.3 | 29.31 | 12 | 7.0 | 0.6 | -1.2 | 0.5 | 282.9 | 4.4 | 194.0 | 4.9 | 160 |
| 30.3 | 27.31 | 11 | 6.9 | 0.5 | -1.0 | 0.5 | 281.7 | 4.4 | 194.4 | 4.8 | 160 |
| 32.3 | 25.31 | 10 | 6.8 | 0.5 | -0.8 | 0.5 | 280.3 | 4.4 | 195.2 | 4.8 | 160 |
| 34.3 | 23.31 | 9 | 6.7 | 0.6 | -0.5 | 0.5 | 278.5 | 4.3 | 196.5 | 4.9 | 150 |
| 36.3 | 21.31 | 8 | 6.6 | 0.6 | -0.2 | 0.5 | 275.9 | 4.5 | 198.3 | 5.1 | 130 |
| 38.3 | 19.31 | 7 | 6.6 | 0.6 | 0.1 | 0.5 | 272.8 | 4.7 | 200.3 | 5.4 | 120 |
| 40.3 | 17.31 | 6 | 6.6 | 0.6 | 0.4 | 0.6 | 269.3 | 5.0 | 202.3 | 5.7 | 110 |
| 42.3 | 15.31 | 5 | 6.8 | 0.7 | 0.6 | 0.6 | 266.0 | 5.2 | 204.3 | 5.9 | 100 |
| 44.3 | 13.31 | 4 | 6.9 | 0.7 | 0.8 | 0.6 | 262.5 | 5.3 | 206.4 | 6.1 | 97 |
| 46.3 | 11.31 | 3 | 7.2 | 0.7 | 1.0 | 0.6 | 259.0 | 5.5 | 208.5 | 6.2 | 95 |
| 48.3 | 9.31 | 2 | 7.5 | 0.8 | 1.3 | 0.7 | 255.8 | 5.6 | 210.4 | 6.3 | 97 |
| 50.3 | 7.31 | 1 | 7.8 | 0.8 | 1.6 | 0.7 | 253.1 | 5.7 | 211.5 | 6.3 | 99 |
| 57.0 | 0.55 | 1 | 5.7 | 0.6 | 2.0 | 0.5 | 245.0 | 6.4 | 185.4 | 7.3 | 95 |
| 57.1 | 0.53 | 1 | 6.1 | 0.6 | 2.1 | 0.6 | 239.5 | 6.5 | 186.6 | 7.0 | 100 |
| 57.2 | 0.40 | 2 | 5.9 | 0.6 | 2.0 | 0.5 | 239.0 | 6.5 | 186.9 | 6.9 | 100 |
| 57.3 | 0.28 | 3 | 5.6 | 0.6 | 1.9 | 0.5 | 238.5 | 6.4 | 187.3 | 6.9 | 100 |
| 57.4 | 0.15 | 4 | 5.3 | 0.5 | 1.7 | 0.5 | 237.8 | 6.4 | 187.7 | 6.8 | 100 |
| 57.6 | 0.02 | 5 | 4.6 | 0.4 | 1.4 | 0.4 | 237.6 | 6.1 | 188.6 | 6.6 | 110 |

*Depth beneath 57.6 m nominal surface height

ADCP 8471

PCADP 8473

ADV 8474

**Table B-22.** $S_2$ tidal characteristics from current meter records at Site B6. [cph, cycles per hour; SNR, signal-to-noise ratio]

| Site B6–$S_2$–0.08333 cph | | | | | | | | | | | |
|---|---|---|---|---|---|---|---|---|---|---|---|
| **Depth*** | **Elevation** | **Bin#** | **Major** | **error** | **Minor** | **error** | **Inclination** | **error** | **Phase** | **error** | **SNR** |
| 6.3 | 51.31 | 23 | 4.6 | 0.9 | -1.5 | 0.8 | 286.0 | 11.3 | 237.0 | 13.3 | 24 |
| 8.3 | 49.31 | 22 | 4.3 | 0.9 | -1.4 | 0.8 | 287.2 | 12.0 | 240.0 | 13.7 | 23 |
| 10.3 | 47.31 | 21 | 4.1 | 0.9 | -1.3 | 0.8 | 285.9 | 12.5 | 238.6 | 14.3 | 22 |
| 12.3 | 45.31 | 20 | 4.0 | 0.9 | -1.3 | 0.8 | 284.7 | 12.9 | 236.7 | 14.6 | 21 |
| 14.3 | 43.31 | 19 | 3.9 | 0.9 | -1.2 | 0.8 | 283.7 | 13.1 | 235.2 | 14.4 | 21 |
| 16.3 | 41.31 | 18 | 3.9 | 0.8 | -1.1 | 0.8 | 284.0 | 12.6 | 235.0 | 13.7 | 22 |
| 18.3 | 39.31 | 17 | 3.9 | 0.8 | -1.1 | 0.7 | 285.0 | 12.1 | 234.9 | 13.0 | 24 |
| 20.3 | 37.31 | 16 | 3.8 | 0.7 | -1.0 | 0.7 | 287.6 | 11.6 | 234.5 | 12.3 | 26 |
| 22.3 | 35.31 | 15 | 3.7 | 0.7 | -0.9 | 0.6 | 290.6 | 11.0 | 233.2 | 11.6 | 29 |
| 24.3 | 33.31 | 14 | 3.5 | 0.6 | -0.7 | 0.6 | 292.9 | 10.2 | 231.1 | 10.8 | 32 |
| 26.3 | 31.31 | 13 | 3.4 | 0.6 | -0.6 | 0.5 | 294.3 | 9.6 | 228.7 | 10.3 | 34 |
| 28.3 | 29.31 | 12 | 3.3 | 0.5 | -0.6 | 0.5 | 295.2 | 9.3 | 226.4 | 10.0 | 36 |
| 30.3 | 27.31 | 11 | 3.2 | 0.5 | -0.5 | 0.5 | 294.8 | 9.5 | 224.4 | 10.1 | 34 |
| 32.3 | 25.31 | 10 | 3.1 | 0.5 | -0.4 | 0.5 | 292.8 | 9.6 | 222.6 | 10.3 | 32 |
| 34.3 | 23.31 | 9 | 3.0 | 0.5 | -0.2 | 0.5 | 289.5 | 9.5 | 221.8 | 10.5 | 30 |
| 36.3 | 21.31 | 8 | 3.0 | 0.6 | -0.1 | 0.5 | 285.6 | 9.7 | 222.8 | 11.0 | 27 |
| 38.3 | 19.31 | 7 | 2.9 | 0.6 | 0.0 | 0.5 | 281.7 | 10.2 | 224.6 | 11.6 | 24 |
| 40.3 | 17.31 | 6 | 2.9 | 0.6 | 0.1 | 0.6 | 278.4 | 10.8 | 227.2 | 12.3 | 22 |
| 42.3 | 15.31 | 5 | 3.0 | 0.7 | 0.1 | 0.6 | 275.8 | 11.3 | 229.5 | 12.9 | 20 |
| 44.3 | 13.31 | 4 | 3.0 | 0.7 | 0.3 | 0.6 | 273.0 | 11.6 | 231.7 | 13.4 | 19 |
| 46.3 | 11.31 | 3 | 3.1 | 0.7 | 0.4 | 0.6 | 270.6 | 12.2 | 233.4 | 14.0 | 18 |
| 48.3 | 9.31 | 2 | 3.1 | 0.8 | 0.6 | 0.7 | 268.8 | 13.1 | 234.7 | 14.8 | 17 |
| 50.3 | 7.31 | 1 | 3.1 | 0.8 | 0.8 | 0.7 | 267.1 | 14.4 | 235.6 | 16.2 | 15 |
| 57.0 | 0.55 | 1 | 2.0 | 0.6 | 0.7 | 0.5 | 257.7 | 16.8 | 205.0 | 20.2 | 11 |
| 57.1 | 0.53 | 1 | 2.2 | 0.6 | 0.7 | 0.5 | 251.9 | 17.1 | 206.3 | 19.4 | 12 |
| 57.2 | 0.40 | 2 | 2.1 | 0.6 | 0.7 | 0.5 | 251.6 | 17.3 | 206.4 | 19.5 | 12 |
| 57.3 | 0.28 | 3 | 2.0 | 0.6 | 0.7 | 0.5 | 251.2 | 17.4 | 206.6 | 19.4 | 12 |
| 57.4 | 0.15 | 4 | 1.9 | 0.5 | 0.6 | 0.5 | 250.6 | 17.2 | 206.6 | 19.2 | 12 |
| 57.6 | 0.02 | 5 | 1.6 | 0.5 | 0.6 | 0.4 | 249.6 | 16.8 | 208.2 | 18.8 | 13 |

*Depth beneath 57.6 m nominal surface height

ADCP 8471

PCADP 8473

ADV 8474

**Table B-23.** $O_1$ tidal characteristics from current meter records at Site B6. [cph, cycles per hour; SNR, signal-to-noise ratio]

| Site B6–$O_1$–.0.03873 cph | | | | | | | | | | | |
|---|---|---|---|---|---|---|---|---|---|---|---|
| **Depth*** | **Elevation** | **Bin#** | **Major** | **error** | **Minor** | **error** | **Inclination** | **error** | **Phase** | **error** | **SNR** |
| 6.3 | 51.31 | 23 | 2.0 | 0.9 | -0.2 | 0.7 | 282.8 | 18.6 | 149.7 | 21.7 | 5 |
| 8.3 | 49.31 | 22 | 1.7 | 0.8 | -0.2 | 0.7 | 282.8 | 21.3 | 141.0 | 25.5 | 4 |
| 10.3 | 47.31 | 21 | 1.6 | 0.8 | -0.1 | 0.6 | 279.8 | 19.3 | 141.3 | 24.8 | 4 |
| 12.3 | 45.31 | 20 | 1.6 | 0.8 | 0.0 | 0.6 | 277.8 | 18.0 | 142.6 | 24.4 | 4 |
| 14.3 | 43.31 | 19 | 1.6 | 0.8 | 0.1 | 0.6 | 277.2 | 17.2 | 143.9 | 23.7 | 4 |
| 16.3 | 41.31 | 18 | 1.7 | 0.7 | 0.2 | 0.5 | 277.5 | 15.9 | 144.8 | 22.0 | 5 |
| 18.3 | 39.31 | 17 | 1.8 | 0.7 | 0.2 | 0.5 | 278.8 | 14.1 | 145.4 | 20.5 | 6 |
| 20.3 | 37.31 | 16 | 1.8 | 0.7 | 0.2 | 0.5 | 281.3 | 13.1 | 144.6 | 19.5 | 7 |
| 22.3 | 35.31 | 15 | 1.8 | 0.7 | 0.1 | 0.5 | 286.6 | 13.0 | 142.0 | 19.2 | 7 |
| 24.3 | 33.31 | 14 | 1.8 | 0.7 | 0.0 | 0.5 | 291.7 | 13.0 | 139.2 | 18.8 | 7 |
| 26.3 | 31.31 | 13 | 1.9 | 0.7 | -0.1 | 0.5 | 296.8 | 13.4 | 137.2 | 18.4 | 7 |
| 28.3 | 29.31 | 12 | 2.0 | 0.7 | -0.2 | 0.6 | 301.8 | 14.0 | 135.9 | 17.7 | 8 |
| 30.3 | 27.31 | 11 | 2.0 | 0.7 | -0.3 | 0.6 | 305.6 | 14.8 | 135.1 | 17.4 | 8 |
| 32.3 | 25.31 | 10 | 2.0 | 0.7 | -0.3 | 0.6 | 308.8 | 15.6 | 135.1 | 17.3 | 9 |
| 34.3 | 23.31 | 9 | 2.0 | 0.7 | -0.3 | 0.6 | 309.6 | 16.3 | 134.8 | 17.8 | 8 |
| 36.3 | 21.31 | 8 | 2.0 | 0.7 | -0.3 | 0.7 | 308.8 | 17.0 | 134.0 | 18.7 | 7 |
| 38.3 | 19.31 | 7 | 1.9 | 0.7 | -0.3 | 0.6 | 306.8 | 17.3 | 133.0 | 19.9 | 7 |
| 40.3 | 17.31 | 6 | 1.9 | 0.8 | -0.3 | 0.6 | 305.0 | 17.1 | 131.9 | 20.3 | 6 |
| 42.3 | 15.31 | 5 | 1.9 | 0.8 | -0.3 | 0.6 | 302.4 | 16.2 | 131.2 | 20.4 | 6 |
| 44.3 | 13.31 | 4 | 1.9 | 0.7 | -0.3 | 0.6 | 301.0 | 15.2 | 130.7 | 19.7 | 7 |
| 46.3 | 11.31 | 3 | 2.0 | 0.7 | -0.3 | 0.5 | 300.5 | 14.1 | 131.3 | 18.6 | 7 |
| 48.3 | 9.31 | 2 | 2.0 | 0.7 | -0.3 | 0.5 | 300.2 | 13.5 | 130.3 | 17.9 | 8 |
| 50.3 | 7.31 | 1 | 2.0 | 0.7 | -0.3 | 0.5 | 300.7 | 13.1 | 129.3 | 17.3 | 9 |
| 57.0 | 0.55 | 1 | 1.3 | 0.5 | -0.2 | 0.4 | 299.5 | 14.3 | 101.9 | 18.9 | 7 |
| 57.1 | 0.53 | 1 | 1.4 | 0.5 | -0.1 | 0.4 | 294.8 | 14.7 | 102.0 | 20.0 | 6 |
| 57.2 | 0.40 | 2 | 1.3 | 0.5 | -0.1 | 0.4 | 294.9 | 14.7 | 101.9 | 20.0 | 6 |
| 57.3 | 0.28 | 3 | 1.2 | 0.5 | -0.1 | 0.4 | 294.5 | 14.7 | 101.6 | 20.1 | 6 |
| 57.4 | 0.15 | 4 | 1.2 | 0.5 | -0.1 | 0.3 | 293.3 | 14.5 | 100.8 | 20.3 | 6 |
| 57.6 | 0.02 | 5 | 1.0 | 0.4 | -0.1 | 0.3 | 291.1 | 13.3 | 101.0 | 20.0 | 6 |

*Depth beneath 57.6 m nominal surface height

ADCP 8471

PCADP 8473

ADV 8474

**Table B-24.** $K_1$ tidal characteristics from current meter records at Site B6. [cph, cycles per hour; SNR, signal-to-noise ratio]

| Site B6 –$K_1$–.0.04178 cph | | | | | | | | | | | |
|---|---|---|---|---|---|---|---|---|---|---|---|
| **Depth*** | **Elevation** | **Bin#** | **Major** | **error** | **Minor** | **error** | **Inclination** | **error** | **Phase** | **error** | **SNR** |
| 6.3 | 51.31 | 23 | 4.2 | 0.9 | -1.7 | 0.7 | 272.5 | 12.3 | 185.4 | 13.9 | 23 |
| 8.3 | 49.31 | 22 | 3.5 | 0.8 | -1.5 | 0.7 | 280.6 | 14.5 | 180.4 | 16.5 | 17 |
| 10.3 | 47.31 | 21 | 3.3 | 0.8 | -1.3 | 0.6 | 285.8 | 13.1 | 171.8 | 15.5 | 17 |
| 12.3 | 45.31 | 20 | 3.2 | 0.8 | -1.1 | 0.6 | 291.3 | 12.5 | 164.9 | 14.9 | 17 |
| 14.3 | 43.31 | 19 | 3.1 | 0.7 | -1.0 | 0.6 | 297.2 | 12.2 | 159.6 | 14.2 | 18 |
| 16.3 | 41.31 | 18 | 3.1 | 0.7 | -1.0 | 0.6 | 303.8 | 12.1 | 155.6 | 13.4 | 20 |
| 18.3 | 39.31 | 17 | 3.1 | 0.6 | -0.9 | 0.6 | 310.7 | 11.9 | 152.5 | 12.4 | 23 |
| 20.3 | 37.31 | 16 | 3.1 | 0.6 | -0.9 | 0.6 | 316.0 | 11.7 | 149.5 | 11.5 | 27 |
| 22.3 | 35.31 | 15 | 3.1 | 0.6 | -1.0 | 0.6 | 319.0 | 11.8 | 146.5 | 11.2 | 29 |
| 24.3 | 33.31 | 14 | 3.2 | 0.6 | -1.1 | 0.6 | 320.7 | 12.3 | 143.8 | 11.4 | 30 |
| 26.3 | 31.31 | 13 | 3.2 | 0.6 | -1.2 | 0.7 | 322.4 | 13.0 | 142.4 | 11.7 | 31 |
| 28.3 | 29.31 | 12 | 3.2 | 0.6 | -1.2 | 0.7 | 323.6 | 13.6 | 141.5 | 12.1 | 30 |
| 30.3 | 27.31 | 11 | 3.2 | 0.6 | -1.2 | 0.7 | 324.3 | 13.6 | 141.1 | 12.0 | 30 |
| 32.3 | 25.31 | 10 | 3.2 | 0.6 | -1.1 | 0.7 | 323.5 | 13.5 | 140.7 | 12.0 | 28 |
| 34.3 | 23.31 | 9 | 3.2 | 0.6 | -1.0 | 0.7 | 323.8 | 13.2 | 140.8 | 11.6 | 27 |
| 36.3 | 21.31 | 8 | 3.2 | 0.6 | -0.9 | 0.7 | 323.5 | 13.0 | 140.0 | 11.4 | 26 |
| 38.3 | 19.31 | 7 | 3.2 | 0.6 | -0.8 | 0.7 | 322.3 | 13.0 | 138.9 | 11.6 | 24 |
| 40.3 | 17.31 | 6 | 3.2 | 0.7 | -0.7 | 0.7 | 320.5 | 12.8 | 138.7 | 11.7 | 24 |
| 42.3 | 15.31 | 5 | 3.1 | 0.7 | -0.8 | 0.7 | 319.0 | 12.9 | 139.7 | 12.1 | 23 |
| 44.3 | 13.31 | 4 | 3.0 | 0.6 | -0.9 | 0.7 | 317.9 | 13.2 | 141.3 | 12.6 | 22 |
| 46.3 | 11.31 | 3 | 3.0 | 0.6 | -0.9 | 0.7 | 317.5 | 13.4 | 143.7 | 12.8 | 23 |
| 48.3 | 9.31 | 2 | 2.9 | 0.6 | -1.0 | 0.6 | 317.1 | 14.0 | 145.2 | 13.6 | 22 |
| 50.3 | 7.31 | 1 | 2.8 | 0.6 | -1.1 | 0.6 | 315.9 | 15.1 | 146.7 | 14.9 | 21 |
| 57.0 | 0.55 | 1 | 1.5 | 0.5 | -1.0 | 0.4 | 304.0 | 31.4 | 126.1 | 34.0 | 10 |
| 57.1 | 0.53 | 1 | 1.5 | 0.5 | -1.0 | 0.4 | 299.7 | 33.5 | 125.7 | 36.7 | 8 |
| 57.2 | 0.40 | 2 | 1.5 | 0.5 | -1.0 | 0.4 | 299.1 | 33.2 | 125.5 | 36.5 | 8 |
| 57.3 | 0.28 | 3 | 1.4 | 0.5 | -0.9 | 0.4 | 297.8 | 32.6 | 124.9 | 36.3 | 8 |
| 57.4 | 0.15 | 4 | 1.3 | 0.5 | -0.8 | 0.3 | 295.7 | 31.3 | 123.7 | 35.5 | 8 |
| 57.6 | 0.02 | 5 | 1.1 | 0.4 | -0.7 | 0.3 | 295.1 | 36.5 | 122.2 | 41.1 | 8 |

*Depth beneath 57.6 m nominal surface height

ADCP 8471

PCADP 8473

ADV 8474

**Table B-25.** $M_2$ tidal characteristics from near-bottom 1,200-kHz ADCP current meter records at Site B6. [cph, cycles per hour; SNR, signal-to-noise ratio]

| Site B6–$M_2$–0.08051 cph | | | | | | | | | | | |
|---|---|---|---|---|---|---|---|---|---|---|---|
| Depth* | Elevation | Bin# | Major | error | Minor | error | Inclination | error | Phase | error | SNR |
| 46.0 | 14.01 | 52 | 7.9 | 0.7 | 1.1 | 0.8 | 259.5 | 6.2 | 24.7 | 5.4 | 130 |
| 47.0 | 13.01 | 48 | 8.0 | 0.8 | 1.2 | 0.8 | 257.5 | 6.2 | 25.9 | 6.0 | 110 |
| 48.0 | 12.01 | 44 | 8.2 | 0.8 | 1.3 | 0.8 | 255.6 | 6.1 | 26.9 | 6.0 | 100 |
| 49.0 | 11.01 | 40 | 8.4 | 0.8 | 1.3 | 0.8 | 254.3 | 6.1 | 27.0 | 6.0 | 110 |
| 50.0 | 10.01 | 36 | 8.6 | 0.8 | 1.5 | 0.9 | 253.4 | 6.2 | 27.4 | 6.0 | 110 |
| 51.0 | 9.01 | 32 | 8.8 | 0.9 | 1.6 | 0.9 | 252.7 | 6.2 | 27.4 | 6.0 | 110 |
| 52.0 | 8.01 | 28 | 9.1 | 0.9 | 1.8 | 0.9 | 251.8 | 6.1 | 27.1 | 6.0 | 110 |
| 52.2 | 7.76 | 27 | 9.2 | 0.9 | 1.9 | 0.9 | 251.6 | 6.1 | 27.0 | 6.1 | 110 |
| 52.5 | 7.51 | 26 | 9.2 | 0.9 | 1.9 | 0.9 | 251.6 | 6.1 | 26.8 | 6.1 | 110 |
| 52.7 | 7.26 | 25 | 9.3 | 0.9 | 2.0 | 0.9 | 251.2 | 6.1 | 26.9 | 6.1 | 110 |
| 53.0 | 7.01 | 24 | 9.4 | 0.9 | 2.0 | 0.9 | 251.0 | 6.1 | 26.9 | 6.1 | 110 |
| 53.2 | 6.76 | 23 | 9.4 | 0.9 | 2.1 | 0.9 | 250.9 | 6.1 | 26.8 | 6.2 | 110 |
| 53.5 | 6.51 | 22 | 9.5 | 0.9 | 2.2 | 0.9 | 250.8 | 6.1 | 26.7 | 6.3 | 100 |
| 53.7 | 6.26 | 21 | 9.5 | 0.9 | 2.3 | 0.9 | 250.7 | 6.1 | 26.6 | 6.3 | 100 |
| 54.0 | 6.01 | 20 | 9.6 | 0.9 | 2.3 | 0.9 | 250.5 | 6.0 | 26.6 | 6.3 | 100 |
| 54.2 | 5.76 | 19 | 9.6 | 0.9 | 2.4 | 0.9 | 250.2 | 6.1 | 26.6 | 6.3 | 100 |
| 54.5 | 5.51 | 18 | 9.7 | 1.0 | 2.4 | 0.9 | 250.1 | 6.1 | 26.5 | 6.4 | 100 |
| 54.7 | 5.26 | 17 | 9.7 | 1.0 | 2.5 | 0.9 | 249.8 | 6.0 | 26.5 | 6.4 | 100 |
| 55.0 | 5.01 | 16 | 9.7 | 1.0 | 2.5 | 0.9 | 249.6 | 6.1 | 26.2 | 6.6 | 100 |
| 55.2 | 4.76 | 15 | 9.7 | 1.0 | 2.6 | 0.9 | 249.5 | 6.1 | 26.3 | 6.6 | 99 |
| 55.5 | 4.51 | 14 | 9.7 | 1.0 | 2.7 | 0.9 | 249.2 | 6.0 | 26.2 | 6.6 | 100 |
| 55.7 | 4.26 | 13 | 9.6 | 1.0 | 2.7 | 0.9 | 249.0 | 6.1 | 25.9 | 6.7 | 97 |
| 56.0 | 4.01 | 12 | 9.6 | 1.0 | 2.8 | 0.9 | 248.7 | 6.1 | 25.8 | 6.8 | 97 |
| 56.2 | 3.76 | 11 | 9.5 | 1.0 | 2.8 | 0.9 | 248.4 | 6.1 | 25.8 | 6.8 | 97 |
| 56.5 | 3.51 | 10 | 9.4 | 1.0 | 2.8 | 0.8 | 248.1 | 6.1 | 25.6 | 6.8 | 97 |
| 56.7 | 3.26 | 9 | 9.3 | 1.0 | 2.9 | 0.8 | 247.9 | 6.1 | 25.3 | 6.9 | 96 |
| 57.0 | 3.01 | 8 | 9.2 | 0.9 | 2.8 | 0.8 | 247.7 | 6.2 | 25.0 | 7.0 | 94 |
| 57.2 | 2.76 | 7 | 9.0 | 0.9 | 2.9 | 0.8 | 247.3 | 6.2 | 24.9 | 7.0 | 94 |
| 57.5 | 2.51 | 6 | 8.8 | 0.9 | 2.9 | 0.8 | 247.0 | 6.3 | 24.6 | 7.1 | 95 |
| 57.7 | 2.26 | 5 | 8.6 | 0.9 | 2.9 | 0.8 | 246.6 | 6.3 | 24.3 | 7.1 | 95 |
| 58.0 | 2.01 | 4 | 8.3 | 0.8 | 2.8 | 0.7 | 246.1 | 6.4 | 24.1 | 7.1 | 96 |
| 58.2 | 1.76 | 3 | 8.0 | 0.8 | 2.7 | 0.7 | 245.5 | 6.4 | 24.3 | 7.1 | 97 |
| 58.5 | 1.51 | 2 | 7.6 | 0.8 | 2.7 | 0.7 | 244.7 | 6.4 | 24.5 | 7.0 | 100 |
| 58.7 | 1.26 | 1 | 7.2 | 0.7 | 2.6 | 0.6 | 243.9 | 6.5 | 24.6 | 7.0 | 100 |

*Depth beneath 57.6 m nominal surface height

**Table B-26.** $S_2$ tidal characteristics from near-bottom 1,200-kHz ADCP current meter records at Site B6. [cph, cycles per hour; SNR, signal-to-noise ratio]

| Site B6–$S_2$–0.08333 cph | | | | | | | | | | | |
|---|---|---|---|---|---|---|---|---|---|---|---|
| **Depth*** | **Elevation** | **Bin#** | **Major** | **error** | **Minor** | **error** | **Inclination** | **error** | **Phase** | **error** | **SNR** |
| 46.0 | 14.01 | 52 | 3.8 | 0.7 | 0.2 | 0.8 | 277.7 | 12.3 | 46.9 | 10.7 | 29 |
| 47.0 | 13.01 | 48 | 3.7 | 0.8 | 0.3 | 0.8 | 276.0 | 12.6 | 48.5 | 12.1 | 23 |
| 48.0 | 12.01 | 44 | 3.7 | 0.8 | 0.3 | 0.8 | 276.3 | 12.8 | 48.4 | 12.6 | 21 |
| 49.0 | 11.01 | 40 | 3.7 | 0.8 | 0.4 | 0.8 | 275.8 | 13.1 | 47.6 | 12.7 | 21 |
| 50.0 | 10.01 | 36 | 3.7 | 0.8 | 0.4 | 0.9 | 275.1 | 13.6 | 46.7 | 13.2 | 19 |
| 51.0 | 9.01 | 32 | 3.6 | 0.9 | 0.4 | 0.9 | 274.1 | 14.2 | 46.1 | 13.7 | 18 |
| 52.0 | 8.01 | 28 | 3.6 | 0.9 | 0.5 | 0.9 | 273.8 | 14.7 | 44.5 | 14.4 | 17 |
| 52.2 | 7.76 | 27 | 3.5 | 0.9 | 0.5 | 0.9 | 273.6 | 14.8 | 44.0 | 14.7 | 16 |
| 52.5 | 7.51 | 26 | 3.5 | 0.9 | 0.5 | 0.9 | 273.4 | 14.9 | 43.4 | 14.8 | 16 |
| 52.7 | 7.26 | 25 | 3.5 | 0.9 | 0.5 | 0.9 | 273.4 | 15.0 | 43.4 | 15.1 | 15 |
| 53.0 | 7.01 | 24 | 3.5 | 0.9 | 0.5 | 0.9 | 272.9 | 15.2 | 43.1 | 15.4 | 15 |
| 53.2 | 6.76 | 23 | 3.5 | 0.9 | 0.5 | 0.9 | 273.2 | 15.4 | 42.9 | 15.7 | 14 |
| 53.5 | 6.51 | 22 | 3.4 | 0.9 | 0.5 | 0.9 | 273.0 | 15.4 | 42.2 | 15.9 | 14 |
| 53.7 | 6.26 | 21 | 3.4 | 0.9 | 0.5 | 0.9 | 272.7 | 15.5 | 41.8 | 16.4 | 13 |
| 54.0 | 6.01 | 20 | 3.4 | 0.9 | 0.5 | 0.9 | 272.7 | 15.7 | 41.4 | 16.6 | 13 |
| 54.2 | 5.76 | 19 | 3.3 | 1.0 | 0.5 | 0.9 | 272.4 | 16.0 | 40.7 | 16.9 | 12 |
| 54.5 | 5.51 | 18 | 3.3 | 1.0 | 0.5 | 0.9 | 271.8 | 16.0 | 40.6 | 17.3 | 12 |
| 54.7 | 5.26 | 17 | 3.3 | 1.0 | 0.5 | 0.9 | 271.9 | 16.0 | 39.9 | 17.4 | 12 |
| 55.0 | 5.01 | 16 | 3.2 | 1.0 | 0.5 | 0.9 | 270.9 | 16.1 | 40.5 | 18.0 | 11 |
| 55.2 | 4.76 | 15 | 3.2 | 1.0 | 0.5 | 0.9 | 270.4 | 16.3 | 39.5 | 18.4 | 10 |
| 55.5 | 4.51 | 14 | 3.1 | 1.0 | 0.5 | 0.9 | 270.1 | 16.2 | 39.0 | 18.5 | 10 |
| 55.7 | 4.26 | 13 | 3.1 | 1.0 | 0.5 | 0.9 | 269.9 | 16.4 | 38.8 | 19.0 | 10 |
| 56.0 | 4.01 | 12 | 3.0 | 1.0 | 0.5 | 0.8 | 269.6 | 16.5 | 38.5 | 19.6 | 9 |
| 56.2 | 3.76 | 11 | 2.9 | 1.0 | 0.5 | 0.8 | 268.8 | 16.9 | 37.8 | 20.0 | 9 |
| 56.5 | 3.51 | 10 | 2.9 | 1.0 | 0.5 | 0.8 | 267.8 | 17.0 | 37.0 | 20.3 | 9 |
| 56.7 | 3.26 | 9 | 2.8 | 1.0 | 0.5 | 0.8 | 267.1 | 17.1 | 36.6 | 20.7 | 8 |
| 57.0 | 3.01 | 8 | 2.7 | 1.0 | 0.5 | 0.8 | 266.8 | 17.1 | 36.4 | 21.0 | 8 |
| 57.2 | 2.76 | 7 | 2.6 | 1.0 | 0.5 | 0.8 | 266.1 | 17.7 | 35.5 | 21.8 | 8 |
| 57.5 | 2.51 | 6 | 2.6 | 0.9 | 0.5 | 0.8 | 265.2 | 17.7 | 34.7 | 21.6 | 8 |
| 57.7 | 2.26 | 5 | 2.5 | 0.9 | 0.4 | 0.7 | 265.0 | 17.3 | 34.0 | 21.3 | 8 |
| 58.0 | 2.01 | 4 | 2.4 | 0.9 | 0.5 | 0.7 | 263.5 | 17.9 | 34.1 | 21.7 | 8 |
| 58.2 | 1.76 | 3 | 2.3 | 0.8 | 0.4 | 0.7 | 263.0 | 17.7 | 33.3 | 21.4 | 8 |
| 58.5 | 1.51 | 2 | 2.3 | 0.8 | 0.4 | 0.7 | 261.9 | 17.4 | 33.0 | 20.6 | 9 |
| 58.7 | 1.26 | 1 | 2.1 | 0.7 | 0.4 | 0.6 | 262.1 | 17.7 | 32.8 | 20.7 | 8 |
| *Depth beneath 57.6 m nominal surface height | | | | | | | | | | | |

**Table B-27.** $O_1$ tidal characteristics from near-bottom 1,200-kHz ADCP current meter records at Site B6. [cph, cycles per hour; SNR, signal-to-noise ratio]

| Site B6 –$O_1$–.0.03873 cph | | | | | | | | | | | |
|---|---|---|---|---|---|---|---|---|---|---|---|
| **Depth*** | **Elevation** | **Bin#** | **Major** | **error** | **Minor** | **error** | **Inclination** | **error** | **Phase** | **error** | **SNR** |
| 46.0 | 14.01 | 52 | 2.1 | 0.9 | -0.2 | 0.7 | 120.6 | 16.2 | 122.2 | 22.2 | 5 |
| 47.0 | 13.01 | 48 | 2.1 | 0.9 | -0.2 | 0.7 | 119.9 | 15.4 | 129.4 | 22.1 | 5 |
| 48.0 | 12.01 | 44 | 2.2 | 0.9 | -0.2 | 0.6 | 119.4 | 14.5 | 131.8 | 20.8 | 6 |
| 49.0 | 11.01 | 40 | 2.2 | 0.9 | -0.1 | 0.6 | 118.5 | 14.0 | 133.5 | 20.4 | 6 |
| 50.0 | 10.01 | 36 | 2.2 | 0.9 | -0.1 | 0.6 | 118.9 | 13.7 | 134.1 | 19.7 | 6 |
| 51.0 | 9.01 | 32 | 2.3 | 0.9 | -0.1 | 0.6 | 119.4 | 13.6 | 134.5 | 18.9 | 7 |
| 52.0 | 8.01 | 28 | 2.3 | 0.8 | -0.1 | 0.6 | 119.7 | 13.3 | 134.7 | 18.2 | 7 |
| 52.2 | 7.76 | 27 | 2.3 | 0.8 | -0.1 | 0.6 | 120.5 | 13.6 | 134.3 | 18.1 | 8 |
| 52.5 | 7.51 | 26 | 2.3 | 0.8 | -0.2 | 0.6 | 120.1 | 13.5 | 134.4 | 18.1 | 8 |
| 52.7 | 7.26 | 25 | 2.3 | 0.8 | -0.2 | 0.6 | 120.9 | 13.7 | 134.1 | 17.9 | 8 |
| 53.0 | 7.01 | 24 | 2.3 | 0.8 | -0.2 | 0.6 | 121.0 | 13.8 | 133.5 | 17.8 | 8 |
| 53.2 | 6.76 | 23 | 2.3 | 0.8 | -0.2 | 0.6 | 121.1 | 14.1 | 133.5 | 18.1 | 8 |
| 53.5 | 6.51 | 22 | 2.3 | 0.8 | -0.2 | 0.7 | 121.5 | 14.2 | 133.6 | 18.1 | 8 |
| 53.7 | 6.26 | 21 | 2.2 | 0.8 | -0.1 | 0.7 | 122.0 | 14.4 | 133.8 | 18.1 | 8 |
| 54.0 | 6.01 | 20 | 2.2 | 0.8 | -0.2 | 0.7 | 122.0 | 14.5 | 133.3 | 18.2 | 7 |
| 54.2 | 5.76 | 19 | 2.2 | 0.8 | -0.2 | 0.7 | 121.9 | 14.7 | 133.4 | 18.4 | 7 |
| 54.5 | 5.51 | 18 | 2.2 | 0.8 | -0.2 | 0.7 | 122.2 | 14.7 | 133.7 | 18.2 | 7 |
| 54.7 | 5.26 | 17 | 2.2 | 0.8 | -0.2 | 0.7 | 122.1 | 15.1 | 134.0 | 18.5 | 7 |
| 55.0 | 5.01 | 16 | 2.1 | 0.8 | -0.2 | 0.7 | 121.9 | 15.3 | 133.2 | 18.8 | 7 |
| 55.2 | 4.76 | 15 | 2.1 | 0.8 | -0.2 | 0.7 | 122.9 | 15.5 | 132.7 | 18.7 | 7 |
| 55.5 | 4.51 | 14 | 2.1 | 0.8 | -0.2 | 0.7 | 122.4 | 15.6 | 132.2 | 18.9 | 7 |
| 55.7 | 4.26 | 13 | 2.0 | 0.8 | -0.2 | 0.7 | 122.7 | 16.3 | 132.2 | 19.4 | 7 |
| 56.0 | 4.01 | 12 | 2.0 | 0.8 | -0.2 | 0.7 | 122.6 | 16.2 | 131.8 | 19.3 | 7 |
| 56.2 | 3.76 | 11 | 2.0 | 0.8 | -0.2 | 0.7 | 123.5 | 16.7 | 131.7 | 19.5 | 7 |
| 56.5 | 3.51 | 10 | 1.9 | 0.8 | -0.1 | 0.7 | 123.4 | 17.1 | 131.6 | 20.0 | 6 |
| 56.7 | 3.26 | 9 | 1.9 | 0.8 | -0.1 | 0.7 | 123.6 | 17.7 | 131.3 | 20.5 | 6 |
| 57.0 | 3.01 | 8 | 1.8 | 0.8 | -0.1 | 0.7 | 123.8 | 17.7 | 131.0 | 20.4 | 6 |
| 57.2 | 2.76 | 7 | 1.8 | 0.7 | -0.1 | 0.7 | 123.4 | 17.8 | 131.5 | 20.4 | 6 |
| 57.5 | 2.51 | 6 | 1.8 | 0.7 | 0.0 | 0.7 | 123.3 | 17.9 | 130.6 | 20.6 | 6 |
| 57.7 | 2.26 | 5 | 1.7 | 0.7 | 0.0 | 0.6 | 123.6 | 18.3 | 130.0 | 21.1 | 5 |
| 58.0 | 2.01 | 4 | 1.7 | 0.7 | 0.0 | 0.6 | 123.5 | 18.4 | 129.8 | 21.1 | 5 |
| 58.2 | 1.76 | 3 | 1.6 | 0.7 | 0.1 | 0.6 | 122.6 | 18.6 | 130.1 | 21.6 | 5 |
| 58.5 | 1.51 | 2 | 1.6 | 0.7 | 0.1 | 0.6 | 123.0 | 18.5 | 128.5 | 21.4 | 5 |
| 58.7 | 1.26 | 1 | 1.5 | 0.6 | 0.1 | 0.6 | 122.7 | 18.9 | 127.8 | 21.8 | 5 |

*Depth beneath 57.6 m nominal surface height

**Table B-28.** $K_1$ tidal characteristics from near-bottom 1,200-kHz ADCP current meter records at Site B6. [cph, cycles per hour; SNR, signal-to-noise ratio]

| Site B6 –$K_1$–.0.04178 cph | | | | | | | | | | | |
|---|---|---|---|---|---|---|---|---|---|---|---|
| **Depth*** | **Elevation** | **Bin#** | **Major** | **error** | **Minor** | **error** | **Inclination** | **error** | **Phase** | **error** | **SNR** |
| 46.0 | 14.01 | 52 | 3.8 | 0.9 | -0.7 | 0.8 | 130.8 | 11.3 | 137.1 | 12.3 | 19 |
| 47.0 | 13.01 | 48 | 3.6 | 0.8 | -0.8 | 0.8 | 131.1 | 11.8 | 138.0 | 12.9 | 18 |
| 48.0 | 12.01 | 44 | 3.5 | 0.8 | -0.8 | 0.8 | 131.2 | 12.1 | 139.2 | 13.1 | 18 |
| 49.0 | 11.01 | 40 | 3.4 | 0.8 | -0.9 | 0.7 | 131.0 | 12.5 | 139.7 | 13.5 | 18 |
| 50.0 | 10.01 | 36 | 3.4 | 0.8 | -0.9 | 0.7 | 131.4 | 12.5 | 141.2 | 13.5 | 18 |
| 51.0 | 9.01 | 32 | 3.4 | 0.8 | -1.0 | 0.7 | 130.6 | 12.7 | 142.2 | 13.8 | 18 |
| 52.0 | 8.01 | 28 | 3.3 | 0.8 | -1.0 | 0.7 | 131.1 | 13.1 | 144.2 | 14.1 | 18 |
| 52.2 | 7.76 | 27 | 3.3 | 0.8 | -1.0 | 0.7 | 131.0 | 13.4 | 144.5 | 14.3 | 18 |
| 52.5 | 7.51 | 26 | 3.2 | 0.8 | -1.1 | 0.7 | 131.7 | 13.6 | 145.4 | 14.3 | 18 |
| 52.7 | 7.26 | 25 | 3.2 | 0.8 | -1.1 | 0.7 | 131.8 | 13.9 | 145.5 | 14.6 | 18 |
| 53.0 | 7.01 | 24 | 3.2 | 0.8 | -1.1 | 0.7 | 131.4 | 14.0 | 145.9 | 14.8 | 18 |
| 53.2 | 6.76 | 23 | 3.2 | 0.8 | -1.1 | 0.7 | 131.8 | 14.6 | 146.2 | 15.3 | 17 |
| 53.5 | 6.51 | 22 | 3.1 | 0.8 | -1.2 | 0.7 | 132.0 | 15.0 | 146.5 | 15.7 | 17 |
| 53.7 | 6.26 | 21 | 3.1 | 0.8 | -1.2 | 0.7 | 132.1 | 15.2 | 146.5 | 15.8 | 17 |
| 54.0 | 6.01 | 20 | 3.1 | 0.8 | -1.2 | 0.7 | 132.3 | 15.6 | 147.1 | 16.2 | 17 |
| 54.2 | 5.76 | 19 | 3.1 | 0.8 | -1.2 | 0.7 | 132.1 | 16.1 | 146.9 | 16.7 | 16 |
| 54.5 | 5.51 | 18 | 3.0 | 0.8 | -1.2 | 0.7 | 132.5 | 16.4 | 147.6 | 16.9 | 16 |
| 54.7 | 5.26 | 17 | 2.9 | 0.7 | -1.3 | 0.7 | 133.0 | 17.1 | 148.0 | 17.5 | 16 |
| 55.0 | 5.01 | 16 | 2.9 | 0.8 | -1.3 | 0.7 | 132.8 | 17.4 | 147.8 | 17.9 | 15 |
| 55.2 | 4.76 | 15 | 2.9 | 0.7 | -1.3 | 0.7 | 133.4 | 18.2 | 148.1 | 18.5 | 15 |
| 55.5 | 4.51 | 14 | 2.8 | 0.7 | -1.3 | 0.7 | 133.8 | 18.5 | 148.7 | 18.7 | 15 |
| 55.7 | 4.26 | 13 | 2.8 | 0.7 | -1.3 | 0.7 | 133.3 | 19.5 | 148.1 | 19.8 | 14 |
| 56.0 | 4.01 | 12 | 2.7 | 0.7 | -1.3 | 0.7 | 134.2 | 20.4 | 148.5 | 20.5 | 14 |
| 56.2 | 3.76 | 11 | 2.7 | 0.7 | -1.3 | 0.7 | 134.5 | 21.1 | 148.8 | 21.2 | 14 |
| 56.5 | 3.51 | 10 | 2.6 | 0.7 | -1.3 | 0.7 | 134.5 | 21.8 | 148.4 | 21.9 | 13 |
| 56.7 | 3.26 | 9 | 2.5 | 0.7 | -1.4 | 0.7 | 135.2 | 23.4 | 148.5 | 23.4 | 13 |
| 57.0 | 3.01 | 8 | 2.5 | 0.7 | -1.3 | 0.7 | 135.8 | 24.3 | 149.0 | 24.2 | 12 |
| 57.2 | 2.76 | 7 | 2.4 | 0.7 | -1.3 | 0.7 | 135.2 | 25.0 | 147.8 | 25.0 | 12 |
| 57.5 | 2.51 | 6 | 2.3 | 0.7 | -1.4 | 0.7 | 134.7 | 26.8 | 147.3 | 26.9 | 11 |
| 57.7 | 2.26 | 5 | 2.3 | 0.7 | -1.3 | 0.7 | 134.3 | 28.2 | 147.3 | 28.3 | 11 |
| 58.0 | 2.01 | 4 | 2.2 | 0.7 | -1.3 | 0.7 | 134.4 | 29.3 | 146.9 | 29.4 | 11 |
| 58.2 | 1.76 | 3 | 2.1 | 0.7 | -1.3 | 0.7 | 132.4 | 30.4 | 145.5 | 30.8 | 10 |
| 58.5 | 1.51 | 2 | 2.0 | 0.6 | -1.2 | 0.6 | 132.9 | 31.6 | 146.2 | 32.0 | 10 |
| 58.7 | 1.26 | 1 | 1.8 | 0.6 | -1.2 | 0.6 | 129.1 | 34.8 | 143.1 | 35.8 | 9 |

*Depth beneath 57.6 m nominal surface height